EPRI
Electric Power
Research Institute

Keywords:
Corrosion
Thermodynamics
Computer Programs
Electrochemical Corrosion
Water Chemistry

EPRI NP-3137
Volume 2
Project 1167-2
Final Report
June 1983

EPRI-NP--3137-Vol.2

DE83 902680

Computer-Calculated Potential pH Diagrams to 300°C

Volume 2:
Handbook of Diagrams

Prepared by
The Babcock & Wilcox Company
Alliance, Ohio

Computer-Calculated Potential pH Diagrams to 300°C.

Volume 2. Handbook of Diagrams

NP-3137, Volume 2
Research Project 1167-2

Final Report, June 1983

Prepared by

THE BABCOCK & WILCOX COMPANY
Research and Development Division
P. O. Box 835
Alliance, Ohio 44601

Principal Investigators
C. M. Chen
K. Aral
G. J. Theus

Prepared for

Electric Power Research Institute
3412 Hillview Avenue
Palo Alto, California 94304

EPRI Project Managers
D. Cubicciotti
T. O. Passell

Materials and Corrosion Program
Nuclear Power Division

ORDERING INFORMATION

Requests for copies of this report should be directed to Research Reports Center (RRC), Box 50490, Palo Alto, CA 94303, (415) 965-4081. There is no charge for reports requested by EPRI member utilities and affiliates, U.S. utility associations, U.S. government agencies (federal, state, and local), media, and foreign organizations with which EPRI has an information exchange agreement. On request, RRC will send a catalog of EPRI reports.

NOTICE

Prepared by
The Babcock & Wilcox Company
Alliance, Ohio

EPRI PERSPECTIVE

PROJECT DESCRIPTION

Corrosion rates of metals in water correlate well with the stabilities of metal oxides. Potential pH diagrams indicate the regions of oxide thermodynamic stability as functions of solution pH and the electrochemical potential of the system. Diagrams of this type are not generally available for metal-water systems at elevated temperatures. The diagrams provide a useful guide to corrosion engineers for solving corrosion problems as they arise and for recommending situations to avoid where problems might arise.

Related EPRI projects are RP311; RP967; and other subprojects in RP1167, namely, RP1167-1, RP1167-3, and RP1167-4. Related reports are EPRI Final Reports NP-2177, NP-2298, and NP-2400.

PROJECT OBJECTIVE

The objective of RP1167-2 was to generate potential pH (Pourbaix) diagrams for high-temperature metal-water systems.

PROJECT RESULTS

Potential pH diagrams for many metal-water systems were obtained at temperatures up to 300°C. These diagrams are complementary to those presented in EPRI NP-2298 in that different metal-water systems were studied in most cases or higher temperatures were used.

Application of the diagrams to several nuclear corrosion problems illustrates one potential use. In general the potential pH diagrams can serve as guides to the corrosion engineer to help devise mechanisms to describe the corrosion processes. Unfortunately the information is still limited, so that mechanisms evolved are only possibilities, and detailed testing is needed to establish their validity.

A computer program to generate potential pH diagrams is one of the valuable results of the project. Part of this final report presents a user's guide to the program. Copies of the program, named POT-pH-TEMP, will be available through the EPRI Software Center.

This report has been divided into three volumes, which are of interest to several kinds of readers. Volume 1, the executive summary, gives an overview including a discussion of the uses of potential pH diagrams for the general technical reader. Volume 2, a handbook of diagrams, discusses the many potential pH diagrams generated on the project for use by corrosion engineers. Volume 3, a user's guide to POT-pH-TEMP, gives the program details for people interested in generating their own diagrams for special cases.

The diagrams represent the available thermodynamic information concerning common metals in contact with corrosive water environments. This data base is still in need of improvement for high temperatures, and thus, the diagrams are subject to change.

D. Cubicciotti, Project Manager
T. O. Passell, Project Manager
Nuclear Power Division

ABSTRACT

This final report summarizes the results of a program to devise a general computer method of estimating potential-pH diagrams for metals in water at temperatures from 25°C to 300°C. The computer program uses literature data for room temperature and either literature data where available or standard estimation procedures, especially for ions in solution, to calculate relative thermodynamic stabilities of the various possible compounds of an element at temepratures up to 300°C. The program identifies the regions in which various phases are stable and presents the stability fields in a potential-pH diagram for a metal in water. In addition to the computer program itself, the report presents numerous potential-pH diagrams for specific elements in water are various temperatures.

ACKNOWLEDGMENTS

The authors wish to thank Drs. D. Cubicciotti and T. O. Passell, of EPRI, for their assistance and Dr. D. D. MacDonald, Ohio State University, for his discussion of the results.

CONTENTS

CONTENTS (Contd.)

ILLUSTRATIONS

TABLES

TABLES (Contd.)

SUMMARY OF ALL THREE VOLUMES

This is the final report for EPRI Contract RP1167-2. The objective of this project was to develop a computerized program for generating potential-pH (Pourbaix) diagrams for metal-water systems at elevated temperatures. The project was a follow on to Project RP967-1, which generated diagrams for systems up to 200°C and presented the results in the Final Report, EPRI NP-2298. In the present project the same methodology was applied, but extended to higher temperatures, namely up to 300°C. Also many other metal systems were treated.

The report consists of three volumes, namely,

- Volume 1 - Executive Summary
- Volume 2 - Handbook of Diagrams
- Volume 3 - Users Guide to Computer Program - POT-pH-TEMP

Volume 1 presents an overview of the entire report. This volume presents a simplified explanation of the complicated chemistry and mathematics (thermodynamics) needed to develop diagrams for diagnosing or predicting corrosion problems in aqueous systems. Examples are given for the power industry, where the diagrams are used to explain why certain corrosion phenomena have occurred or might occur. These diagrams can readily be used in other industries where corrosion is also a concern.

Volume 2 gives the results of the computer calculations in the form of binary, potential-pH diagrams at 25°, 100°, 200°, 250° and 300°C for 10 elements in water: S, Fe, Ni, Cr, C, B, N, Cu, Ti and Zr. In addition, ternary diagrams are presented for Fe-H_2O from room temperature to 200°C and for Ni-H_2O from room temperature up to 300°C.

A computer program was developed for calculating, at any temperature from 25° to 300°C, the electrode potentials of a variety of compounds as a function of pH. The program delineates and graphs the predominant areas of chemical and ionic species. The free energies of formation of the compounds are from standard literature sources. The partial molar quantities of ionic species in aqueous solutions at room temperature are usually from National Bureau of Standards (NBS) Technical Notes, and those at high temperatures are determined by the Criss-Cobble correspondence principle.

The resulting diagrams consist of lines corresponding to both homogeneous and heterogeneous reactions, where the homogeneous reactions are shown as broken lines and heterogeneous reactions as solid lines. A broken line separates the areas of stability of two ions and expresses the conditions under which the activities of the two dissolved species are equal. A solid line represents equilibrium between two solid species or a solid and a dissolved species. The values assumed for the activities or fugacities of all gaseous, liquid, solid or dissolved species are shown in each diagram title. In each diagram, two additional broken lines are drawn to delineate the conditions for oxygen and hydrogen formation from water for one atmosphere of gas. For each system a discussion of the relevant chemistry is presented.

Volume 3 is a Users Guide for the computer program. The basic principles are presented in the first three sections of this volume. The fourth section gives the steps involved for entering data into the program and running it. The subsequent section gives six specific examples of input and output data to assist in running the program.

Section 1

INTRODUCTION

This volume presents the simple, binary, potential-pH diagrams at 25°, 100°, 200°, 250° and 300°C for 10 elements in water: S, Fe, Ni, Cr, C, B, N, Cu, Ti and Zr. In addition, ternary diagrams are presented for Fe-H_2O from room temperature to 200°C and for Ni-H_2O from room temperature up to 300°C. Volume III presents a description of the computer program and User's Manual, while Volume IV is a list of the source program. Volume I of this report is a summary of the entire project, and it gives a few examples of how potential-pH diagrams can be used to obtain information concerning corrosion problems or water chemistry.

Section 2 of this volume summarizes the results of the diagrams, and Section 3 is an explanation of some of the details of each set of diagrams. Section 4 lists the thermodynamic data and the equilibrium reactions to delineate the diagrams, and Section 5 presents the diagrams.

A computer program was developed for calculating, at any temperature from 25° to 300°C, the electrode potentials of a variety of compounds as a function of pH. The program delineates and graphs the predominant areas of chemical and ionic species. The free energies of formation of the compounds are from standard literature sources. The partial molar quantities of ionic species in aqueous solutions at room temperature are usually from National Bureau of Standards (NBS) technical notes, and those at high temperatures are determined by the Criss-Cobble correspondence principle. For details of the computer program and estimating methods, see Volumes III and IV.

The resulting diagrams consist of lines corresponding to both homogeneous and heterogeneous reactions, where the homogeneous reactions are shown as broken lines and heterogeneous reactions as solid lines. A broken line separates the areas of stability of two ions and expresses the conditions under which the activities of the two dissolved species are equal. A solid line represents equilibrium between two solid species or a solid and a dissolved species. The values assumed for the activities or fugacities of all gaseous, liquid, solid or dissolved species are shown in each diagram title. In each diagram, two additional broken lines are drawn at a hydrogen or oxygen pressure of one atmosphere for the following reactions:

$H_2 = 2H^+ + 2e$ ---------------------- (line a)

$2H_2O = O_2 + 4H^+ + 4e$ ----------------- (line b)

The electrochemical potential of each electrochemical reaction in the diagram is referred to the universal convention, for which the potential of the standard hydrogen reference electrode is assumed to be zero at the temperature of measurements.

A complete discussion of potential-pH diagrams for water systems is given in the book by Pourbaix (1), which provides a careful assessment of the diagrams for all element-water systems at 25°C.

Section 2

RESULTS

S-H_2O SYSTEM

The thermodynamic data used for the diagram of a S-H_2O system are shown in Table 1-a. One solid and/or one liquid species (S), three gaseous species (SO, SO_2 and SO_3) and eleven dissolved species (S^{2-}, HS^-, $S_2O_3{}^{2-}$, $S_2O_4{}^{2-}$, $SO_3{}^{2-}$, $HSO_3{}^-$, $HSO_4{}^-$, H_2SO_3, H_2SO_4 and H_2S) are considered, and the reactions that delineate areas of the diagrams are shown in Table 1-b. The diagrams are shown in Figure 1-a, b, c, d, and e for temperatures of 25°, 100°, 200°, 300° and 250°C, respectively. Each diagram contains two additional broken lines ("a and b") for the hydrogen and oxygen reactions respectively, whose thermodynamic data are shown in Table 1-c.

Fe-H_2O SYSTEM

The thermodynamic data used to construct the diagrams for the Fe-H_2O system are shown in Table 2-a. Four solid species (Fe, FeO, Fe_3O_4 and Fe_2O_3) and six dissolved species (Fe^{2+}, Fe^{3+}, $Fe(OH)^{2+}$, $FeO_4{}^{2-}$ and $HFeO_2{}^-$) are considered, and the reactions that delineate areas of the diagrams are shown in Table 2-b. The resulting diagrams are shown in Figures 2-a, b, c, d and e for temperatures of 25°, 100°, 200°, 300° and 250°C, respectively. The diagrams generally agree well with those published previously (1,2,3,4,5,6). Figures 2-f, g, h and i show those diagrams presented by Townsend (2,3) for temperatures of 25°, 60°, 100° and 200°C. Note that the species of $Fe(OH)^{2+}$ (aq), $Fe(OH)_2{}^+$ (aq) and $FeO_4{}^{2-}$ (aq) were not taken into consideration, and the entropy value of $HFeO_2{}^-$ (aq) was taken as 10 ± 5 e.u. at room temperature.

Fe-S-H_2O SYSTEM

The thermodynamic data used to construct the diagrams for the Fe-S-H_2O system are shown in Tables 1-a and 2-a. For the iron sulfide compounds, four solid species (FeS(α), FeS(β), FeS_2 and $FeSO_4$) are considered, and the reactions that delineate areas of the diagrams are shown in Table 2-b. The diagrams are shown in Figure 3-a, b, c, d and e for temperatures of 25°, 100°, 200°, 300° and 250°C, respectively. The resulting diagrams generally agree with those published by Biernat and

Robins (7) and are shown in Figure 3-f, g, h and i for temperatures of 25°, 100°, 200° and 300°C. For comparison, it should be noted that in Biernat and Robins' paper, the additional species of $Fe(OH)^{2+}$ (aq), $Fe_2(OH)_2^{4+}$ (aq), $Fe(OH)_2$ (c), $Fe(OH)_3$ (c) and FeOOH (c) are considered and that the electrode potential referred to is the "alternate" convention. Furthermore, the activity of all dissolved species in Reference 7 was assumed to be unity.

Fe-Cl^--H_2O SYSTEM

The thermodynamic data used to construct the diagrams for the Fe-Cl^--H_2O system are shown in Table 2-a. For the chloride compounds two solid species ($FeCl_2$ and $FeCl_3$) and two dissolved species (Cl^- and $FeCl^{2+}$) are considered, and the reactions that delineate areas of the diagrams are shown in Table 2-b. The diagrams are shown in Figure 4-a, b, c, d and e for temperatures of 25°, 100°, 200°, 300° and 250°C, respectively.

Ni-H_2O SYSTEM

The thermodynamic data used to construct the diagrams for the Ni-H_2O system are shown in Table 3-a. Five solid species (Ni, NiO, Ni_3O_4, Ni_2O_3 and NiO_2) and two dissolved species (Ni^{2+} and $HNiO_2^-$) are considered, and the reactions that delineate areas of the diagrams are shown in Table 3-b. The diagrams are shown in Figure 5-a, b, c, d and e for temperatures of 25°, 100°, 200°, 300° and 250°C, respectively.

Ni-S-H_2O SYSTEM

The thermodynamic data used to construct the diagrams for the Ni-S-H_2O system are shown in Tables 1-a. and 3-a. For the nickel sulfide compounds, three solid species (NiS, Ni_3S_2 and $NiSO_4$) are considered, and the reactions that delineate areas of the diagrams are shown in Table 3-b. The diagrams are shown in Figure 6-a, b, c, d and e for temperatures of 25°, 100°, 200°, 300° and 250°C, respectively.

Ni-Cl^--H_2O SYSTEM

The thermodynamic data used to construct the diagrams for the Ni-Cl^--H_2O system are shown in Table 3-a. For the chloride compounds, one solid species ($NiCl_2$) and one dissolved species (Cl^-) are considered, and the reactions that delineate areas of the diagrams are shown in Table 3-b. The diagrams are shown in Figure 7-a, b, c, d and e for temperatures of 25°, 100°, 200°, 300° and 250°C, respectively.

Cr-H_2O SYSTEM

The thermodynamic data used to construct the diagrams for the Cr-H_2O system are shown in Table 4-a. Five solid species (Cr, CrO, Cr_2O_3, $Cr(OH)_3$ and CrO_2) and nine dissolved species (Cr^{2+}, Cr^{3+}, CrO_4^{2-}, $Cr_2O_7^{2-}$, CrO_2^-, CrO_3^{3-}, $Cr(OH)^{2+}$, $Cr(OH)_2^+$ and $HCrO_4^-$) are taken into consideration, and the reactions that delineate areas of the diagrams are shown in Table 4-b. The diagrams are shown in Figure 8-a, b, c, d and e for temperatures of 25°, 100°, 200°, 300° and 250°C, respectively.

C-H_2O SYSTEM

The thermodynamic data used to construct the diagrams for the C-H_2O system are shown in Table 5-a. One solid species (C), three gaseous species (CH_4, CO and CO_2) and nine dissolved species (HCO_2^-, $HC_2O_4^-$, $C_2O_4^{2-}$, HCO_3^-, CO_3^{2-}, H_2CO_2, H_2CO_3, CH_3OH and HCHO) are considered, and the reactions that delineate areas of the diagrams are shown in Table 5-b. The diagrams are shown in Figure 9-a, b, c, d and e for temperatures of 25°, 100°, 200°, 300° and 250°C, respectively.

B-H_2O SYSTEM

The thermodynamic data used to construct the diagram for the B-H_2O system are shown in Table 6-a. Three solid species ($B_{10}H_{14}$, B and B_2O_3), two liquid species ($B_{10}H_{14}$ and B_5H_9), 10 gaseous species ($B_{10}H_{14}$, B_5H_9, B_2H_6, BH, BH_2, BH_3, BO, BO_2, B_2O and B_2O_2) and four dissolved species ($H_2BO_3^-$, HBO_3^{2-}, BO_3^{3-} and H_3BO_3 are considered, and the reactions that delineate areas of the diagrams are shown in Table 6-b. The diagrams are shown in Figure 10-a, b, c, d and e for temperatures of 25°, 100°, 200°, 300° and 250°C, respectively. When boron hydrides are not taken into consideration, the diagram is as shown in Figure 10-f for 250°C.

N-H_2O SYSTEM

The thermodynamic data used to construct the diagrams for the N-H_2O system are shown in Table 7-a. One liquid species (N_2H_4), 15 gaseous species (N_2, N_2O, NO, N_2O_3, NO_2, N_2O_4, N_2O_5, NO_3, HNO_3, NH_3, NH, NH_2, HNO_2, N and N_2H_4) and six dissolved species (NH_4^+, NH_4OH, NO_2^-, NO_3^-, HNO_2 and HNO_3) are considered, and the reactions that delineate areas of the diagrams are shown in Table 7-b. The diagrams are shown in Figure 11-a, b, c, d and e for temperatures of 25°, 100°, 200°, 300° and 250°C, respectively.

Cu-H_2O SYSTEM

The thermodynamic data used to construct the diagrams for the Cu-H_2O system are shown in Table 8-a. Four solid species (Cu, Cu_2O, CuO, $Cu(OH)_2$) and four dissolved species (Cu^+, CU^{2+}, $HCuO_2^-$ and CuO_2^{2-}) are considered, and the reactions that delineate areas of the diagrams are shown in Table 8-b. The diagrams are shown in Figure 12-a, b, c, d and e for temperatures of 25°, 100°, 200°, 300° and 250°C, respectively.

Cu-S-H_2O SYSTEM

The thermodynamic data used to construct the diagram for the Cu-S-H_2O system are shown in Tables 1-a and 8-a. For the copper sulfide compounds, 10 solid species (CuS, $Cu_2S(\alpha)$, $Cu_2S(\beta)$, $CuSO_4$, $CuO \cdot CuSO_4$, $CuSO_4 \cdot H_2O$, $CuSO_4 \cdot 3H_2O$, $CuSO_4 \cdot 5H_2O$, $CuSO_4 \cdot 2Cu(OH)_2$, $CuSO_4 \cdot 3Cu(OH)_2$) are considered, and the reactions that delineate areas of the diagrams are shown in Table 8-b. The diagrams are shown in Figure 13-a, b, c, d and e for temperatures of 25°, 100°, 200°, 300° and 250°C, respectively. For comparison, the diagrams published by Kwok and Robins (8) are shown in Figure 13-f, g and h for temperatures of 25°, 100°, 200°C, respectively. Here, it should be noted the unit activity is assumed for all species considered, and the electrode potential is based on the "alternate" convention. The "alternate" convention assumes that the standard hydrogen reference electrode is a function of temperature and is zero only at room temperature (that is, 298°K).

Ti-H_2O SYSTEM

The thermodynamic data used to construct the diagrams for the Ti-H_2O system are shown in Table 9-a. Nine solid species (Ti, TiO, $Ti_2O_3(\alpha)$, $Ti_2O_3(\beta)$, $Ti_3O_5(\alpha)$, $Ti_3O_5(\beta)$, TiO_2(ru.) TiO_2(an.) and TiH_2) and three dissolved species (Ti^{2+}, Ti^{3+} and $HTiO_3^-$) are considered, and the reactions that delineate areas of the diagrams are shown in Table 9-b. The diagrams are shown in Figure 14-a, b, c, d and e for temperatures of 25°, 100°, 200°, 300° and 250°C, respectively. When $TiH_2(c)$ is not taken into consideration, the diagram is as shown in Figure 14-f for 250°C.

Ti-F^--H_2O SYSTEM

The thermodynamic data used to construct the diagrams for the Ti-F^--H_2O system are shown in Table 9-a. For the fluoride compounds, two solid species (TiF_3 and TiF_4), three gaseous species (F_2, TiF_2 and TiF_4) and two dissolved species (F^- and TiF_6^{2-})

are considered, and the reactions that delineate areas of the diagrams are listed in Table 9-b. The diagrams are shown in Figure 15-a, b, c, d and e for temperatures of 25°, 100°, 200°, 300° and 250°C, respectively. When $TiH_2(c)$ is not taken into consideration, the diagram is as shown in Figure 15-f for 250°C.

$Zr-H_2O$ SYSTEM

The thermodynamic data used to construct the diagrams for the $Zr-H_2O$ system are shown in Table 10-a. Three solid species (Zr, $Zr(OH)_4$ and ZrH_2) and three dissolved species (Zr^{4+}, ZrO_2^{2+} and $HZrO_3^-$) are considered, and the reactions that delineate areas of the diagrams are shown in Table 10-b. The diagrams are shown in Figure 16-a, b, c, d and e for temperatures of 25°, 100°, 200°, 300° and 250°C, respectively. When $ZrH_2(c)$ is not taken into consideration, the diagram is as shown in Figure 16-f for 250°C.

TERNARY DIAGRAMS FOR $Fe-H_2O$ AND $Ni-H_2O$ SYSTEMS

The two-dimensional potential-pH diagrams calculated thus far for various temperatures in a certain system can be succinctly summarized in a ternary potential-pH temperature diagram. Figure 17 shows a ternary diagram for a $Fe-H_2O$ system from room temperature to 200°C; Figure 18 shows a ternary diagram for a $Ni-H_2O$ system from room temperature up to 300°C. Although the ternary diagrams seem complicated, trends in the stability regions can be discerned readily after careful examination.

Section 3

DISCUSSION OF DIAGRAMS

SULFUR SYSTEM

Sulfur (Figure 1) has an oxidation number of +2 in sulfides (H_2S, HS^-, S^{2-}) and forms polysulfides, whose average oxidation number is negative (S_2^{2-}, S_3^{2-}, S_4^{2-}). The oxidation number of sulfur oxides (SO, SO_2, SO_3), thiosulfate, dithionite and sulfate ions range from +2 to +6. At room temperature, only H_2S, HS^-, S^{2-}, S(c), HSO_4^- and SO_4^{2-} are stable enough to appear in the diagram. The stability domain of solid sulfur is a narrow triangle that lies within the stability region of water and extends from the acid to the neutral region. H_2S, HS^- and S^{2-} are stable in reducing conditions and can be oxidized to solid sulfur or sulfate ions.

When the temperature is increased, the solid sulfur becomes liquid and the stability area is reduced. Sulfur dioxide and thiosulfate ions become stable at high temperatures: the former in acidic solutions; the latter in near-neutral solutions.

IRON SYSTEMS

Iron and low-alloy steels (Figures 2, 3 and 4) are the primary metals of industrial concern and are very susceptible to corrosion in aqueous solutions. The important oxidation numbers are +2(Fe^{2+}), +3(Fe^{3+}), +4(FeO_3^{2-}) and +6(FeO_4^{2-}). Six dissolved species (Fe^{2+}, Fe^{3+}, $HFeO_2^-$, $FeOH^{2+}$, $Fe(OH)_2^+$ and FeO_4^{2-}) and three solid substances (Fe, Fe_3O_4 and Fe_2O_3) show thermodynamic stability and appear in the diagram.

Iron is considered a base metal since its domain lies in the region where water is unstable. Therefore, iron will corrode to ferrous ions with the evolution of hydrogen in acid solutions. The reaction will be abated when the pH of the solution increases and will almost cease at a pH of about 10, where iron becomes covered with a film of magnetite. In alkaline solutions, with the pH above 14, iron corrodes again to $HFeO_2^-$ ions.

Under oxidizing conditions, magnetite (Fe_3O_4) and hematite (Fe_2O_3) can form on the surface and passivate the iron, except in very low or very high pH solutions, where iron passivation is impossible. When the electrode potential is above the passivation region, iron becomes transpassive and corrodes to FeO_4^{2-}. When the temperature is increased, the corrosion region of $HFeO_2^-$ expands and the passivation region contracts.

In the iron-sulfur system, iron dissolves to ferrous ions in acid solutions and forms iron monosulfide in weak acid, neutral and weak alkaline solutions. In alkaline solutions, iron again dissolves to $HFeO_2^-$ ions. When the electrode potential of iron is increased in the noble direction, the ferrous ion and monosulfide react to form iron disulfide, while the dihypoferrite ion is oxidized to either magnetite or hematite (depending on pH). Further oxidation changes the disulfide to sulfate or bisulfate ions in acid solutions, and to hematite or magnetite in neutral and weak alkaline solutions. Iron monosulfide and disulfide are stable from acid solutions to alkaline solutions, and the stability areas replace most of the Fe_3O_4 area; magnetite (Fe_3O_4) is stable only in a narrow triangular strip in weak alkaline solutions. In strong alkaline solutions, the monosulfide or disulfide are not stable, and Fe_3O_4 is in its usual stability area.

Although the diagrams show that Fe_2O_3 can be formed on the metal surface under strong oxidizing conditions and protect iron from corrosion in neutral solutions, the incompatibility between FeS_2 and Fe_2O_3 prevents growth of an adhesive Fe_2O_3 layer. The Fe_2O_3 outer layer would exfoliate from the FeS_2 sublayer because of the stress and strain at the interface when the oxide grows to a certain thickness. The presence of solid iron sulfides instead of soluble iron in part of the acid corrosion region would suggest that hydrogen sulfide addition to acid solutions might retard corrosion by passivation. Since the iron sulfides are good ionic conductors, however, they offer little protection against corrosion, particularly at high temperatures, where the diffusion coefficient of ions is considerable. When the temperature is increased, the stability area of the $HFeO_2^-$ ion expands and those of the sulfides and oxides contract.

In modern power boilers, chloride ion is the most aggravating agent for acid attack. Chloride ion ingress is often due to condenser leak of sea-water-cooled units. If this occurs, the acidity is increased locally, particularly in crevices and on heat transfer surfaces, and local attack due to wastage or pitting results. In the iron-chloride system, dissolved $FeCl^{2+}$ and solid $FeCl_2$ show thermodynamic stability areas in the diagrams. Both species are stable only in acid solutions: the former is found around the oxygen evolution line; the latter is around the hydrogen evolution line. As the temperature is increased, the stability area of solid $FeCl_2$ expands. Conversely, the area of dissolved $FeCl^{2+}$ contracts and disappears at around 200°C and then reappears in the 250°C diagram. Of course, the reactions that delineate this area are different in the two cases.

NICKEL SYSTEMS

The oxidation number of nickel and its compounds range from 0 to +6. The more important oxidation states are +2 (Ni^{2+}, NiO and $HNiO_2^-$), +3 (Ni_2O_3) and +4 (NiO_2).

Nickel is considered a slightly noble metal, since its stability domain has a small zone in common with the water stability area and thus cannot reduce water. Therefore, it is distinctly more noble than iron, which -- as noted previously -- has no zone of stability in common with that of water. Although this common zone is small in the stability diagram, a nickel electrode will behave as a reversible hydrogen electrode similar to a platinized platinum within a restricted pH range, depending on the temperature (9). Therefore, in some research laboratories, including ours, the more economical nickel electrode is sometimes used as a hydrogen reference electrode instead of the expensive platinum electrode.

Nickel will dissolve to Ni^{2+} ions in acid solutions and becomes covered by insoluble NiO in neutral solutions. In alkaline solutions, nickel dissolves again to $HNiO_2^-$ ions. With oxidizing conditions, Ni^{2+} ion will be oxidized to Ni_3O_4 or Ni_2O_3 in weak acid solutions and to NiO_2 in strong acid solutions. The NiO and $HNiO_2^-$ ion will be oxidized to Ni_3O_4 in neutral and alkaline solutions, respectively.

As the temperature is increased, the stability domain of $HNiO_2^-$ ion expands and the area of stability of the oxides shifts to the more acid side of the diagram.

In the nickel-sulfur system, nickel dissolves to Ni^{2+} ions in acid solutions and forms nickel disulfide in weak acid, neutral, and alkaline solutions. In very strong alkaline solutions, nickel will dissolve as $HNiO_2^-$ ions. When the electrode potential of nickel is raised in the noble direction, Ni_3S_2 dissolves to Ni^{2+} ions in acid solutions and sulfurizes to NiS in weak acid, neutral, and weak alkaline solutions. In stronger alkaline solutions the Ni_3S_2 is oxidized to $HNiO_2^-$ ions.

Upon further oxidation, the monosulfide will be dissolved to Ni^{2+} ions in the acid corrosion region and will be converted to Ni_3S_2 again in the neutral and weak alkaline solutions to produce sulfate ions. The reaction sequence is as follows:

$$3Ni + 2S^{2-} = Ni_3S_2 + 4e$$

$$Ni_3S_2 + S^{2-} = 3NiS + 2e$$

$$3NiS + 4H_2O = Ni_3S_2 + SO_4^{2-} + 8H^+ + 6e$$

The nickel disulfide can then be oxidized to Ni^{2+} ion, NiO or $HNiO_2^-$ ions, depending on the pH of the solution. In the acidic corrosion region, there is a stability area of solid nickel sulfate for the 25°C diagram. When the electrode potential is further enhanced in the noble direction, a nickel electrode will behave as it would in a solution without sulfides and will thus be oxidized to nickel oxides.

The stability area of sulfides replaces a large part of the nickel stability domain. Although the nickel disulfide can be converted to NiO in neutral solutions, passivation cannot be attained because of incompatibility between the oxide and sulfide.

When the temperature is increased, the stability area of the $HNiO_2^-$ ion expands, while those of the sulfides contract. The stability area of the solid sulfate disappears totally from the diagrams at high temperatures.

In the nickel-chloride system, the diagram is the same as that of a solution without chloride ion addition, except that a stability area of solid nickel chloride appears in the acidic corrosion region. This area expands with increasing temperature.

CHROMIUM SYSTEM

The important oxidation states of chromium are +2 (Cr^{2+}, CrO), +3 (Cr^{3+}, Cr_2O_3), +4 (CrO_2) and +6 (CrO_4^{2-}). Chromium is a very base metal, and its stability domain lies considerably below that of the hydrogen evolution line. In acid solutions, chromium dissolves to Cr^{2+} ions, and it tends to become covered with chromic oxide or hydroxide in neutral and weak alkaline solutions. In stronger alkaline solutions, it dissolves to CrO_3^{3-} and CrO_2^- ions. When oxidized, Cr^{2+} ions change to Cr^{3+} ions, which can be further oxidized to $HCrO_4^-$ or $Cr_2O_7^{2-}$ ions in acid solutions; chromic oxide or hydroxide, CrO_2^- and CrO_3^- ions can be oxidized to CrO_4^{2-} ion.

When the temperature is increased, the stability region for chromic oxide or hydroxide contracts, while the stability region for $Cr(OH)_2^+$, CrO_2^- and CrO_3^- ions expands. When the temperature is greater than about 250°C, CrO becomes stable, and chromium will be oxidized to CrO first and then to $Cr(OH)_3$ and/or Cr_2O_3.

CARBON SYSTEM

The oxidation states for carbon range from -4 to +4. The more important oxidation states are -4 (CH_4), -2(CH_3OH), 0 (HCHO), +2 (HCOOH) and +4 (CO_2). At room temperature, only H_2CO_3, $CO_2(g)$, CH_3OH, $CH_4(g)$, HCO_3^-, CO_3^{2-} and C(c) are stable. The stability domain of solid carbon is a narrow strip and lies in the stability region of water, extending from the acid side to the weak alkaline region. Carbon can be reduced to $CH_4(g)$ and CH_3OH and oxidized to CO_2 and/or H_2CO_3 in acid solutions, to HCO_3^- ions in neutral solutions and to CO_3^{2-} ions in alkaline solutions. When the temperature is increased, carbon becomes unstable; at 200°C, the stability area disappears completely from the diagram. Instead, the stability domain for formate ion (HCO_2^-) emerges in alkaline solutions at high temperatures.

BORON SYSTEM

The oxidation number of boron ranges from -3 to +5. The more important oxidation states are -3 (B_2H_6) and +3 (B_2O_3). Boron is a very base element, because its stability area lies considerably below that of water. Actually boron in contact with water is thermodynamically unstable and forms boron hydrides (BH_3 and B_2H_6) if cathodically polarized. In the water stability zone, boron is oxidized to boric oxide (B_2O_3) in acid solutions, to orthoboric acid (H_3BO_3) in neutral solutions, to dihydrogen orthoborate ion ($H_2BO_3^{2-}$) in weak alkaline solutions, to monohydrogen orthoborate ion (HBO_3^-) in stronger alkaline solutions and to orthoborate ion (BO_3^{3-}) in very strong alkaline solutions. When the temperature is increased, the stability areas of B_2O_3 and BO_3^{3-} expand, while that of HBO_3^{2-} contracts. At temperature higher than 150°C, HBO_3^{2-} ion becomes unstable and disappears completely from the diagram.

NITROGEN SYSTEM

Nitrogen forms compounds with all the oxidation states from -3 to 6. The more important oxidation states are -3 (NH_3), -2 (N_2H_4), -1 (NH), 0(N_2), +1 (N_2O), +2 (NO), +3 (HNO_2), +4 (NO_2), +5 (HNO_3) and +6 (NO_3). The stability area of nitrogen extends over most of the stability region of water. Therefore, nitrogen is thermodynamically stable under ordinary conditions in aqueous solutions. However, nitrogen is thermodynamically unstable outside the water stability region. If an aqueous solution is polarized so that hydrogen evolves at the cathode and if nitrogen is bubbled over this cathode, the nitrogen gas can be changed to NH_4^+ ion in acidic and neutral solutions, to $NH_4(OH)$ in weak alkaline solutions and to $NH_3(g)$ in alkaline solutions. On the other hand, if an aqueous solution is polarized so that oxygen evolves at the anode, and if nitrogen is bubbled over this anode, then the nitrogen can be oxidized to HNO_3 in acid solution and to NO_3^- ion in weak acid, neutral and alkaline solutions. At extremely high anodic conditions, the nitric acid and nitrate ion will be oxidized to $NO_3(g)$.

When the temperature is increased, the stability area of NH_4^+ ion contracts, while those of $NH_4(OH)$, $NH_3(g)$ and $NO_3(g)$ expand. When the temperature is beyond 250°C, the stability area for $HNO_3(g)$ appears in the diagrams and expands with increasing temperature.

COPPER SYSTEM

The oxidation states of copper compounds are +1 (Cu^+) and +2 (Cu^{2+}). The existence of the +3 oxidation state is shown by the formation of acid oxide salts (Cu_2O_3). However, these salts and the +3 ion are such powerful oxidizing agents that they are unstable in aqueous solutions.

Copper is a relatively noble metal and is stable in the lower part of the water stability region. Copper will not corrode in deaerated water solutions free from oxidizing agents, because the electrode potential of Cu/Cu^{2+} is more noble than the H_2/H^+ hydrogen electrode. However, aerated solutions can cause copper to corrode in acid solutions and to oxidize in neutral and alkaline solutions.

With oxidizing conditions, copper dissolves to Cu^{2+} ions in acid solutions, oxidizes to Cu_2O in neutral and alkaline solutions and dissolves to CuO_2^{2-} ions in alkaline solutions. When the potential is further increased in the noble direction, Cu_2O will be converted to $Cu(OH)_2$ and/or CuO in neutral and weak alkaline solutions and dissolve to CuO_2^{2-} ions in alkaline solutions. When the temperature is increased, Cu^+ and $HCuO_2^-$ ions become stable and their stability areas expand with further increases in temperature. At high temperatures, copper dissolves to Cu^+ ions, which will then oxidize to Cu^{2+} ions in acid solutions. In weak alkaline solutions, copper is either oxidized to Cu_2O and then to $HCuO_2^-$ ion, or it may be oxidized to $HCuO_2^-$ ion directly.

In the copper-sulfur system, copper is sulfurized to cuprous sulfide (Cu_2S) first and then to cupric sulfide (CuS) in acid and neutral solutions. The sulfur of CuS will be further oxidized to sulfate ion; as a result, it will be converted back to Cu_2S again. With further anodic polarization, hydrated solid copper sulfates precipitate in weak acid solution and $CuSO_4 \cdot 3Cu(OH)_2(c)$ will be formed in neutral solutions. In alkaline solutions, copper is sulfurized to Cu_2S, whose sulfur is then oxidized to sulfate ion. As a result, Cu_2S is converted back to copper again. After these considerations, the polarization behavior behaves the same as that of the copper system. When the temperature is increased, the stability areas of copper sulfates and $CuSO_4 \cdot 3Cu(OH)_2(c)$ contract and disappear completely from the diagrams at high temperatures.

TITANIUM SYSTEM

Titanium forms compounds of the +2, +3 and +4 oxidation states. Titanium is thermodynamically a very active metal and tends to react with water to form titanium hydride in the hydrogen stability region. Titanium hydride dissolves to Ti^{2+} and/or Ti^{3+} ions in strong acid solutions and forms an insoluble passive film (TiO_2) in weak acid, neutral and alkaline solutions. Note that TiO_2 is stable over practically the whole water stability region, and it is this oxide that protects the active metal from corrosion. At high temperatures, the titanium oxide becomes less stable, and a narrow stability region for $HTiO_3^-$ ions at high pH begins to appear in the diagram at 150°C and thereafter expands considerably with increasing temperature.

When titanium hydride is not considered, the stability areas of TiO and Ti_2O_3 appear in the diagram. However, they are stable only in the hydrogen stability region; again, only the TiO_2 oxide is stable in the stability domain of water.

Although titanium is a very corrosion-resistant metal (due to formation of the TiO_2 passive film), it is vulnerable to fluoride ion attack. In the titanium-fluoride system, titanium hydride is fluoridated to $TiF_3(c)$ in acid and neutral solutions and to TiO_2 in neutral and alkaline solutions. Other than these considerations, the behavior is the same as that of the titanium system. When the potential is increased in the anodic direction, $TiF_3(c)$ is converted to TiF_6^{2-} ions or $TiF_4(c)$ in strong acid solutions and to TiO_2 in weak acid and neutral solutions. The aggravating action of fluoride ions can be easily explained by observing that a portion of the passive TiO_2 area in the acid region is replaced by $TiF_3(c)$, which has no corrosion protection. Higher temperatures do not markedly change the diagrams; but the stability area of the fluorides expands gradually.

ZIRCONIUM SYSTEM

The only important oxidation state of zirconium is +4 (ZrO_2). Like titanium, zirconium is a very active metal and tends to react with water to form zirconium hydride in the hydrogen stability region. Zirconium hydride dissolves to Zr^{4+} ions in very strong acids, to ZrO^{2+} ion in weaker acid solutions, to an insoluble oxide film (ZrO_2) in very weak acid, neutral and weak alkaline solution, and corrodes to $HZrO_3^-$ ions in alkaline solutions. When the temperature is increased, the stability area of $HZrO_3^-$ ion expands, and those of $ZrO_2 \cdot 2H_2O(c)$ and ZrO^{2+} ions contract.

Section 4

THERMODYNAMIC DATA AND REACTION EQUILIBRIA

Thermodynamic data and reaction equilibria for the diagrams are listed in this section. Although the computer program can calculate free-energy values continuously from room temperature up to 300°C, the tables present only the entropy value at 25°C and free-energy values at 25°, 100°, 200°, 250° and 300°C. The code number for reaction in the tables refers to the appropriate line number in the diagram.

Table 1-a

FREE-ENERGY VALUES (cal/mole) FOR SULFUR AND ITS COMPOUNDS FROM 25° TO 300°C

Chemical Species	$S^\circ(25)$	$G_f^\circ(25)$	$G^\circ(100)$	$G^\circ(200)$	$G^\circ(250)$	$G^\circ(300)$	References
S(c,rh)	7.62	0	-620	-1,585	-2,120	-2,688	10,11
S(c,mo)	7.78	23	-622	-1,615	-2,163	-2,741	10,11
S(l)	8.444	93	-597	-1,745	-2,391	-3,079	11,12
SO(g)	53.02	-4,741	-8,782	-14,344	-17,189	-20,072	11,13,14
SO_2(g)	59.30	-71,748	-76,281	-82,564	-85,795	-89,080	11,13,14
SO_3(g)	61.34	-88,690	-93,402	-100,005	-103,432	-106,934	11,13,14
S^{2-}(aq)	6.5	20,500	20,518	22,219	23,815	26,237	14,15
HS^-(aq)	20.0	2,880	1,886	2,261	3,194	4,962	14,15
$S_2O_3^{2-}$(aq)	39.0	-127,200	-129,641	-131,461	-131,668	-131,389	10,15
$S_2O_4^{2-}$(aq)	32.0	-143,500	-145,287	-145,863	-145,257	-144,038	14,15
SO_4^{2-}(aq)	14.8	-177,970	-178,148	-175,670	-173,064	-169,537	14,15
SO_3^{2-}(aq)	3.0	-116,300	-115,375	-110,801	-106,824	-101,713	14,15
HSO_3^-(aq)	38.4	-126,150	-129,187	-133,366	-135,670	-138,087	14,15
HSO_4^-(aq)	36.5	-180,690	-183,518	-187,223	-189,191	-191,208	14,15
H_2SO_3(aq)	55.5	-128,560	-133,153	-140,294	-144,523	-149,117	14,16,17,18
H_2SO_4(aq)	4.8	-177,970	-178,688	-180,474	-181,928	-183,680	14,16,17,18
H_2S(aq)	29.0	-6,660	-9,221	-12,222	-13,794	-15,252	7,14,19

Table 1-b

REACTIONS AND THEIR CODE NUMBERS TO DELINEATE DIAGRAM OF S-H_2O SYSTEM

Code Number	Reaction
1	$H_2S(aq) = S(c) + 2H^+ 2e$
2	$S(C,1) + 4H_2O = SO_4^{2-} + 8H^+ + 6e$
3	$HS^- = S(C,1) + H^+ + 2e$
4	$S(C,1) + 4H_2O = HSO_4^- + 7H^+ + 6e$
5	$H_2S + 4H_2O = SO_4^{2-} + 10H^+ + 8e$
6	$H_2S = HS^- + H^+$
7	$H_2S + 4H_2O = HSO_4^- + 9H^+ + 8e$
8	$S^{2-} + 4H_2O + SO_4^{2-} + 8H^+ + 8e$
9	$HS^- = S^{2-} + H^+$
10	$HS^- + 4H_2O = SO_4^{2-} + 9H^+ + 8e$
11	$HSO_4^- = SO_4^{2-} + H^+$
12	$2S(1) + 3H_2O = S_2O_3^{2-} + 6H^+ + 4e$
13	$S_2O_3^{2-} + 5H_2O = 2SO_4^{2-} + 10H^+ + 8e$
14	$S_2O_3^{2-} + 5H_2O = 2HSO_4^- + 8H^+ + 8e$
15	$2HS^- + 3H_2O = S_2O_3^{2-} + 8H^+ + 8e$
16	$2H_2S + 3H_2O = S_2O_3^{-2} + 10H^+ + 8e$
17	$2S^{2-} + 3H_2O = S_2O_3^{2-} + 6H^+ + 8e$
18	$S(1) + 2H_2O = SO_2(g) + 4H^+ 4e$
19	$SO_2(g) + 2H_2O = HSO_4^- + 3H^+ + 2e$

Table 1-c

FREE-ENERGY VALUES (cal/mole) FOR HYDROGEN, OXYGEN AND THEIR COMPOUNDS FROM 25° TO 300°C

Chemical Species	S°(25)	$G°_f(25)$	G°(100)	G°(200)	G°(250)	G°(300)	References
$H_2(g)$	31.208	0	-2,401	-5,761	-7,499	-9,270	13,20
$O_2(g)$	49.003	0	-3,737	-8,888	-11,524	-14,197	13,20
$H_2O(1)$	16.71	-56,687	-58,098	-60,396	-61,694	-63,078	13,20
$H^+(aq)$	-5.0	0	+104	-648	-1,468	-2,539	15,20,21
$OH^-(aq)$	2.43	-37,594	-37,271	-35,170	-33,375	-30,755	15,20,21

Table 2-a

FREE-ENERGY VALUES (cal/mole) FOR IRON SYSTEMS FROM 25° TO 300°C

Chemical Species	$S^\circ(25)$	$G^\circ_f(25)$	$G^\circ(100)$	$G^\circ(200)$	$G^\circ(250)$	$G^\circ(300)$	References
Fe(c)	6.52	0	-542	-1,411	-1,902	-2,427	11,13,20
FeO(c)	13.74	-58.590	-59,730	-61,544	-62,558	-63,634	11,13,20
Fe_3O_4(c)	35.0	-242,700	-245,652	-250,515	-253,308	-256,326	11,13,20
Fe_2O_3(c)	20.89	-177,400	-179,194	-182,233	-184,002	-185,924	11,13,20
Fe^{2+}(aq)	-42.9	-18,850	-16,240	-14,706	-14,827	-15,584	15,20,21
Fe^{3+}(aq)	-90.5	-1,100	4,850	10,078	11,467	11,978	15,20,21
$Fe(OH)^{2+}$(aq)	-44.0	-54,830	-52,143	-50,523	-50,610	-51,337	15,20,21
$Fe(OH)_2{}^{+}$(aq)	-14.5	-104,700	-104,083	-104,752	-105,775	-107,288	15,20,22
$FeO_4{}^{2-}$(aq)	18.2	-111,685	-112,181	-110,307	-108,096	-84,749	2,15,20,23
$HFeO_2{}^{-}$(aq)	15	-90,300	-90,768	-89,100	-87,274	-84,749	2,15,20,23
FeS(c,α)	14.41	-24,000	-25,200	-27,152	-28,269	-29,478	11,13,20
FeS(c,β)	16.4	-23,700	-25,093	-27,338	-28,604	-29,953	11,13,21
FeS_2(c)	12.65	-39,900	-40,983	-42,801	-43,850	-44,983	11,13,20
$FeSO_4$(c)	28.909	-197,176	-199,579	-203,541	-205,846	-208,353	12
Cl^-(aq)	18.5	-31,372	-32,254	-31,731	-30,725	-28,884	15,20,21
$FeCl^{2+}$(aq)	-37.0	-34,400	-32,204	-31,128	-31,436	-32,350	15,20,21
$FeCl_2$(c)	28.19	-72,260	-74,536	-78,007	-29,902	-81,890	13,20
$FeCl_3$(c)	34.0	-79.840	-82,596	-86,854	-89,202	-91,680	13,20

Table 2-b

REACTIONS AND CODE NUMBERS TO DELINEATE DIAGRAM OF Fe-H_2O, Fe-S-H_2O AND Fe-Cl-H_2O SYSTEMS

Code Number	Reaction
1	$Fe^{2+} + 2H_2O = HFeO_2^- + 3H^+$
2	$Fe^{3+} + H_2O = FeOH^{2+} + H^+$
3	$FeOH^{2+} + H_2O = Fe(OH)_2^+ + H^+$
4	$Fe^{2+} = Fe^{3+} + e$
5	$Fe^{2+} + H_2O = FeOH^{2+} + H^+ + e$
6	$Fe^{2+} + 2H_2O = Fe(OH)_2+ + 2H+ + e$
7	$HFeO_2^- + H^+ = Fe(OH)_2^+ + e$
8	$HFeO_2^- + 2H_2O = FeO_4^{2-} + 5H^+ + 4e$
9	$Fe^{3+} + 4H_2O = FeO_4^{2-} + 8H^+ + 3e$
10	$FeOH^{2+} + 3H_2O = FeO_4^{2-} + 7H^+ + 3e$
11	$Fe(OH)_2^+ + 2H_2O = FeO_4^{2-} + 6H^+ + 3e$
12	$Fe(c) + H_2O = FeO(c) + 2H^+ + 2e$
13	$3Fe(c) + 4H_2O = Fe_3O_4(c) + 8H^+ + 8e$
14	$2Fe(c) + 3H_2O = Fe_2O_3(c) + 6H^+ + 6e$
15	$3FeO(c) + H_2O = Fe_3O_4(c) + 2H^+ + 2e$
16	$2FeO(c) + H_2O = Fe_2O_3(c) + 2H^+ + 2e$
17	$2Fe_3O_4(c) + H_2O = 3Fe_2O_3(c) + 2H^+ + 2e$
18	$Fe^{2+} + H_2O = FeO(c) + 2H^+$
19	$FeO(c) + H_2O = HFeO_2^- + H^+$
20	$2Fe^{3+} + 3H_2O = Fe_2O_3(c) + 6H^+$
21	$2FeOH^{2+} + H_2O = Fe_2O_3(c) + 4H^+$
22	$2Fe(OH)_2^+ = Fe_2O_3(c) + H_2O + 2H^+$
23	$Fe(c) = Fe^{2+} + 2e$
24	$Fe(c) + 2H_2O + HFeO_2^- + 3H^+ + 2e$
25	$Fe(c) = Fe^{3+} + 3e$
26	$2Fe^{2+} + 4H_2O = Fe_3O_4(c) + 8H^+ + 2e$
27	$3HFeO_2^- + H^+ = Fe_3O_4(c) + 2H_2O + 2e$
28	$2Fe^{2+} + 3H_2O = Fe_2O_3(c) + 6H^+ + 2e$
29	$2HFeO_2^- = Fe_2O_3(c) + H_2O + 2e$
30	$Fe_2O_3(c) + 5H_2O = 2FeO_4^{2-} + 10H^+ + 6e$
31	$Fe^{2+} + 2H_2S = FeS_2(c) + 4H^+ + 2e$
32	$Fe^{2+} + H_2S = FeS(c) + 2H^+$
33	$Fe(c) + H_2S = FeS(c) + 2H^+ + 2e$

Table 2-b (Contd.)

REACTIONS AND CODE NUMBERS TO DELINEATE DIAGRAM OF $Fe-H_2O$, $Fe-S-H_2O$ AND $Fe-Cl-H_2O$ SYSTEMS

Code Number	Reaction
34	$FeS(c) + H_2S = FeS_2(c) + 2H^+ + 2e$
35	$Fe(c) + HS^- = FeS(c) + H^+ + 2e$
36	$FeS(c) + HS^- = FeS_2(c) + H^+ + 2e$
37	$Fe(c) + S^{2-} = FeS(c) + 2e$
38	$FeS(c) + S^{2-} = FeS_2(c) + 2e$
39	$FeS(c) + 2H_2O = HFeO_2^- + S^{2-} + 3H^+$
40	$3FeS(c) + 4H_2O = Fe_3O_4(c) + 3S^{2-} + 8H^+ 2e$
41	$Fe_3O_4(c) + 6S^{2-} + 8H^+ = 3FeS_2(c) + 4H_2O + 4e$
42	$FeS_2(c) + 8H_2O = Fe^{2+} + 2SO_4^{2-} + 16H^+ + 14e$
43	$2FeS_2(c) + 19H_2O = Fe_2O_3(c) + 4SO_4^{2-} + 38H^+ + 30e$
44	$3FeS_2(c) + 28H_2O = Fe_3o_4(c) + 6SO_4^{2-} + 56H^+ + 44e$
45	$FeS_2(c) = Fe^{2+} + 2S(c\ or\ l) + 2e$
46	$FeS_2(c) + 8H_2O = Fe^{2+} + 2HSO_4^- + 14H^+ + 14e$
47	$2FeS_2(c) + 19H_2O = Fe_2O_3(c) + 4HSO_4^- + 34H^+ + 30e$
48	$3FeS_2(c) + 28H_2O = Fe_3O_4(c) + 6HSO_4^- + 50H^+ 44e$
49	$Fe(c) + 2Cl^- = FeCl_2(c) + 2e$
50	$3FeCl_2(c) + 4H_2O = Fe_3O_4(c) + 6Cl^- + 8H^+ + 2e$
51	$FeCl_2(c) = Fe^{3+} + 2Cl^- + e$
52	$Fe^{2+} + Cl^- = FeCl^{2+} + e$
53	$2FeCl^{2+} + 3H_2O = Fe_2O_3(c) + 2Cl^- + 6H^+$
54	$FeCl^{2+} + 4H_2O = FeO_4^{2-} + Cl^- + 8H^+ + 3e$
55	$FeCl_2(c) + H_2O = Fe(OH)^{2+} + 2Cl^- + H^+ + e$
56	$2FeCl_2(c) + 3H_2O = Fe_2O_3(c) + 4Cl^- + 6H_+ + 2e$
57	$FeCl^{2+} + H_2O = Fe(OH)^{2+} + Cl^- + H^+$

Table 3-a

FREE-ENERGY VALUES (cal/mole) OF NICKEL SYSTEMS FROM 25° TO 300°C

Chemical Species	S°(25)	G_f°(25)	G°(100)	G°(200)	G°(250)	G°(300)	References
$Ni(c)$	7.14	0	-591	-1,534	-2,066	-2,634	11,13,20
$NiO(c)$	9.08	-50,600	-51,376	-52,689	-53,461	-54,310	11,13,20
$Ni_3O_4(c)$	33.5	-170,150	-172,941	-177,482	-180,055	-182,810	1,16,17,18,24
$Ni_2O_3(c)$	22.5	-112,270	-114,151	-117,235	-118,989	-120,871	1,16,17,18,24
$NiO_2(c)$	12.5	-51,420	-52,469	-54,199	-55,185	-56,244	1,16,17,18,24
$Ni^{2+}(aq)$	-40.8	-10,900	-8,438	-7,066	-7,254	-8,067	15,20
$HNiO_2^-(aq)$	15	-83,465	-83,933	-82,265	-80,439	-77,914	1,15,23,25
$NiS(c)$	12.66	-19,000	-20,048	-21,716	-22,650	-23,645	11,13,20
$Ni_3S_2(c)$	32.0	-47,100	-50,465	-56,008	-59,128	-62,442	18,20
$NiSO_4(c)$	22.0	-181,600	-183,541	-186,912	-188,883	-191,023	13,20
$Cl^-(aq)$	18.5	-31,372	-32,254	-31,731	-30,725	-28,884	15,20,21
$NiCl_2(c)$	23.34	-61,918	-63,820	-66,769	-68,395	-70,110	11,13,20

Table 3-b

REACTIONS AND CODE NUMBERS TO DELINEATE DIAGRAM OF $Ni-H_2O$, $Ni-S-H_2O$ AND $Ni-Cl^{-}-H_2O$-SYSTEMS

Code Number	Reaction
1	$Ni(c) = Ni^{2+} + 2e$
2	$Ni^{2+} + H_2O + NiO(c) + 2H^+$
3	$3Ni^{2+} + 4H_2O = Ni_3O_4(c) + 8H^+ 2e$
4	$2Ni^{2+} + 3H_2O = Ni_2O_3(c) + 6H^+ + 2e$
5	$Ni^{2+} + 2H_2O = NiO_2(c) + 4H^+ + 2e$
6	$Ni(c) + H_2O = NiO(c) + 2H^+ 2e$
7	$Ni(c) + 2H_2O = HNiO_2^- + 3H^+ + 2e$
8	$3NiO(c) + H_2O = Ni_3O_4(c) + 2H^+ + 2e$
9	$NiO(c) + H_2O = HNiO_2^- + H^+$
10	$3HNiO_2^- + H^+ = Ni_3O_4(c) + 2H_2O + 2e$
11	$2Ni_3O_4(c) + H_2O = 3Ni_2O_3(c) + 2H^+ + 2e$
12	$Ni_2O_3(c) + H_2O = 2NiO_2(c) + 2H^+ + 2e$
13	$Ni^{2+} + 2H_2O = HNiO_2^- + 3H^+$
14	$2HNiO_2^- = Ni_2O_3(c) + H_2O + 2e$
15	$HNiO_2^- = NiO_2(c) + H^+ + 2e$
16	$Ni_3S_2(c) + 4H^+ = 3Ni^{2+} + 2H_2S + 2e$
17	$3Ni(c) + 2H_2S = Ni_3S_2(c) + 4H^+ + 4e$
18	$Ni_3S_2(c) + H_2S = 3NiS(c) + 2H^+ + 2e$
19	$3Ni(c) + 2HS^- = Ni_3S_2(c) + 2H^+ + 4e$
20	$Ni_3S_2(c) + HS^- = 3NiS(c) + H^+ 2e$
21	$3Ni(c) + 2S^{2-} = Ni_3S_2(c) + 4e$
22	$Ni_3S_2(c) + S^{2-} = 3NiS(c) + 2e$
23	$Ni_3S_2(c) + 6H_2O = 3HNiO_2^- + 2S^{2-} + 9H^+ + 2e$
24	$Ni_3S_2(c) + 8H_2O = 3Ni^{2+} + 2SO_4^{2-} + 16H^+ + 18e$
25	$3NiS(c) + 4H_2O = Ni_3S_2(c) + SO_4^{2-} + 8H^+ + 6e$
26	$Ni_3S_2(c) + 11H_2O = 3NiO(c) + 2SO_4^{2-} + 22H^+ + 28e$
27	$Ni_3S_2(c) + 14H_2O = 3HNiO_2^- + 2SO_4^{2-} + 25H^+ + 18e$
28	$Ni^{2+} + H_2S = NiS(c) + 2H^+$
29	$NiS(c) = Ni^{2+} + S(c) + 2e$
	$NiS(c) = Ni^{2+} + S(l) + 2e$
30	$NiS(c) + 4H_2O = Ni^{2+} + SO_4^{2-} + 8H^+ 8e$
31	$3NiSO_4(c) + 4H_2O = Ni_3O_4(c) + 3SO_4^{2-} + 8H^+ + 2e$

Table 3-b (Contd.)

REACTIONS AND CODE NUMBERS TO DELINEATE DIAGRAM OF Ni-H_2O, Ni-S-H_2O AND Ni-Cl^--H_2O-SYSTEMS

Code Number	Reaction
32	$NiSO_4(c) + H_2O = NiO(c) + SO_4^{2-} + 2H^+$
33	$NiS(c) + 4H_2O = NiSO_4(c) + 8H^+ + 8e$
34	$Ni_3S_2(c) + 8H_2O + SO_4^{2-} = 3NiSO_4(c) + 16H^+ + 18e$
35	$6NiS(c) + 3H_2O = 2Ni_3S_2(c) + S_2O_3^{2-} + 6H^+ + 4e$
36	$NiS(c) + 4H_2O = Ni^{2+} + HSO_4^- + 7H^+ + 8e$
37	$Ni_3S_2(c) + 8H_2O = 3Ni^{2+} + 2HSO_4^- + 14H^+ + 18e$
38	$Ni_3S_2(c) + 11H_2O = 3NiO(c) + 2HSO_4^- + 20H^+ + 18e$
39	$3NiS(c) + 4H_2O = Ni_3S_2(c) + HSO_4^- + 7H^+ + 6e$
40	$Ni(c) + 2Cl^- = NiCl_2(c) + 2e$
41	$NiCl_2(c) + H_2O = NiO(c) + 2Cl^- + 2H^+$
42	$3NiCl_2(c) + 4H_2O = Ni_3O_4(c) + 6Cl^- + 8H^+ + 2e$
43	$2NiCl_2(c) + 3H_2O = Ni_2O_3(c) + 4Cl^- + 6H^+ + 2e$
44	$NiCl_2(c) + 2H_2O = NiO_2(c) + 2Cl^- + 4H^+ + 2e$

Table 4-a

FREE-ENERGY VALUES (cal/mole) OF CHROMIUM AND ITS COMPOUNDS

Chemical Species	S°(25)	G_f°(25)	G°(100)	G°(200)	G°(250)	G°(300)	References
Cr(c)	5.68	0	-476	-1,252	-1,694	-2,168	11,13,20
CrO(c)	10.7	-83,810	-84,689	-86,091	-86,875	-87,711	1,16,17,18,24
Cr_2O_3(c)	19.4	-252,900	-254,579	-257,434	-259,090	-260,882	11,13,20
$Cr(OH)_3$(c)	19.2	-215,300	-216,957	-219,820	-221,482	-223,28	1,16,17,18,24
CrO_2(c)	12.2	-129,000	-130,076	-132,005	-133,146	-134,39	1,16,17,18,24
Cr^{2+}(aq)	-28.9	-42,100	-40,473	-40,025	-40,590	-41,720	1,15,24,26
Cr^{3+}(aq)	-88.5	-51,500	-45,690	-40,617	-39,292	-38,835	1,15,24
CrO_4^{2-}(aq)	22.0	-173,960	-174,811	-173,612	-171,843	-169,282	15,20
$Cr_2O_7^{2-}$(aq)	72.6	-311,000	-316,583	-324,369	-328,483	-332,712	15,20
CrO_2^-(aq)	28.04	-128,090	-129,506	-129,379	-128,313	-126,563	1,15,23,24
CrO_3^{3-}(aq)	-41.94	-144,220	-139,092	-126,538	-117,336	-106,195	1,15,23
$Cr(OH)^{2+}$(aq)	-26.4	-103,000	-101,548	-101,294	-101,939	-103,135	1,15,24
$Cr(OH)_2^+$(aq)	-12.13	-151,210	-150,759	-151,613	-152,710	-154,287	1,15,27,28
$HCrO_4^-$(aq)	49.0	-182,800	-187,000	-193,828	-198,003	-202,659	15,20,21

Table 4-b

REACTIONS AND CODE NUMBERS TO DELINEATE DIAGRAM OF $Cr-H_2O$ SYSTEM

Code Number	Reaction
1	$Cr^{2+} = Cr^{3+} + e$
2	$Cr^{2+} + 3H_2O = Cr(OH)_3$
3	$Cr(c) = Cr^{2+} + 2e$
4	$2Cr^{3+} + 7H_2O = Cr_2O_7^{2-} + 14H^+ + 6e$
5	$Cr^{3+} + 3H_2O = Cr(OH)_3(c) + 3H^+$
6	$Cr(OH)_3(c) + H_2O = CrO_4^{2-} + 5H^+ + 3e$
7	$CrO_3^{3-} + H_2O = CrO_4^{2-} + 2H^+ + 3e$
8	$Cr_2O_7^{2-} + H_2O = 2CrO_4^{2-} + 2H^+$
9	$2Cr(OH)_3(c) + H_2O = CrO_7^{2-} + 8H^+ + 6e$
10	$Cr(c) + 3H_2O = CrO_3^{3-} + 6H^+ + 3e$
11	$Cr(OH)_3(c) = CrO_3^{3-} + 3H^+$
12	$Cr^{3+} + 4H_2O = HCrO_4^- + 7H^+ + 3e$
13	$HCrO_4^- = CrO_4^{2-} + H^+$
14	$Cr(c) + 3H_2O = Cr(OH)_3(c) + 3H^+ + 3e$
15	$Cr_2O_3(c) + 5H_2O = 2CrO_4^{2-} + 10H^+ + 6e$
16	$2Cr^{2+} + 3H_2O = Cr_2O_3(c) + 6H^+ + 2e$
17	$2Cr(c) + 3H_2O = Cr_2O_3(c) + 6H^+ + 6e$
18	$2Cr(OH)^{2+} + H_2O = Cr_2O_3(c) + 4H^+$
19	$Cr_2O_3(c) + 3H_2O = 2CrO_3^- + 6H^+$
20	$Cr^{3+} + H_2O = Cr(OH)^{2+} + H^+$
21	$2Cr(OH)^{2+} + 5H_2O = Cr_2O_7^{-2} + 12H^+ + 6e$
22	$Cr(OH)^{2+} + 3H_2O = CrO_4^{2-} + 7H^+ + 3e$
23	$Cr(OH)^{2+} + H_2O = Cr(OH)_2^+ + H^+$
24	$Cr^{2+} + H_2O = Cr(OH)^{2+} + H^+ + e$
25	$Cr(OH)_2^+ + 2H_2O = CrO_4^{2-} + 6H^+ + 3e$
26	$Cr^{2+} + 2H_2O = Cr(OH)_2^+ + 2H^+ + e$
27	$Cr(OH)_2^+ = CrO_2^- + 2H^+$
28	$Cr^{2+} + 2H_2O = CrO_2^- + 4H^+ + e$
29	$Cr^{2+} + 3H_2O = CrO_3^{3-} + 6H^+ + e$
30	$CrO_2^- + 2H_2O = CrO_4^{2-} + 4H^+ + 3e$
31	$CrO_2^- + H_2O = CrO_3^{3-} + 2H^+$
32	$Cr(OH)^{2+} +2H_2O = Cr(OH)_3(c) + 2H^+$
33	$Cr_2O_3(c) + H_2O = 2CrO_2^- + 2H^+$

Table 4-b (Contd.)

REACTIONS AND CODE NUMBERS TO DELINEATE DIAGRAM OF $Cr-H_2O$ SYSTEM

Code Number	Reaction
34	$Cr(OH)_3(c) = CrO_2^- + H_2O + H^+$
35	$Cr + 2H_2O = CrO_2^- + 4H^+ + 3e$
36	$Cr(OH)^{2+} + 3H_2O = HCrO_4^- + 6H^+ + 3e$
37	$2Cr_2O_3(c) + 8H_2O = 2Cr_2O_7^{2-} + 16H^+ + 12e$
38	$2Cr(OH)_2^+ + 3H_2O = Cr_2O_7^{2-} + 10H^+ + 6e$
39	$Cr^{2+} + H_2O = CrO(c) + 2H^+$
40	$CrO(c) + H_2O = CrO_2^- + 2H^+ + e$
41	$Cr(c) + H_2O = CrO(c) + 2H^+ + 2e$
42	$2CrO(c) + H_2O = Cr_2O_3(c) + 2H^+ + 2e$
43	$CrO(c) + 2H_2O = Cr(OH)_3(c) + H^+ + e$
44	$2CrO_2^- + 3H_2O = Cr_2O_7^{-2} + 6H^+ + 6e$

Table 5-a

FREE-ENERGY VALUES (cal/mole) FOR CARBON AND ITS COMPOUNDS FROM 25° TO 300°C

Chemical Species	$S°(25)$	$G_f°(25)$	$G°(100)$	$G°(200)$	$G°(250)$	$G°(300)$	References
C(c)	1.372	0	-123	-348	-488	-644	13,14
CH_4(g)	44.492	-12,130	-15,545	-20,320	-22,796	-25,326	11,13,14
CO(g)	47.219	-32,780	-36,383	-41,350	-43,893	-46,470	11,13,14
CO_2(g)	51.06	-94,254	-98,164	-103,607	-106,416	-109,276	11,13,14
HCO_2^-(aq)	27.0	-83,900	-85,685	-87,016	-87,307	-87,318	14,15,21
$HC_2O_4^-$(aq)	40.7	-166,930	-170,219	-174,973	-177,683	-180,586	14,15,21
$C_2O_4^{2-}$(aq)	20.9	-161,100	-161,849	-160,454	-158,557	-155,849	14,15,21
HCO_3^-(aq)	26.8	-140,260	-142,023	-143,304	-143,560	-143,528	14,15,21
CO_3^{2-}(aq)	-3.6	-126,170	-124,627	-118,882	-114,137	-108,141	14,15,21
H_2CO_2(aq)	39.0	-89,000	-91,958	-95,741	-97,703	-99,634	14,16,17,18
H_2CO_3(aq)	44.8	-148,940	-152,327	-156,660	-158,887	-161,075	14,16,17,18
CH_3OH(aq)	31.8	-41,920	-44,481	-48,375	-50,502	-52,736	14,16,17,18
HCHO(aq)	40.1	-31,000	-34,174	-38,719	-41,113	-43,582	1,14,16,17,18,24

Table 5-b

REACTIONS AND CODE NUMBERS TO DELINEATE DIAGRAM OF C-H_2O SYSTEM

Code Number	Reaction
1	$CH_4(g) = C(c) + 4H^+ + 4e$
2	$C(c) + 2H_2O = CO_2(g) + 4H^+ + 4e$
3	$C(c) + 3H_2O = HCO_3^- + 5H^+ + 4e$
4	$C(c) + 3H_2O = CO_3^{2-} + 6H^+ + 4e$
5	$CH_4(g) + 3H_2O = CO_3^{2-} + 10H^+ + 8e$
6	$CO_2(g) + H_2O = HCO_3^- + H^+$
7	$HCO_3^- = CO_3^{2-} + H^+$
8	$C(c) + 3H_2O = H_2CO_3 + 4H^+ + 4e$
9	$H_2CO_3 = HCO_3^- + H^+$
10	$CH_3OH + 2H_2O = HCO_3^- + 7H^+ + 6e$
11	$CH_3OH + 2H_2O = CO_3^{2-} + 8H^+ + 6e$
12	$CH_3OH + 2H_2O = H_2CO_3 + 6H^+ + 6e$
13	$CH_4(g) + 3H_2O = HCO_3^- + 9H^+ + 8e$
14	$CH_4(g) + 2H_2O = CO_2(g) + 8H^+ + 8e$
15	$HCO_2^- + H_2O = HCO_3^- + 2H^+ + 2e$
16	$HCO_2^- + H_2O = CO_3^{2-} + 3H^+ + 2e$
17	$CH_3OH + H_2O = HCO_2^- + 5H^+ + 4e$

Table 6-a

FREE-ENERGY VALUES (cal/mole) FOR BORON AND ITS COMPOUNDS FROM 25° TO 300°C

Chemical Species	S°(25)	G_f°(25)	G°(100)	G°(200)	G°(250)	G°(300)	References
$B_{10}H_{14}(c)$	42.20	49,834	46,164	39,622	35,610	31,089	12
$B_{10}H_{14}(c)$	56.299	50,830	46,146	38,152	33,492	28,423	12
$B_{10}H_{14}(g)$	84.147	55,527	48,440	38,483	32,960	27,074	12
$B_5H_9(l)$	44.056	41,067	37,436	31,611	28,272	24,639	12,14
$B_5H_9(g)$	65.803	41,843	36,689	29,140	25,075	20,819	12,14
$B_2H_6(g)$	55.45	20,700	16,414	10,308	7,094	3,777	11,12,14
BH(g)	41.047	98,632	95,493	91,146	88,914	86,649	12,14
$BH_2(g)$	43.045	44,889	41,588	36,983	34,604	32,178	12
$BH_3(g)$	44.880	26,494	23,051	18,249	15,768	13,238	12
B(c)	1.40	0	-132	-392	-558	-745	11,13,14,21
$B_2O_3(c)$	12.9	-285,300	-286,407	-288,295	-289,404	-290,615	13,14,21
BO(g)	48.60	-6,678	-10,474	-15,582	-18,195	-20,844	12,14
$BO_2(g)$	54.90	-69,339	-73,549	-79,421	-82,454	-85,546	12,14
$B_2O(g)$	54.405	14,921	10,759	4,984	2,011	-1,012	12
$B_2O_2(g)$	57.958	-110,833	-115,303	-121,604	-125,882	-128,238	12,14
$H_2BO_3^-(aq)$	12.3	-217,600	-217,772	-215,429	-213,126	-210,032	1,10,15,21,24
$HBO_3^{2-}(aq)$	-13.46	-200,290	-197,634	-188,854	-182,004	-173,470	1,15,23
$BO_3^{3-}(aq)$	-41.94	-181.489	-176,352	-163,798	-154,596	-143,455	1,15,23
$H_3BO_3(aq)$	38.8	-231,560	-233,994	-235,554	-235,646	-235,197	1,14,15,17,18,24

Table 6-b

REACTIONS AND CODE NUMBERS TO DELINEATE DIAGRAM OF B-H_2O SYSTEM

Code Number	Reaction
1	$B_2H_6(g) + 6H_2O = 2H_3BO_3 + 12H^+ + 12e$
2	$B_2H_6(g) + 6H_2O = 2H_2BO_3^- + 14H^+ + 12e$
3	$B_2H_6(g) + 6H_2O = 2HBO_3^{2-} + 16H^+ + 12e$
4	$B_2H_6(g) + 6H_2O = 2BO_3^{3-} + 18H^+ + 12e$
5	$BH_3(g) + 3H_2O = H_3BO_3 + 6H^+ + 6e$
6	$BH_3(g) + 3H_2O = H_2BO_3^- + 7H^+ + 6e$
7	$BH_3(g) + 3H_2O = HBO_3^{2-} + 8H^+ + 6e$
8	$BH_3(g) + 3H_2O = BO_3^{3-} + 9H^+ + 6e$
9	$2B_2H_6(g) + 6H_2O = 2B_2O_3(c) + 24H^+ + 24e$
10	$B_2O_3(c) + 3H_2O = 2H_2BO_3^- + 2H^+$
11	$H_3BO_3 = H_2BO_3^- + H^+$
12	$H_2BO_3^- = HBO_3^{2-} + H^+$
13	$HBO_3^{2-} = BO_3^{-3} + H^+$
14	$H_2BO_3^- = BO_3^{3-} + 2H^+$
15	$2BH_3(g) + 3H_2O = B_2O_3(c) + 12H^+ + 12e$
16	$B(c) + 3H_2O = H_3BO_3 + 3H^+ + 3e$
17	$2B(c) + 3H_2O = B_2O_3(c) + 6H^+ + 6e$
18	$B(c) + 3H_2O = H_2BO_3^- + 4H^+ + 3e$

Table 7-a

FREE-ENERGY VALUES (cal/mole) FOR NITROGEN AND ITS COMPOUNDS

Chemical Species	$S^\circ(25)$	$G_f^\circ(25)$	$G^\circ(100)$	$G^\circ(200)$	$G^\circ(250)$	$G^\circ(300)$	References
$N_2(g)$	45.77	0	-3,494	-8,315	-10,785	-13,289	11,13,14
$N_2O(g)$	52.52	24,900	20,877	15,277	12,387	9,443	11,13,14
$NO(g)$	50.347	20,690	16,851	11,564	8,860	6,120	11,13,14
$N_2O_3(g)$	73.915	33,324	27,640	19,667	15,531	11,305	12,14
$NO_2(g)$	57.35	12,260	7,879	1,812	-1,307	-4,476	11,14
$N_2O_4(g)$	72.70	23,380	17,756	9,769	5,589	1,296	11,14
$N_2O_5(g)$	82.801	28,186	21,767	12,612	7,806	2,859	12,14
$NO_3(g)$	60.352	27,745	23,116	16,645	13,292	9,866	12
$HNO_3(g)$	63.663	-17,690	-22,581	-29,441	-33,004	-36,649	12
$NH_3(g)$	45.97	-3,940	-7,464	-12,373	-14,907	-17,489	11,14
$NH(g)$	43.295	79,567	76,259	71,687	69,344	66,966	12
$NH_2(g)$	46.488	42,337	38,780	33,848	31,313	28,737	12
$HNO_2(g)$	59.586	-10,020	-14,587	-20,953	-24,242	-27,596	12
$N(g)$	36.614	108,870	106,081	102,246	100,288	98,306	12
$N_2H_4(l)$	29.050	35,694	33,305	29,536	27,430	25,190	12
$N_2H_4(g)$	56.030	38,042	33,652	27,472	24,250	20,947	12
$NH_4^+(aq)$	22.10	-18,970	-20,922	-24,431	-26,614	-29,102	14,15,21
$NH_4OH(aq)$	43.30	-63.040	-66,518	-71,787	-74,650	-77,647	14,16,17,18
$NO_2^-(aq)$	38.5	-8,900	-11,295	-13,025	-13,174	-12,828	14,15,21
$NO_3^-(aq)$	40.0	-26,610	-29,145	-31,142	-31,465	-31,320	14,15,21
$HNO_2(aq)$	36.5	-13,300	-15,703	-18,336	-19,380	-20,179	14,16,17,18
$HNO_3(aq)$	35.0	-26,610	-29,040	-31,790	-32,934	-33,859	14,29

Table 7-b

REACTIONS AND CODE NUMBERS TO DELINEATE DIAGRAM OF N-H_2O SYSTEM

Code Number	Reaction
1	$NH_4^+ + H_2O = NH_4(OH) + H^+$
2	$NH_4^+ + 2H_2O = NO_2^- + 8H^+ + 6e$
3	$NH_4^+ + 2H_2O = HNO_2(aq) + 7H^+ + 6e$
4	$HNO_2(aq) + H_2O = HNO_3(aq) + 2H^+ + 2e$
5	$HNO_2(aq) + H_2O = NO_3^- + 3H^+ + 2e$
6	$HNO_2(aq) = NO_2^- + H^+$
7	$NH_4OH + H_2O = NO_2^- + 7H^+ + 6e$
8	$NO_2^- + H_2O = NO_3^- + 2H^+ + 2e$
9	$HNO_3(aq) = NO_3^- + H^+$
10	$2NH_4^+ = N_2(g) + 8H^+ + 6e$
11	$2NH_4(OH) = N_2(g) + 6H^+ + 2H_2O + 6e$
12	$N2(g) + 6H_2O = 2HNO_3(aq) + 10H^+ + 10e$
13	$N_2(g) + 6H_2O = 2NO_3^- + 12H^+ + 10e$
14	$2NH_4^+ + H_2O = N_2O(g) + 10H^+ + 8e$
15	$2NH_4(OH) = N_2O(g) + H_2O + 8H^+ + 8e$
16	$N_2O(g) + 5H_2O = 2HNO_3(g) + 8H^+ + 8e$
17	$N_2O(g) + 5H_2O = 2NO_3^- + 10H^+ + 8e$
18	$NH_4^+ + H_2O = NO(g) + 6H^+ + 5e$
19	$NO(g) + 2H_2O = HNO_3(aq) + 3H^+ + 3e$
20	$NO(g) + 2H_2O = NO_3^- + 4H^+ + 3e$
21	$NO(g) + H_2O = NO_2^- + 2H^+ + e$
22	$2NH_3(g) = N_2(g) + 6H^+ + 6e$
23	$NH_4^+ = NH_3(g) + H^+$
24	$HNO_3(aq) = NO_3(g) + H^+ + e$
25	$NO_3^- = NO_3(g) + e$
26	$N_2O(g) + 3H_2O = 2NO_2^- + 6H^+ + 4e$
27	$NH_4(OH) = NO(g) + 5H^+ + 5e$
28	$N_2(g) + 6H_2O = 2HNO_3(g) + 10H^+ 10e$
29	$HNO_3(g) = NO_3(g) + H^+ + e$
30	$HNO_3(g) = NO_3^- + H^+$

Table 8-a

FREE-ENERGY VALUES (cal/mole) FOR COPPER SYSTEMS FROM 25° TO 300°C

Chemical Species	S°(25)	G_f°(25)	G°(100)	G°(200)	G°(250)	G°(300)	References
Cu(C)	7.923	0	-646	-1,645	-2,195	-2,774	11,13,20,21
$Cu_2O(c)$	22.26	-34,900	-36,716	-39,531	-41,083	-42,721	11,13,20,21
CuO(c)	10.19	-31,000	-31,859	-33,260	-34,055	-34,907	11,13,20,21
$Cu(OH)_2(c)$	25.90	-89,088	-91,231	-94,634	-96,536	-98,558	12
$Cu^+(aq)$	4.7	11,950	11,220	9,060	7,429	5,404	15,20,21
$Cu^{2+}(aq)$	-33.8	15,660	17,631	18,460	18,050	17,050	15,20,21,24
$HCuO_2^-(aq)$	15	-61,800	-62,268	-60,600	-58,774	-56,249	15,20,23,24
$CuO_2^{2-}(aq)$	-13.46	-43,900	-41,435	-33,939	-28,048	-20,729	15,20,23,24
CuS(c)	15.9	-12,800	-14,093	-16,084	-17,177	-18,328	11,13,20,21
$Cu_2S(c,\alpha)$	28.9	-20,600	-22,938	-26,506	-28,451	-30,489	11,13,20,21
$Cu_2S(c,\beta)$	32.0	-20,250	-22,853	-26,862	-29,058	-31,365	11,13,2
$CuSO_4(c)$	26.0	-158,200	-160,360	-163,830	-165,783	-167,870	11,13,20,21
$CuO \cdot CuSO_4(c)$	37.6	-189,390	-192,515	-197,546	-200,392	-203,437	12,13,21
$CuSO_4 \cdot H_2O(c)$	34.9	-219,460	-222,356	-226,991	-229,597	-232,376	16,17,18,20,21
$CuSO_4 \cdot 3H_2O(c)$	52.9	-334,650	-339,052	-346,109	-350,077	-354,306	16,17,18,20,21
$CuSO_4 \cdot 5H_2O(c)$	71.8	-449,344	-455,320	-646,893	-470,269	-475,995	16,17,18,20,21
$CuSO_4 \cdot 2Cu(OH)_2(c)$	63.9	-345,800	-351,165	-359,884	-364,320	-370,098	16,17,18,21,30
$CuSO_4 \cdot 3Cu(OH)_2(c)$	84.1	-435,500	-442,556	-453,999	-460,466	-467,374	16,17,18,21,30

Table 8-b

REACTIONS AND CODE NUMBER TO DELINEATE DIAGRAM OF $Cu-H_2O$ AND $Cu-S-H_2O$ SYSTEMS

Code Number	Reaction
1	$Cu(c) = Cu^{2+} + 2e$
2	$2Cu(c) + H_2O = Cu_2O(c) + 2H^+ + 2e$
3	$Cu(c) + 2H_2O = CuO_2^{2-} + 4H^+ + 2e$
4	$Cu_2O(c) + 2H^+ = 2cu^{2+} + H_2O + 2e$
5	$Cu_2O(c) + 3H_2O = 2Cu(OH)_2(c) + 2H^+ + 2e$
6	$Cu_2O(c) + 3H_2O = 2CuO_2^{2-} + 6H^+ + 2e$
7	$Cu^{2+} + 2H_2O = Cu(OH)_2(c) + 2H^+$
8	$Cu(OH)_2(c) = CuO_2^{2-} + 2H^+$
9	$Cu_2O(c) + H_2O = 2CuO(c) + 2H^+ + 2e$
10	$Cu^{2+} + H_2O = CuO(c) + 2H^+$
11	$CuO(c) + H_2O = CuO_2^{2-} + 2H^+$
12	$Cu^+ = Cu^{2+} + e$
13	$Cu^+ + 2H_2O = HCuO_2^- + 3H^+ + e$
14	$Cu^+ + 2H_2O = CuO_2^{2-} + 4H^+ + e$
15	$Cu^{2+} + 2H_2O = HCuO_2^- + 3H^+$
16	$HCuO_2^- = CuO_2^{2-} + H^+$
17	$Cu(c) = Cu^+ + e$
18	$2Cu^+ + H_2O = Cu_2O(c) + 2H^+$
19	$Cu_2O(c) + 3H_2O = 2HCuO_2^- + 4H^+ + 2e$
20	$CuO(c) + H_2O = HCuO_2^- + H^+$
21	$Cu(OH)_2(c) = HCuO_2^- + H^+$
22	$Cu^+ + 2H_2O = Cu(OH)_2(c) + 2H^+ + e$
23	$Cu(c) + 2H_2O = HCuO_2^- + 3H^+ + 2e$
24	$Cu^+ + H_2O = CuO(c) + 2H^+ + e$
25	$2Cu(c) + H_2S = Cu_2S(c) + 2H^+ + 2e$
26	$2Cu(c) + HS^- = Cu_2S(c) + H^+ + 2e$
27	$2Cu(c) + S^{2-} = Cu_2S(c) + 2e$
28	$Cu_2S(c) + H_2S = 2CuS(c) + 2H^+ + 2e$
29	$CuS(c) + HS^- = 2CuS(c) + H^+ + 2e$
30	$2CuS(c) + 4H_2O = Cu_2S(c) + SO_4^{2-} + 8H^+ + 6e$
31	$2CuS(c) + 4H_2O = Cu_2S(c) + HSO_4^- + 7H^+ + 6e$
32	$CuS(c) + 4H_2O = cu^{2+} + HSO_4^- + 7H^+ + 8e$

Table 8-b (Contd.)

REACTIONS AND CODE NUMBER TO DELINEATE DIAGRAM OF Cu-H_2O AND Cu-S-H_2O SYSTEMS

Code Number	Reaction
33	$CuS(c) = Cu^{2+} + S(c \text{ or } l) + 2e$
34	$Cu_2S(c) + 4H_2O = 2Cu^{2+} + HSO_4^- + 7H^+ + 10e$
35	$Cu_2S(c) + 4H_2O = 2Cu^{2+} + SO_4^{2-} + 8H^+ + 10e$
36	$Cu_2S(c) + 4H_2O = 2Cu(c) + SO_4^{2-} + 8H^+ + 6e$
37	$4Cu_2O(c) + 8H_2O + 2SO_4^{2-} = 2CuSO_4 \cdot 3Cu(OH)_2(c) + 4H^+ + 8e$
38	$4Cu^{2+} + 6H_2O + SO_4^{2-} = CuSO_4 \cdot 3Cu(OH)_2(c) + 6H^+$
39	$CuSO_4 \cdot 3Cu(OH)_2(c) = 4CuO(c) + SO_4^{2-} + 2H_2O + 2H^+$
40	$4CuSO_4 \cdot H_2O(c) + 2H_2O = CuSO_4 \cdot 3Cu(OH)_2(c) + 3SO_4^{2-} + 6H^+$
41	$Cu_2O(c) + H_2O + 2SO_4^{2-} + 2H^+ = 2CuSO_4 \cdot H_2O(c) + 2e$
42	$4CuSO_4 \cdot 3H_2O(c) = CuSO_4 \cdot 3Cu(OH)_2(c) + 3SO_4^{2-} + 6H_2O + 6H^+$
43	$Cu_2O(c) + 5H_2O + 2SO_4^{2-} + 2H^+ = 2CuSO_4 \cdot 3H_2O(c) + 2e$
44	$Cu(c) + 3H_2O + SO_4^{2-} = CuSO_4 \cdot 3H_2O(c) + 2e$
45	$Cu_2S(c) + 10H_2O + SO_4^{2-} = 2CuSO_4 \cdot 3H_2O(c) + 8H^+ + 10e$
46	$4CuSO_4 \cdot 5H_2O(c) = CuSO_4 \cdot 3Cu(OH)_2(c) + 3SO_4^{2-} + 14H_2O + 6H^+$
47	$Cu_2O(c) + 9H_2O + 2SO_4^{2-} + 2H^+ = 2CuSO_4 \cdot 5H_2O(c) + 2e$
48	$Cu(c) + 5H_2O + SO_4^{2-} = CuSO_4 \cdot 5H_2O(c) + 2e$
49	$Cu_2S(c) + 14H_2O + SO_4^{2-} = 2CuSO_4 \cdot 5H_2O(c) + 8H^+ + 10e$
50	$Cu_2S(c) + 4H_2O = 2Cu^+ + SO_4^{2-} + 8H^+ + 8e$
51	$Cu^+ + H_2O + SO_4^{2-} = CuSO_4 \cdot H_2O(c) + e$
52	$Cu^+ + 3H_2O + SO_4^{2-} = CuSO_4 \cdot 3H_2O(c) + e$
53	$Cu^+ + 5H_2O + SO_4^{2-} = CuSO_4 \cdot 5H_2O(c) + e$
54	$Cu_2S(c) + 4H_2O = 2Cu^+ + HSO_4^- + 7H^+ + 8e$
55	$Cu_2S(c) + 2H^+ = 2Cu^{2+} + H_2S + 2e$
56	$Cu^{2+} + H_2S = CuS(c) + 2H^+$
57	$Cu_2S(c) + 4H_2O = 2Cu(c) + HSO_4^- + 7H^+ + 6e$
58	$2Cu^+ + H_2S = Cu_2S(c) + 2H^+$
59	$Cu_2S(c) + S^{2-} = 2CuS(c) + 2e$
60	$Cu^+ + H_2S = CuS(c) + 2H^+ + 2e$
61	$CuS(c) = Cu^+ + S(c \text{ or } l) + e$

Table 9-a

FREE-ENERGY (cal/mole) VALUES OF TITANIUM AND ITS COMPOUNDS FROM 25° TO 300°C

Chemical Species	S°(25)	G_f°(25)	G°(100)	G°(200)	G°(250)	G°(300)	References
Ti(c)	7.3	0	-600	-1,544	-2,068	-2,624	11,13,21,31
TiO(c)	8.3	-117,200	-117,909	-119,100	-119,788	-120,533	13,21,31
Ti_2O_3(c,α)	18.8	-342,800	-344,424	-347,228	-348,890	-350,722	11,13,21,31
Ti_2O_3(c,β)	21.2	-342,200	-344,170	-347,228	-349,007	-350,936	11,13,21
Ti_3O_5(c,α)	30.9	-553,900	-556,610	-561,303	-564,052	-567,045	11,13,21,31
Ti_3O_5(c,β)	40.5	-552,700	-555,909	-561,505	-564,677	-568,068	11,13,21
TiO_2(c,ru)	12.0	-212,600	-213,621	-215,328	-216,313	-217,377	11,13,21,31
TiO_2(c,an)	11.9	-211,400	-212,414	-214,112	-215,093	-216,153	11,13,21,31
TiH_2(c)	7.101	-25,127	-25,727	-26,734	-27,324	-27,968	12
Ti^{2+}(aq)	-33.2	-75,100	-73,171	-72,389	-72,818	-73,833	1,15,24,26
Ti^{3+}(aq)	-85.3	-83,600	-78,015	-73,190	-71,966	-71,594	1,15,24,26
$HTiO_3^-$(aq)	28.04	-228.460	-230,360	-231,950	-232,425	-232,655	1,15,23
F_2(g)	48.44	0	-3,700	-8.815	-11,440	-14,104	11,13,14,21
TiF_2(g)	61.081	-166,083	-70,805	-177,464	-180,921	-184,451	12
TiF_3(c)	21.00	-325,510	-327,278	-330,15	-331,773	-333,507	12,21
TiF_4(c)	32.016	-372,673	-375,318	-379,528	-381,892	-384,411	12,21
TiF_4(g)	75.243	-362,161	-367,564	-376,008	-380,443	-385,001	12
F^-(aq)	1.7	-66,640	-66,262	-64,089	-62,258	-59,604	14,15,21,24
TiF_6^{2-}	30	-506,300	-508,044	-508,651	-508,209	-506,925	15,24

Table 9-b

REACTIONS AND CODE NUMBERS TO DELINEATE DIAGRAM OF Ti-H_2O AND Ti-F^--H_2O SYSTEMS

Code Number	Reaction
1	$Ti^{2+} = Ti^{3+} + e$
2	$Ti^{2+} + 3H_2O = HTiO_3^- + 5H^+ + 2e$
3	$Ti^{3+} + 3H_2O = HTiO_3^- + 5H^+ + e$
4	$Ti(c) = Ti^{2+} + 2e$
5	$Ti(c) + H_2O = TiO(c) + 2H^+ + 2e$
6	$Ti^{2+} + 2H_2O = TiO_2(ru) + 4H^+ + 2e$
7	$2Ti^{2+} + 3H_2O = Ti_2O_3(c) + 6H^+ + 2e$
8	$Ti^{2+} + H_2O = TiO(c) + 2H^+$
9	$2TiO(c) + H_2O = Ti_2O_3(c) + 2H^+ + 2e$
10	$Ti_2O_3(c) + H_2O = 2TiO_2(ru) + 2H^+ + 2e$
11	$Ti^{3+} + 2H_2O = TiO_2(ru) + 4H^+ + e$
12	$Ti^{3+} + 2H_2O = TiO_2(an) + 4H^+ + e$
13	$Ti^{2+} + 2H_2O = TiO_2(an) + 4H^+ + 2e$
14	$Ti_2O_3(c) + H_2O = 2TiO_2(an) + 2H^+ + 2e$
15	$Ti_2O_3(c) + 3H_2O = 2HTiO_3^- + 4H^+ + 2e$
16	$TiO_2(ru) + H_2O = HTiO_3^- + H^+$
17	$TiO_2(an) + H_2O = HTiO_3^- + H^+$
18	$TiH_2(c) = Ti^{2+} + 2H^+ + 4e$
19	$TiH_2(c) + 2H_2O = TiO_2(ru) + 6H^+ + 6e$
20	$TiH_2(c) + 2H_2O = TiO_2(an) + 6H^+ + 6e$
21	$TiH_2(c) + 3H_2O = HTiO_3^- + 7H^+ + 6e$
22	$TiH_2(c) + 3H_2O = Ti_2O_3(c) + 10H^+ + 10e$
23	$Ti_2O_3(c) + H_2O = 2TiO_2(ru) + 2H^+ + 2e$
24	$Ti_2O_3(c) + H_2O = 2TiO_2(an) + 2H^+ + 2e$
25	$TiF_6^{2-} + 2H_2O = TiO_2(ru) + 6F^- + 4H^+$
26	$TiF_6^{2-} + 2H_2O = TiO_2(an) + 6F^- + 4H^+$
27	$Ti^{2+} + 6F^- = TiF_6^{2-} + 2e$
28	$TiF_6^{2-} + 3H_2O = HTiO_3^- + 6F^- + 5H^+$
29	$Ti^{2+} + 4F^- = TiF_4(c\ or\ g) + 2e$
30	$TiF_4(c\ or\ g) + 2H_2O = TiO_2(ru) + 4F^- + 4H^+$
31	$Ti_2O_3(c) + 12F^- + 6H^+ = 2TiF_6^{2-} + 3H_2O + 2e$
32	$TiH_2(c) + 6F^- = TiF_6^{2-} + 2H^+ + 6e$

Table 9-b (Contd.)

REACTIONS AND CODE NUMBERS TO DELINEATE DIAGRAM OF $Ti-H_2O$ AND $Ti-F^--H_2O$ SYSTEMS

Code Number	Reaction
33	$TiH_2(c) + 4F^- = TiF_4(c\ or\ g) + 2H^+ + 6e$
34	$Ti(c) + 3F^- + 2H^+ = TiF_3(c) + H_2O + e$
35	$2TiF_3(c) + 3H_2O = Ti_2O_3(c) + 6F^- + 6H^+$
36	$TiF_3(c) + 2H_2O = TiO_2(ru) + 3F^- + 4H^+ + e$
37	$TiF_3(c) + 2H_2O = TiO_2(an) + 3F^- + 4H_+ + e$
38	$Ti^{2+} + 3F^- = TiF_3(c) + e$
39	$TiF_3(c) + 3F^- = TiF_6^{2-} + e$
40	$TiF_3(c) + F^- = TiF_4(c\ or\ g) + e$
41	$Ti(c) + 3F^- = TiF_3(c) + 3e$
42	$TiH_2(c) + 3F^- = TiF_3(c) + 2H^+ + 5e$

Table 10-a

FREE-ENERGY VALUES (cal/mole) OF ZIRCONIUM AND ITS COMPOUNDS FROM 25° TO 300°C

Chemical Species	S°(25)	G_f°(25)	G°(100)	G°(200)	G°(250)	G°(300)	References
Zr(c)	9.3	0	-751	-1,899	-2,526	-3,185	13,21,31
$Zr(OH)_4(c)$	31.0	-370,000	-372,759	-377,621	-380,480	-383,589	1,17,18,24
$Zr^{4+}(aq)$	-107.3	-142,000	-134,871	-128,339	-126,418	-125,459	1,15,24,32
$ZrO_2^{2+}(aq)$	-85.0	-200,900	-195,336	-190,534	-189,320	-188,956	1,15,21,24
$HZrO_3^-(aq)$	28.0	-287,700	-289,595	-291,176	-291,644	-291,865	1,15,23,24
$ZrH_2(c)$	8.4	-30,926	-31,665	-32,962	-33,722	-34,547	13,16,17,18,30

Table 10-b

REACTIONS AND CODE NUMBERS TO DELINEATE DIAGRAM OF $Zr-H_2O$ SYSTEM

Code Number	Reaction
1	$Zr^{4+} + H_2O = ZrO^{2+} + 2H^+$
2	$ZrO^{2+} + 2H_2O = HZrO_3^- + 3H^+$
3	$Zr(c) = Zr^{4+} + 4e$
4	$Zr(c) + H_2O = ZrO^{2+} + 2H^+ + 4e$
5	$Zr(c) + 4H_2O = ZrO_2 \cdot 2H_2O + 4H^+ + 4e$
6	$Zr(c) + 3H_2O = HZrO_3^- + 5H^+ + 4e$
7	$ZrO^{2+} + 3H_2O = ZrO_2 \cdot 2H_2O + 2H^+$
8	$ZrO_2 \cdot 2H_2O = HZrO_3^- + H_2O + H^+$
9	$ZrH_2(c) = Zr^{4+} + 2H^+ + 6e$
10	$ZrH_2(c) + H_2O = ZrO^{2+} + 4H^+ + 6e$
11	$ZrH_2(c) + 4H_2O = ZrO_2 \cdot 2H_2O(c) + 6H^+ + 6e$
12	$ZrH_2(c) + 3H_2O = HZrO_3^- + 7H^+ + 6e$

Section 5

STABILITY DIAGRAMS

This section presents the diagrams discussed in the previous sections. The diagram at 250°C is shown at full scale, while diagrams at 25°, 100°, 200° and 300°C are shown in reduced scale. The line number in the diagrams corresponds to the appropriate code number in the tables in Section 4.

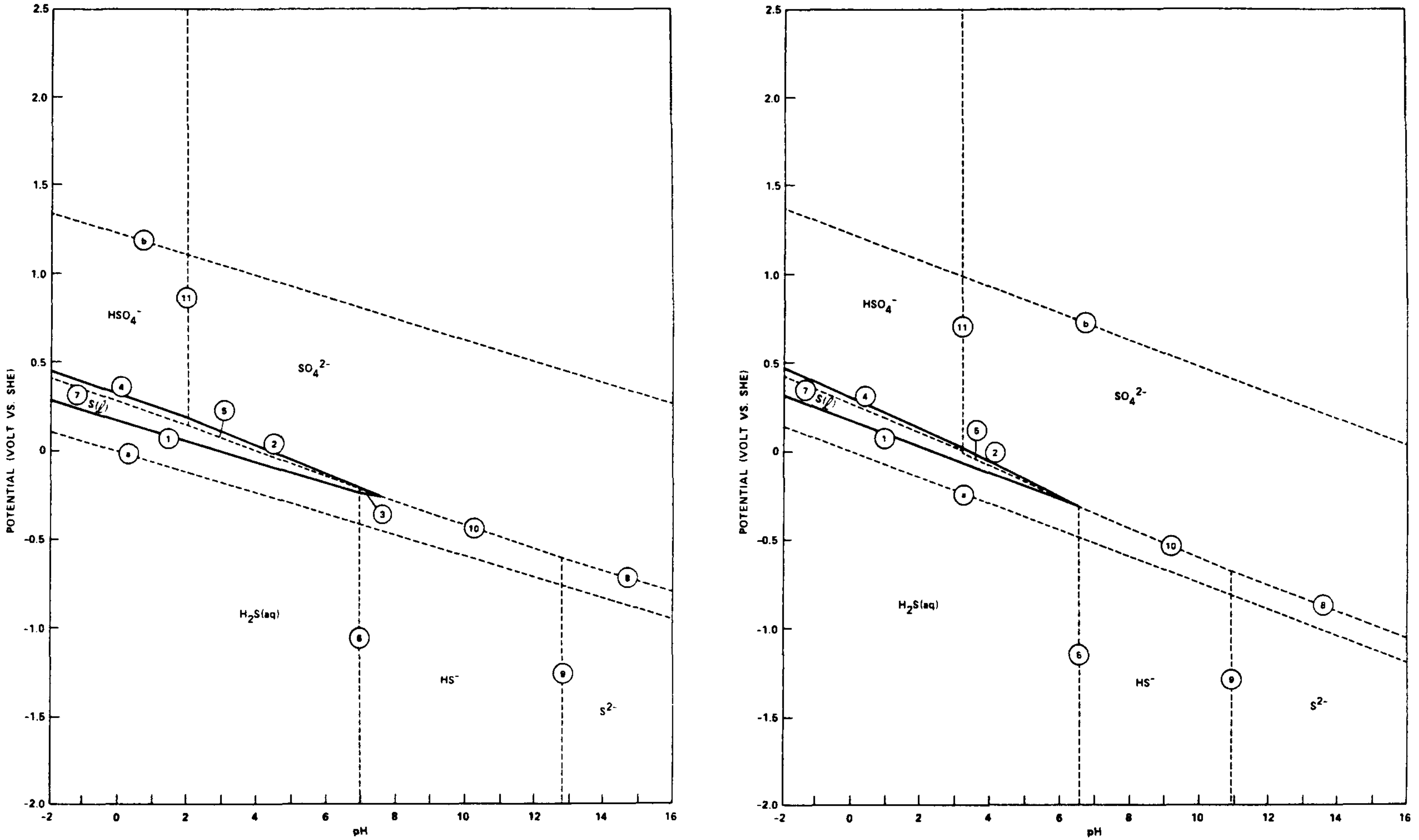

(a) @ 25°C

(b) @ 100°C

FIGURE 1 POTENTIAL-pH DIAGRAM FOR S-H_2O SYSTEM $A_{\text{dissolved sulfide}} = 10^{-1}$, $A_{\text{gas}} = 1$, $A_{\text{solid}} = 1$

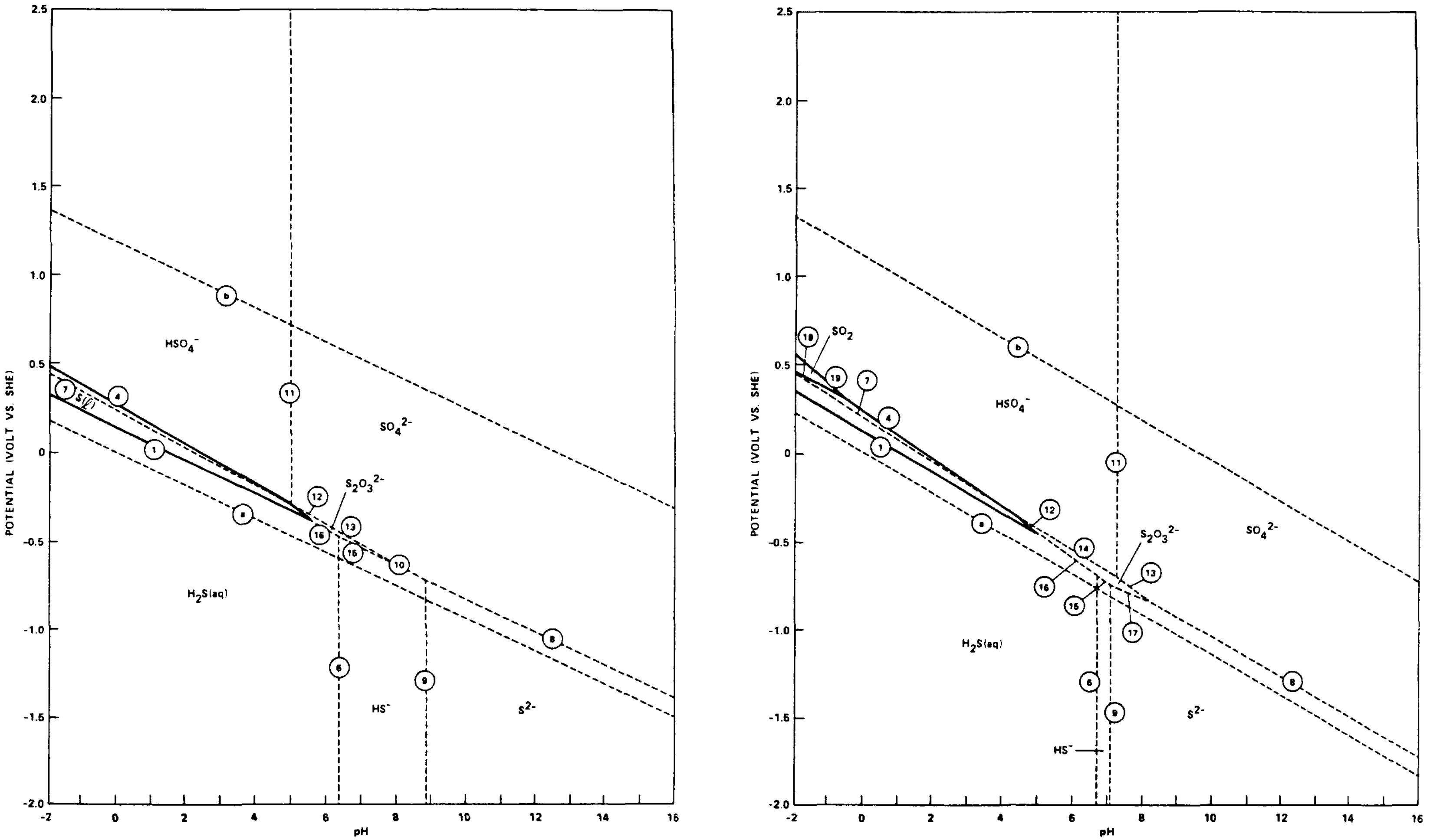

(c) @ 200°C

(d) @ 300°C

FIGURE 1 (Cont'd)

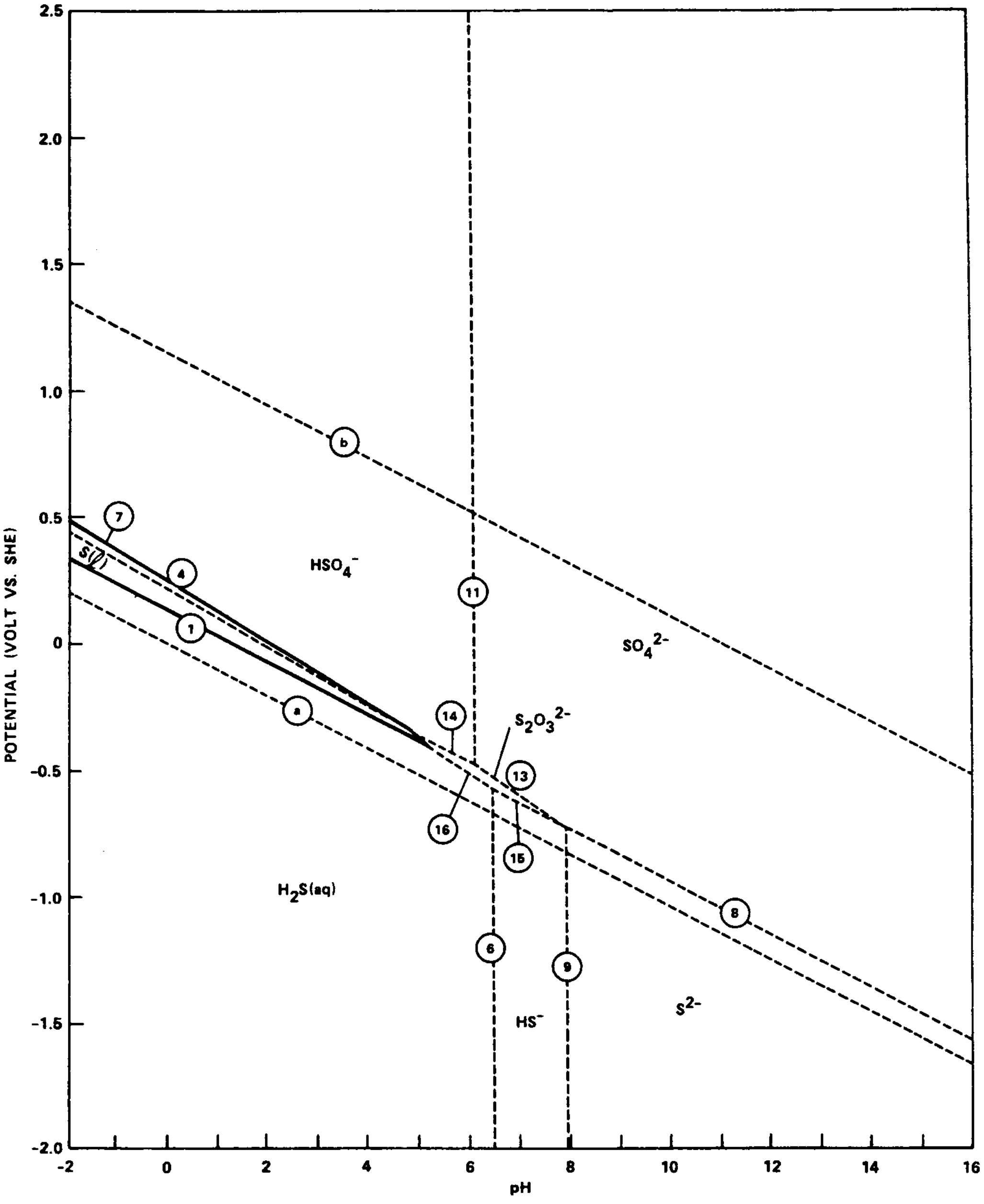

(e) @ 250°C

FIGURE 1 (Cont'd)

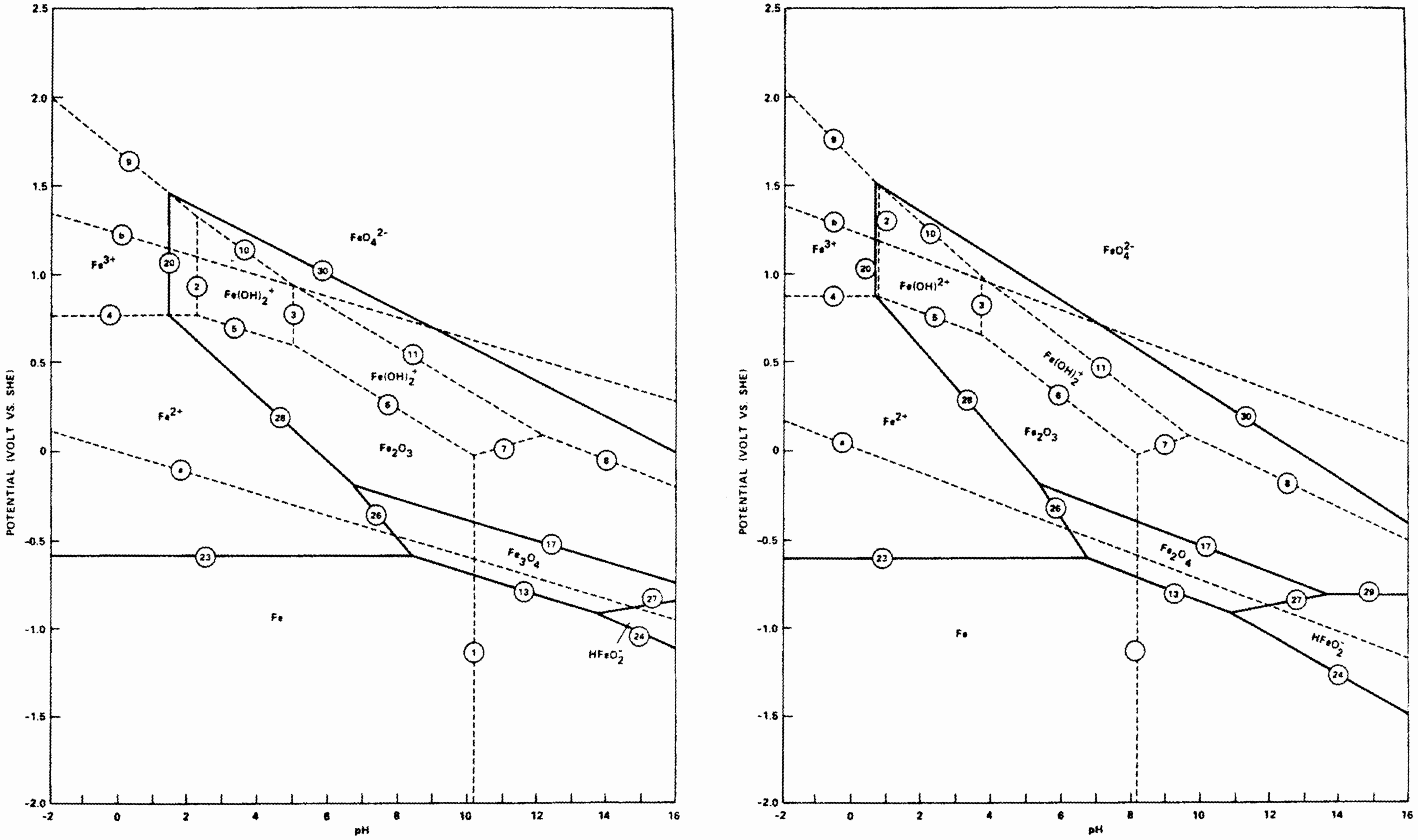

(a) @ 25°C

(b) @ 100°C

FIGURE 2 POTENTIAL-pH DIAGRAM FOR Fe-H_2O SYSTEM
$A_{ion} = 10^{-6}$, $A_{gas} = 1$, $A_{solid} = 1$

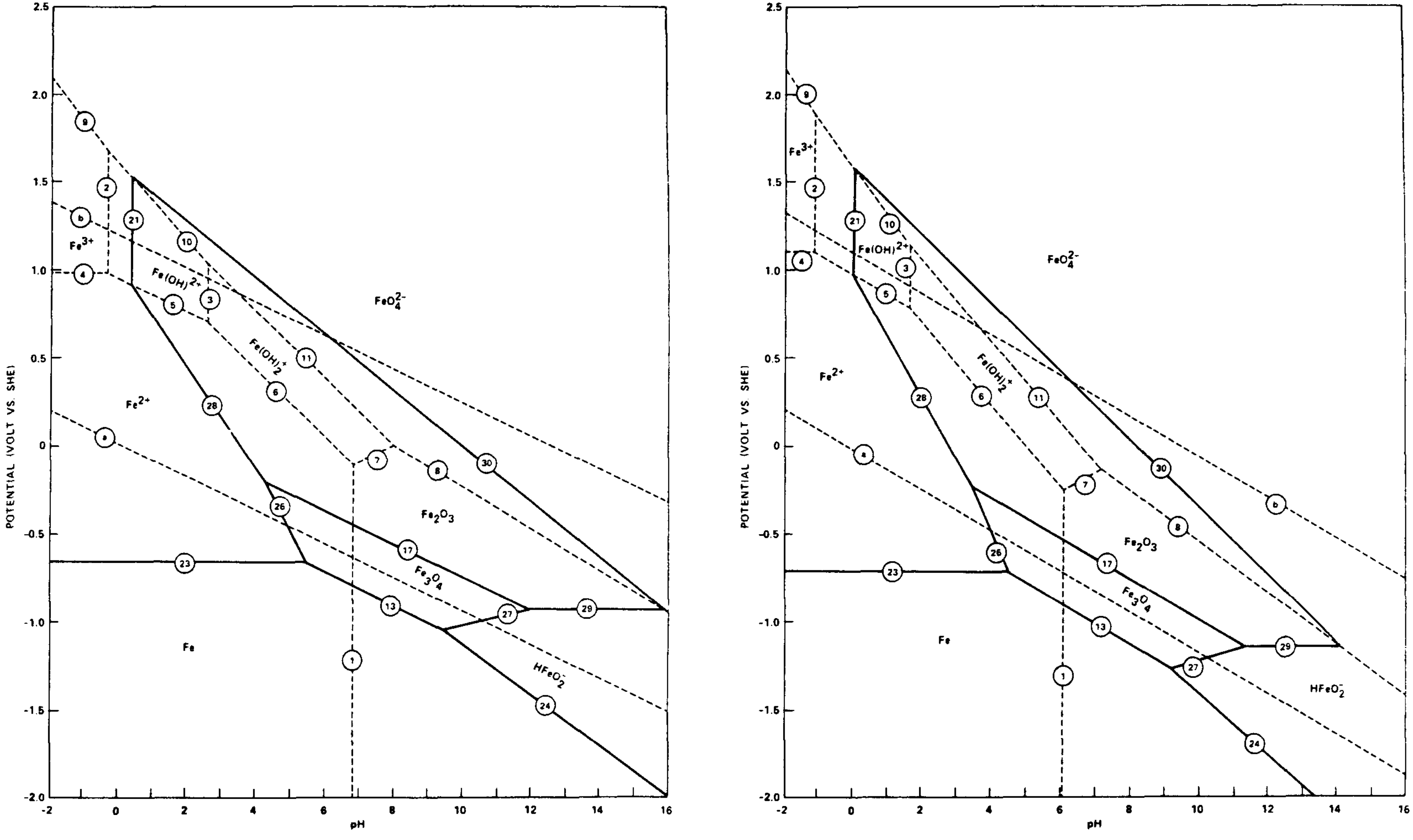

(c) @ 200°C

(d) @ 300°C

FIGURE 2 (Cont'd)

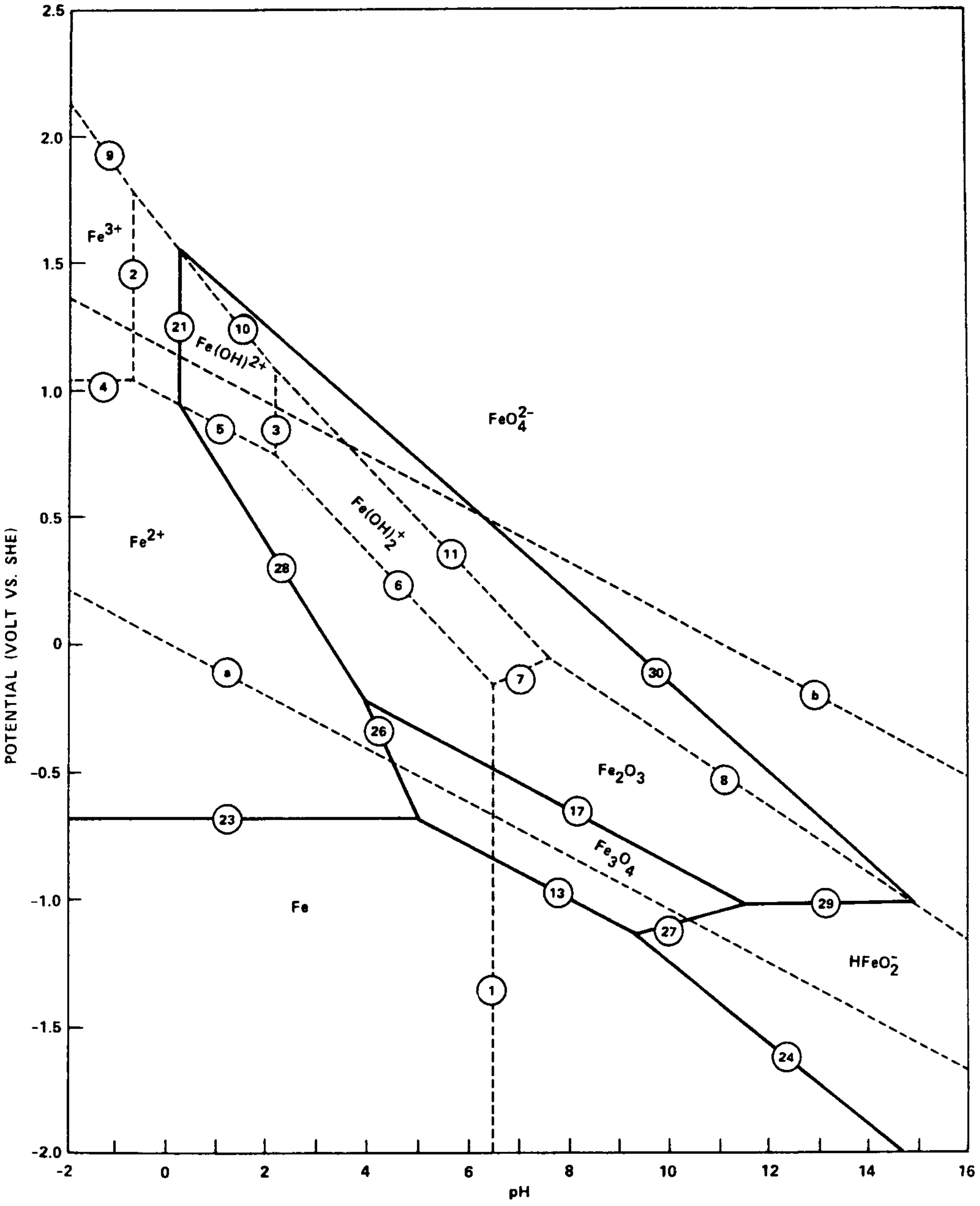

(e) @ 250°C

FIGURE 2 (Cont'd)

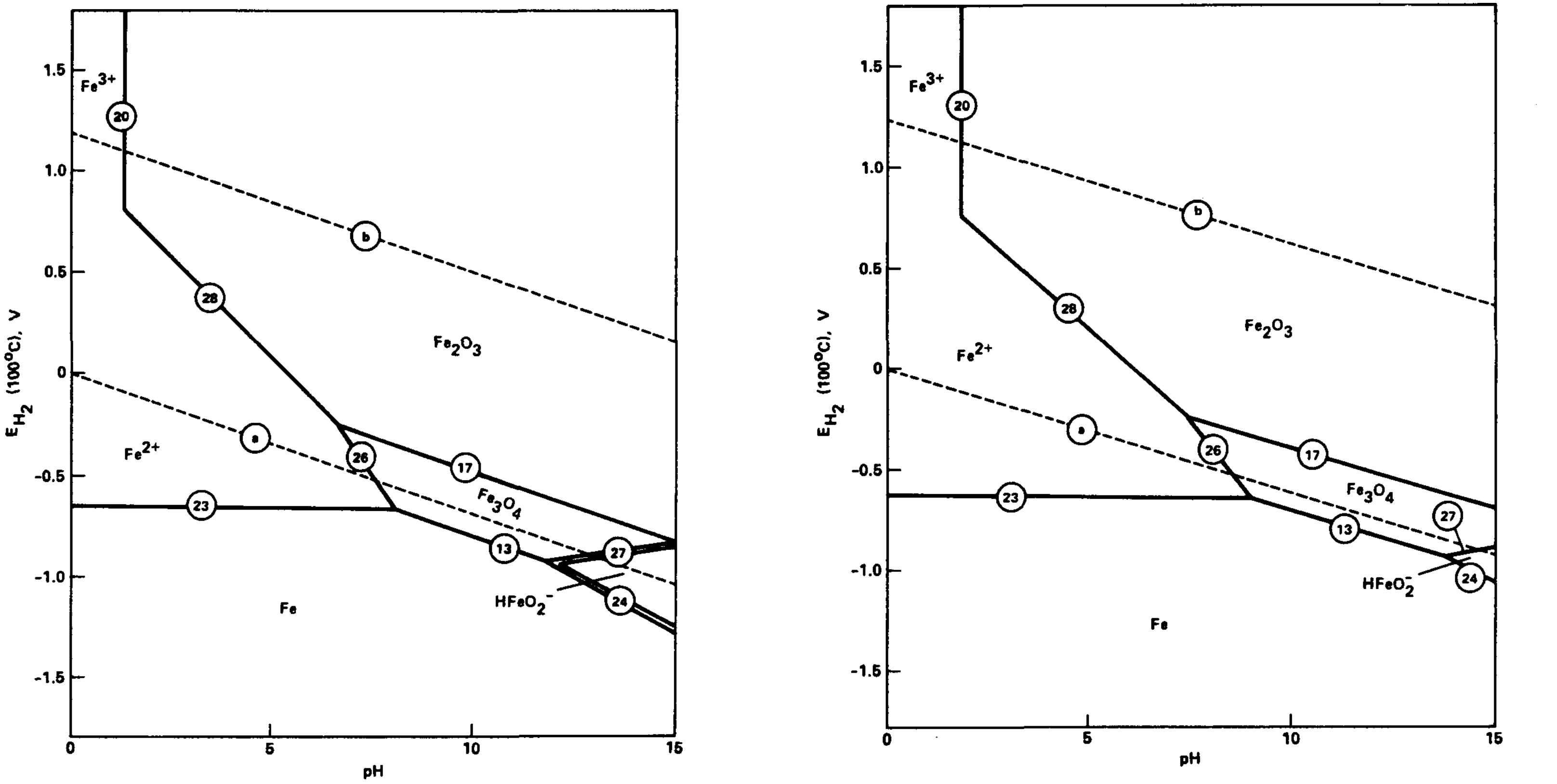

(f) POTENTIAL-pH DIAGRAM (FROM TOWNSEND, REFERENCE 2) FOR Fe-H_2O AT 25°C.

(g) POTENTIAL-pH DIAGRAM (FROM TOWNSEND, REFERENCE 2) FOR Fe-H_2O AT 60°C.

FIGURE 2 (Cont'd)

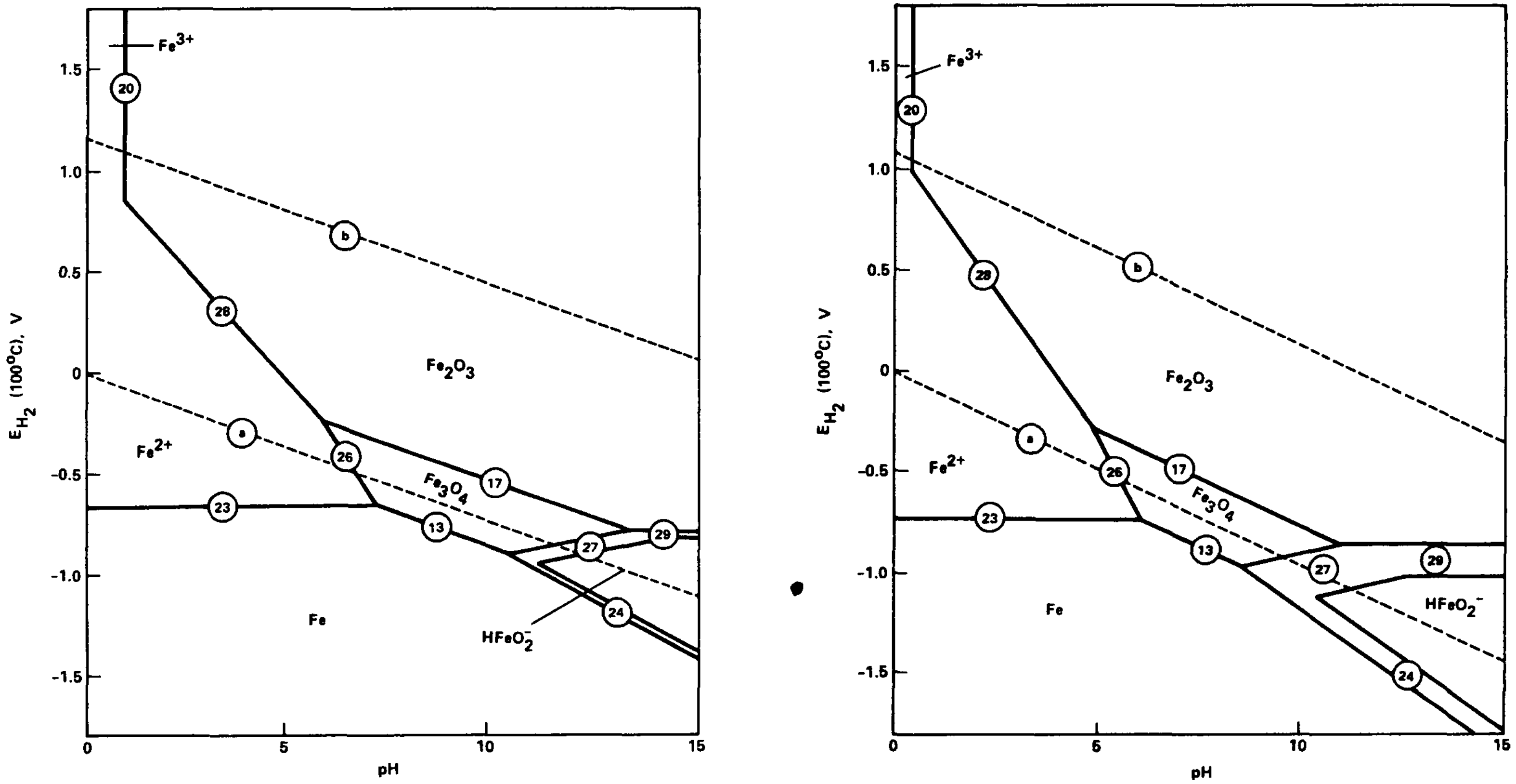

(h) POTENTIAL-pH DIAGRAM (FROM TOWNSEND, REFERENCE 2) FOR Fe-H_2O AT 100°C.

(i) POTENTIAL-pH DIAGRAM (FROM TOWNSEND, REFERENCE 2) FOR Fe-H_2O AT 200°C.

FIGURE 2 (Cont'd)

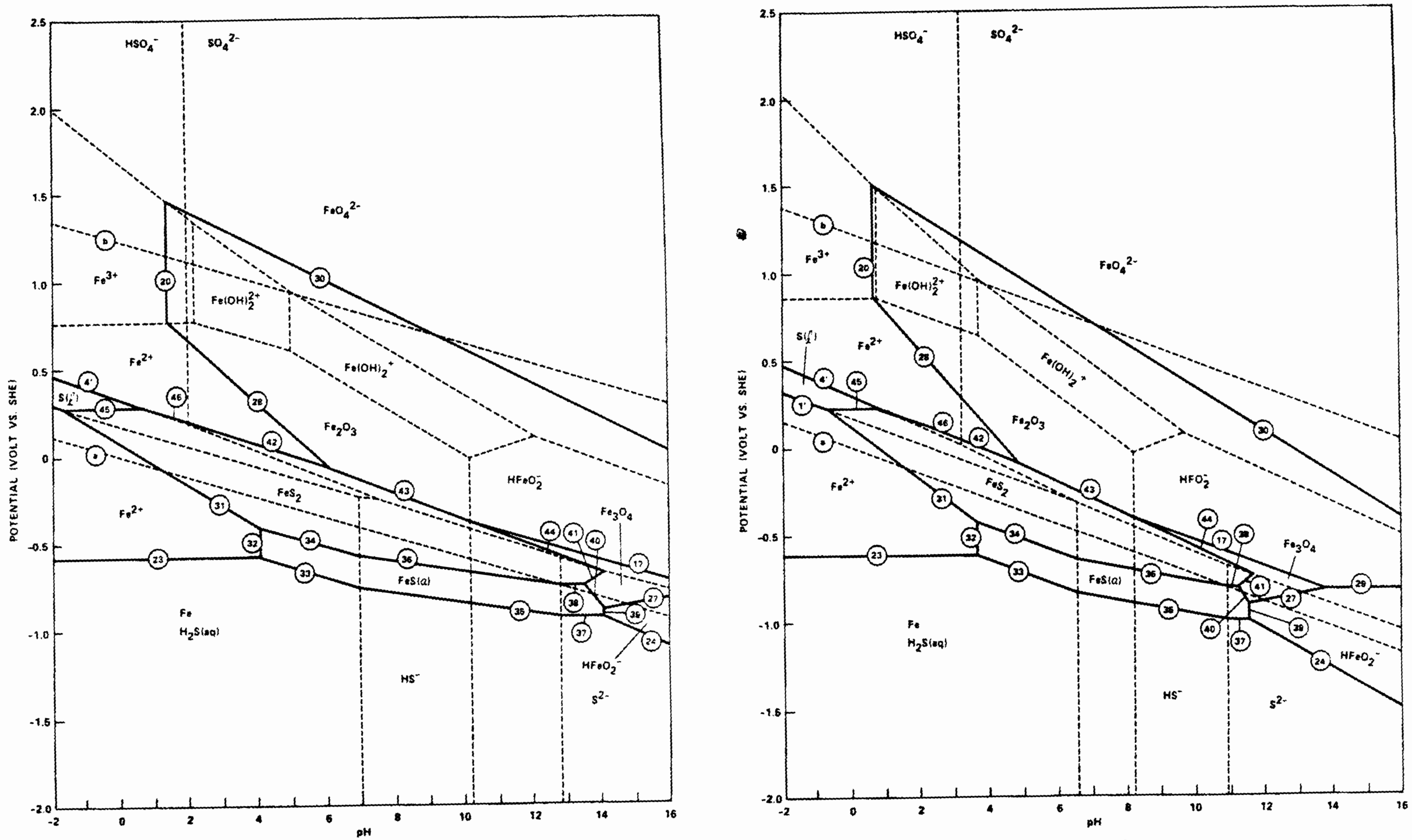

(a) @ 25°C

(b) @ 100°C

FIGURE 3 POTENTIAL-pH DIAGRAM FOR Fe-S-H_2O SYSTEM
$A_{ion} = 10^{-6}$, $A_{dissolved\ sulfide} = 10^{-1}$, $A_{gas} = 1$, $A_{solid} = 1$

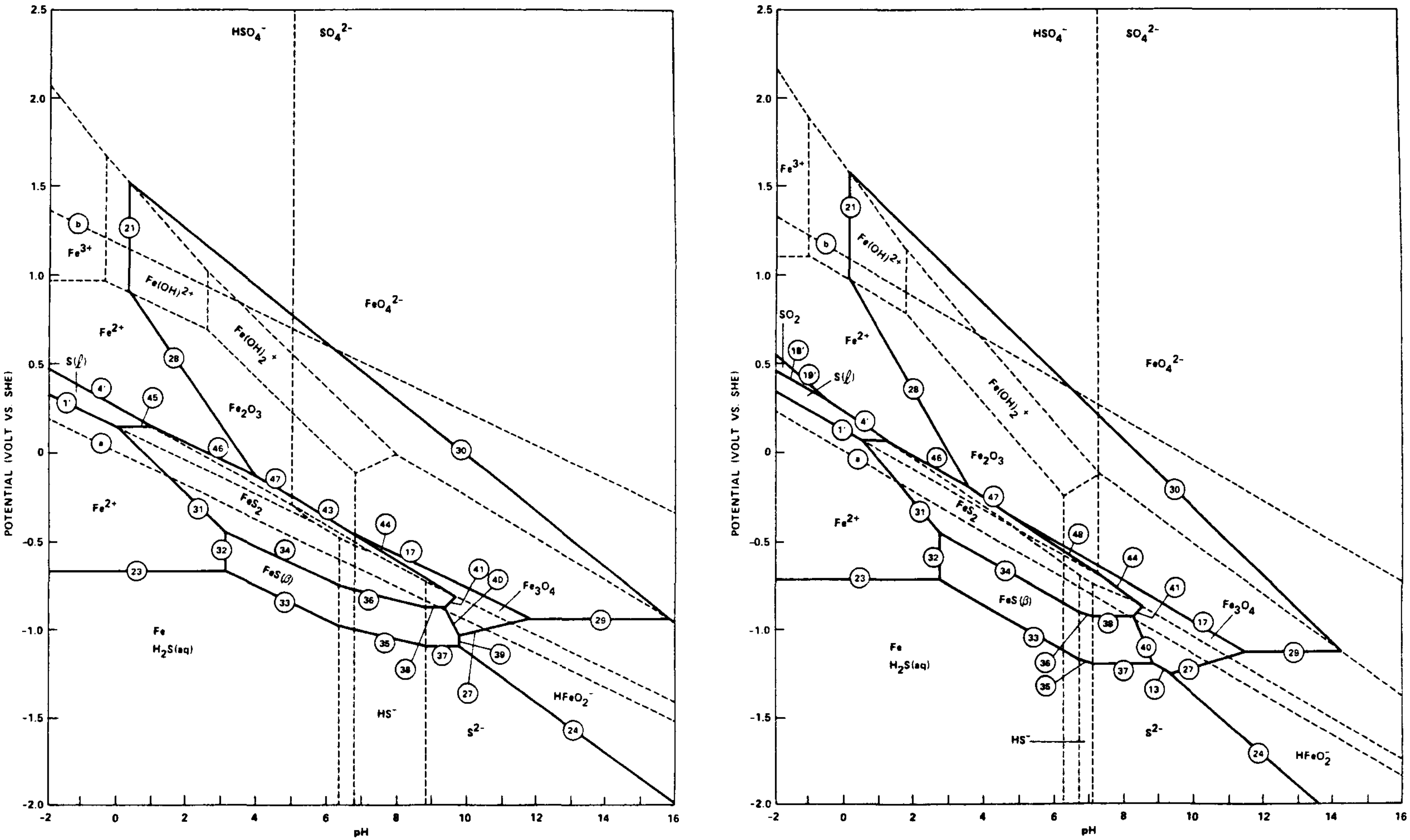

(c) @ 200°C

(d) @ 300°C

FIGURE 3 (Cont'd)

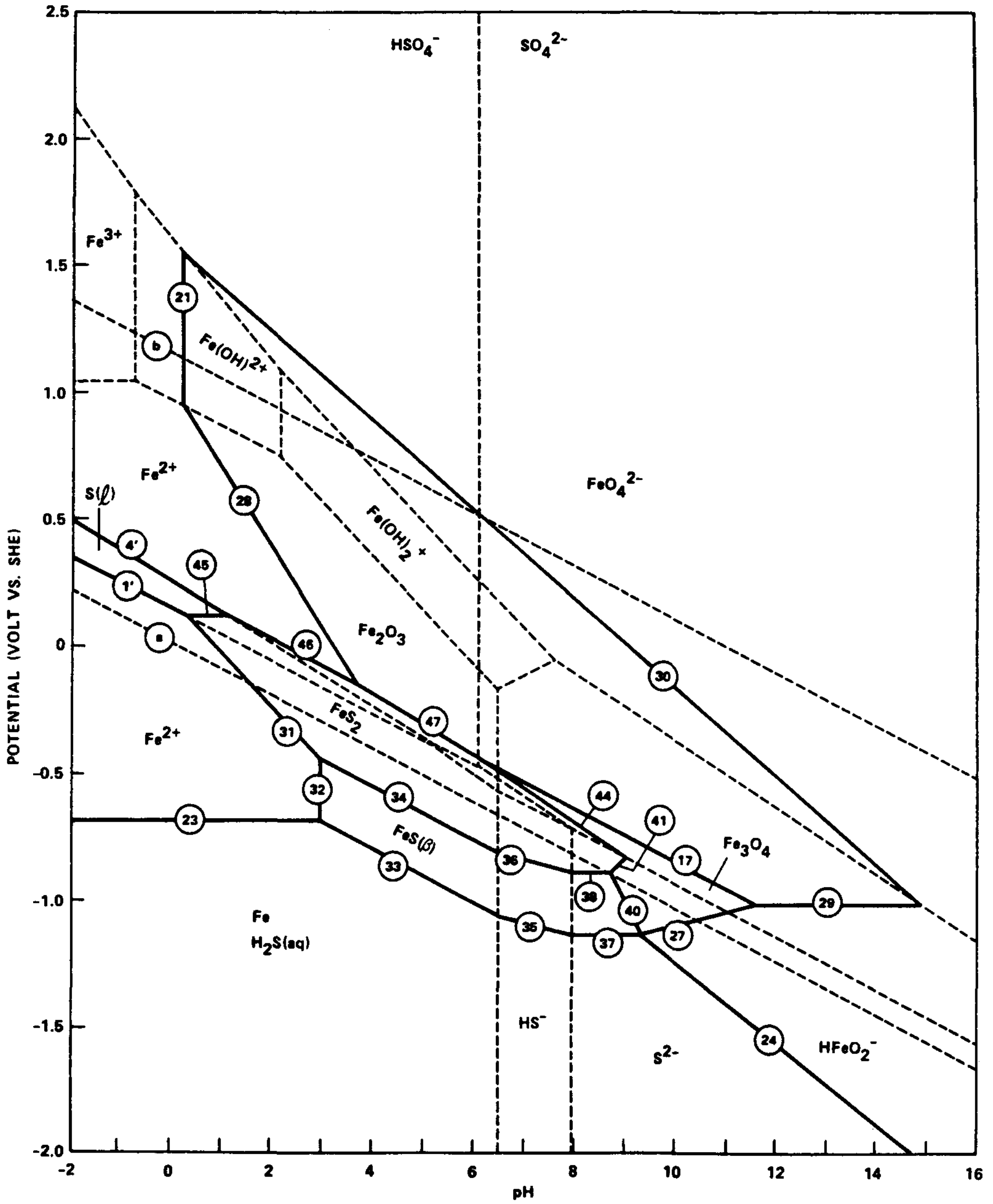

(e) @ 250°C

FIGURE 3 (Cont'd)

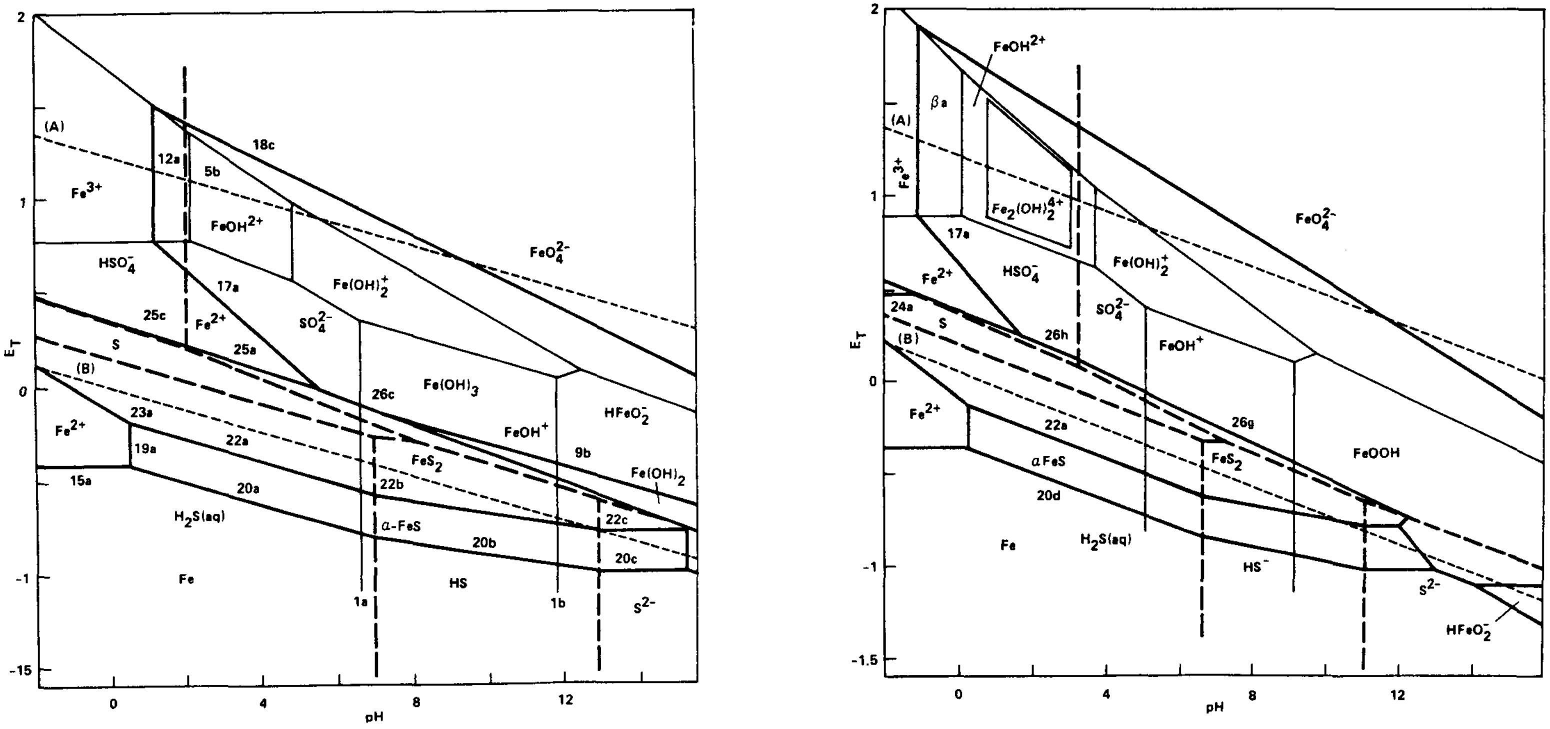

(f) @ 25°C

(g) @ 100°C

FIGURE 3 (Cont'd) POTENTIAL-pH DIAGRAM FOR Fe-H_2O-S SYSTEM [REF. 7]

-------- WATER STABILITY (A) AND (B)

———— DISSOLVED IRON SPECIES

— — — S-H_2O SYSTEM

━━━━ INVOLVING SOLID IRON SPECIES

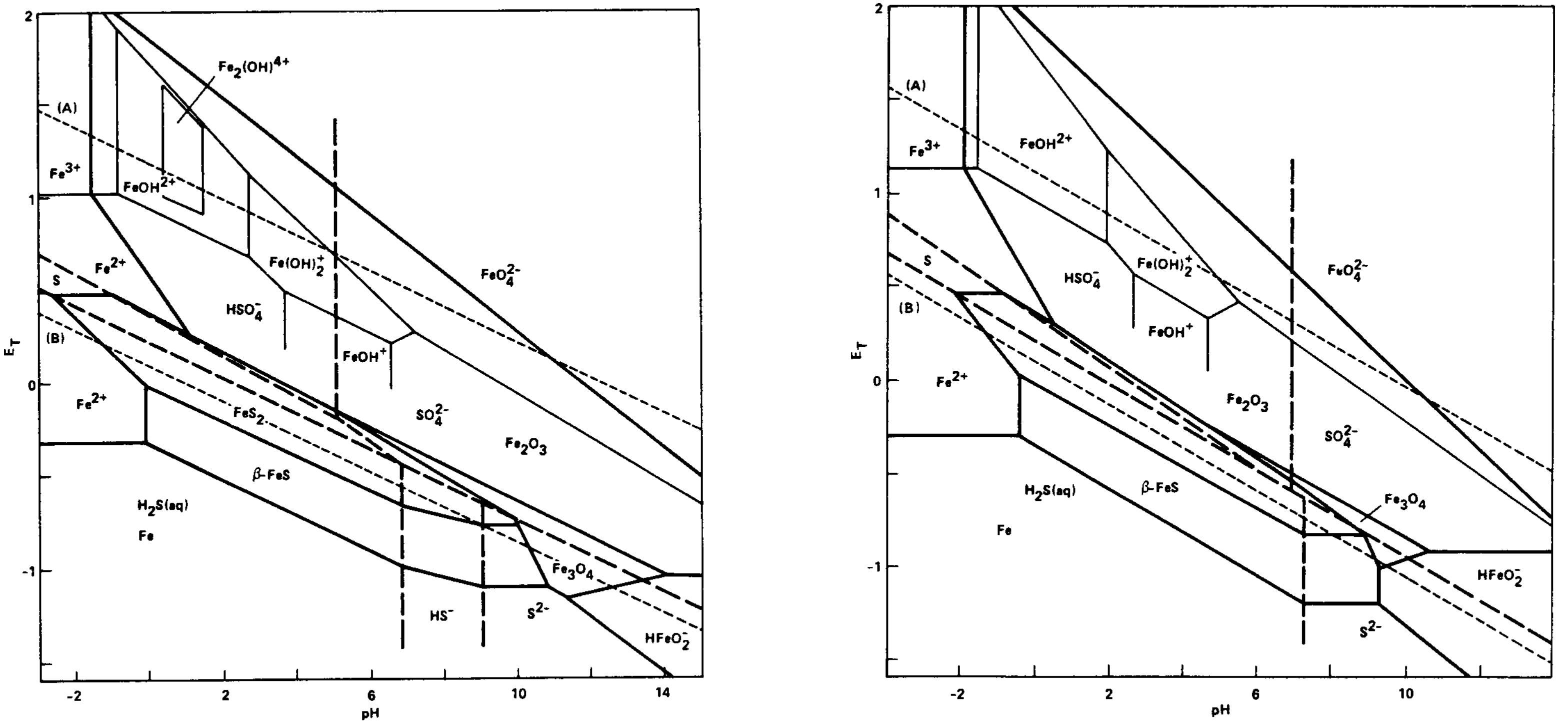

(h) @ 200°C

(i) @ 300°C

FIGURE 3 (Cont'd) POTENTIAL-pH DIAGRAM FOR Fe-H_2O-S SYSTEM [REF. 7]

- - - - - - - - WATER STABILITY (A) AND (B)

———— DISSOLVED IRON SPECIES

— — — S-H_2O SYSTEM

▬▬▬ INVOLVING SOLID IRON SPECIES

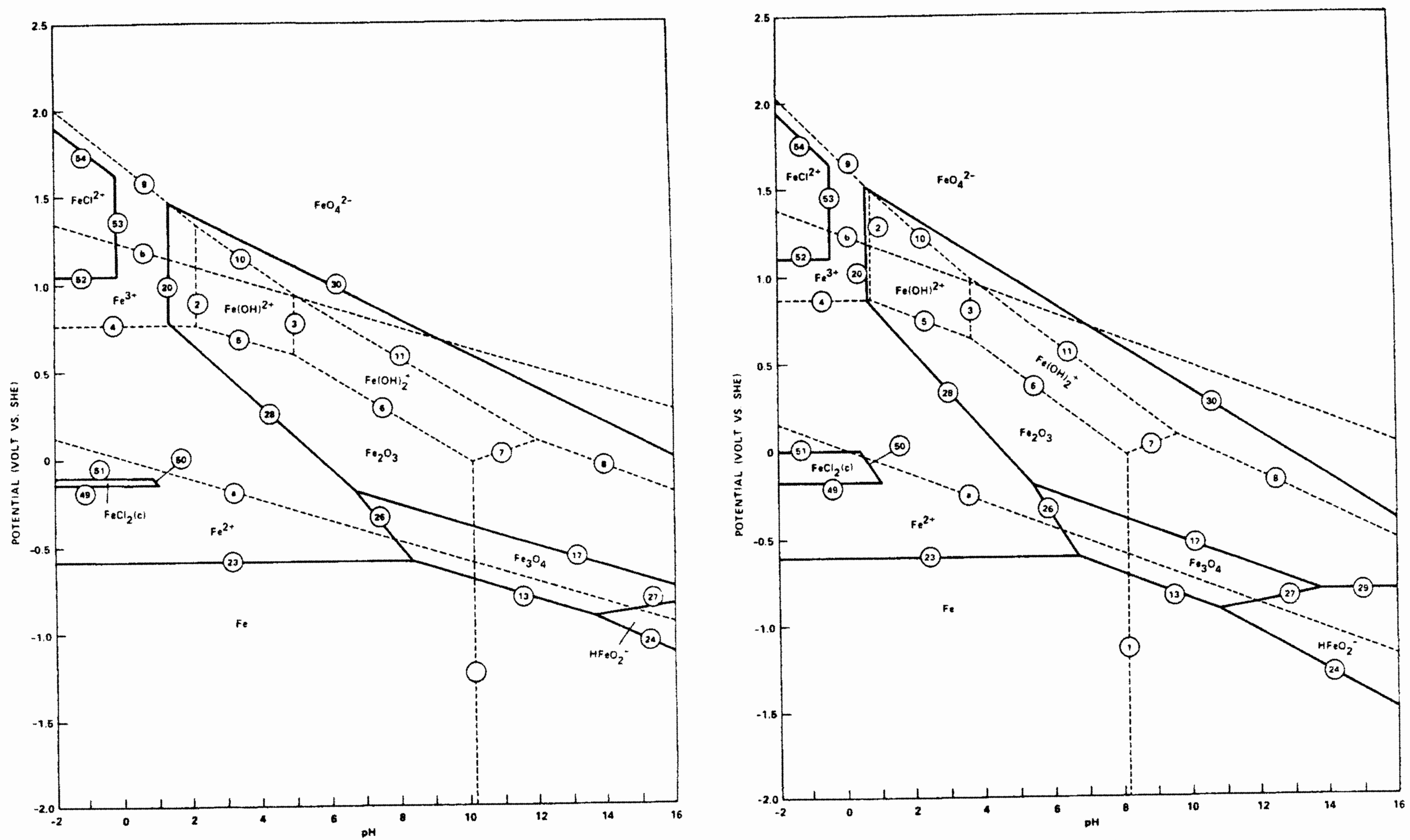

(a) @ 25°C

(b) @ 100°C

FIGURE 4 POTENTIAL-pH DIAGRAM FOR Fe-Cl^--H_2O SYSTEM
$A_{ion} = 10^{-6}$, $A_{dissolved\ chloride} = 10^{-1}$, $A_{gas} = 1$, $A_{solid} = 1$

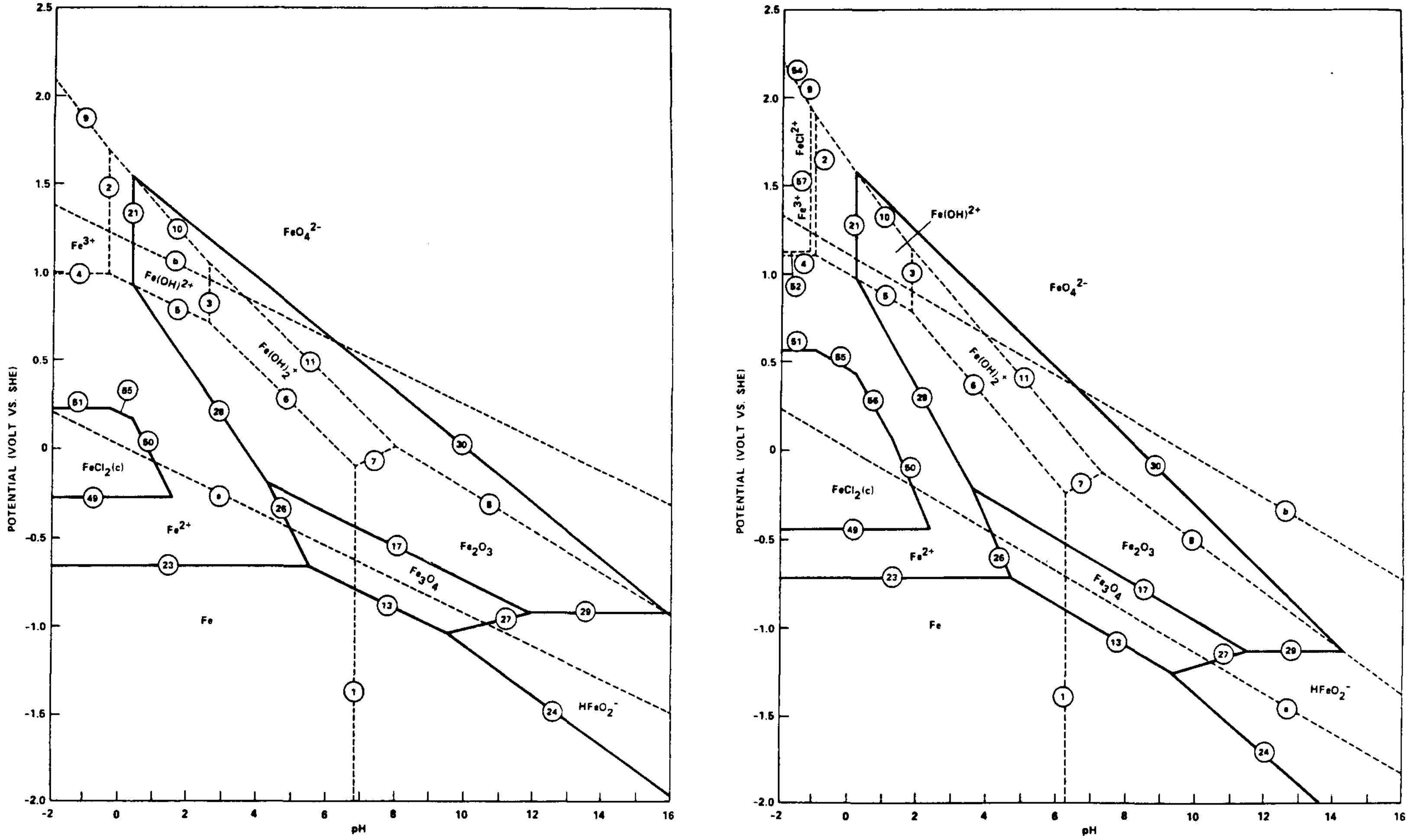

(c) @ 200°C

(d) @ 300°C

FIGURE 4 (Cont'd)

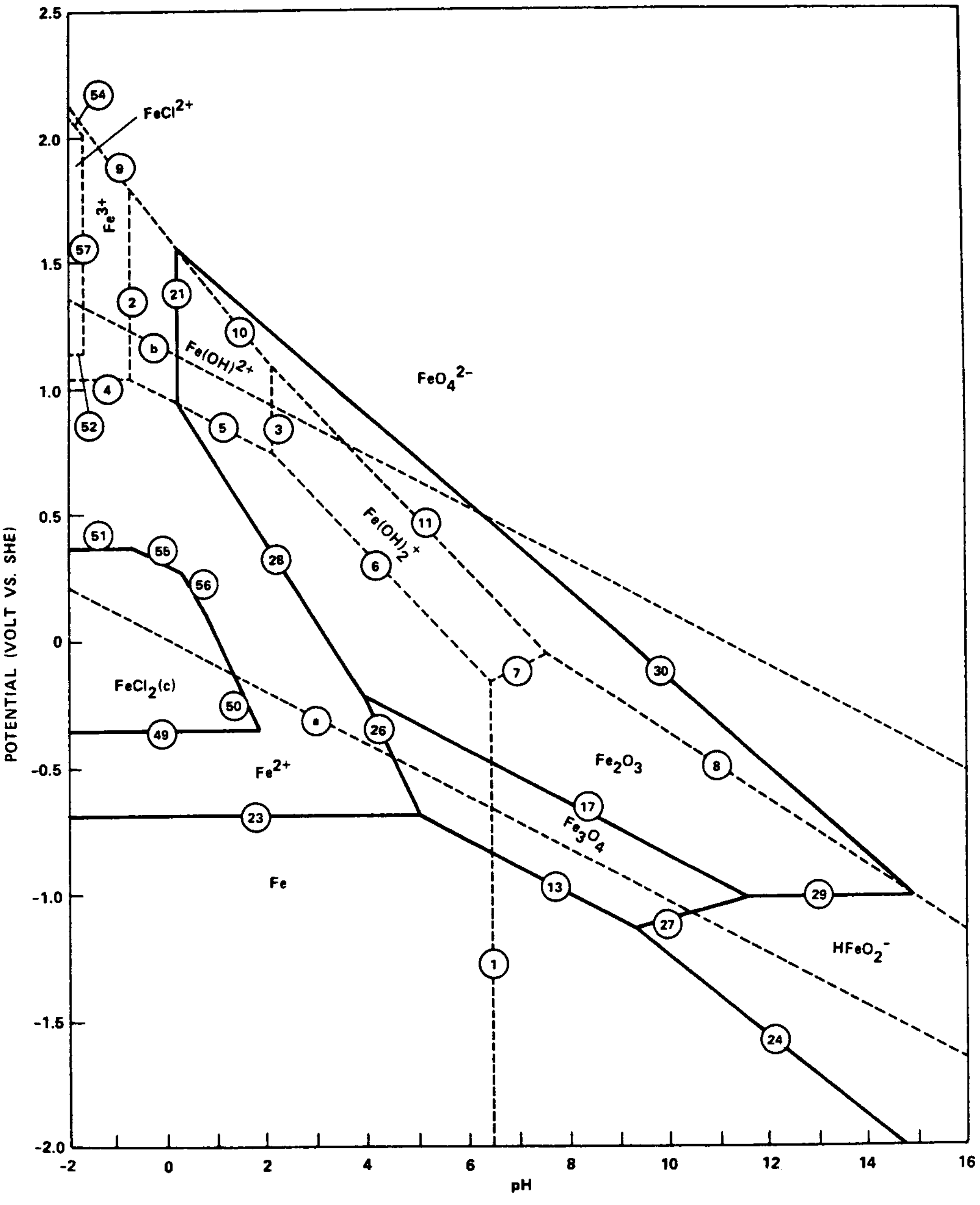

(e) @ 250°C

FIGURE 4 (Cont'd)

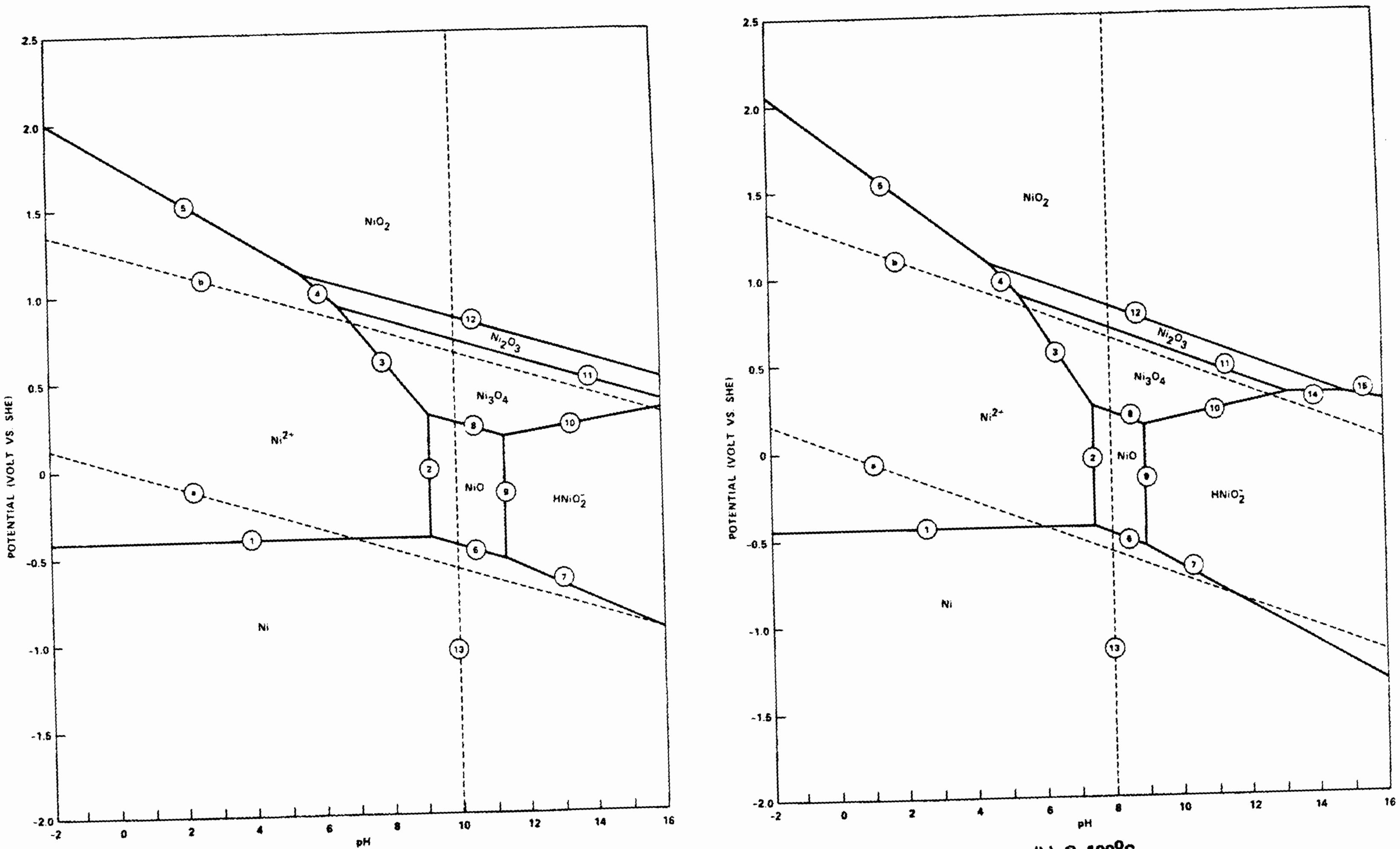

(a) @ 25°C

(b) @ 100°C

FIGURE 5 POTENTIAL-pH DIAGRAM FOR Ni-H_2O SYSTEM
$A_{ion} = 10^{-6}$, $A_{gas} = 1$, $A_{solid} = 1$

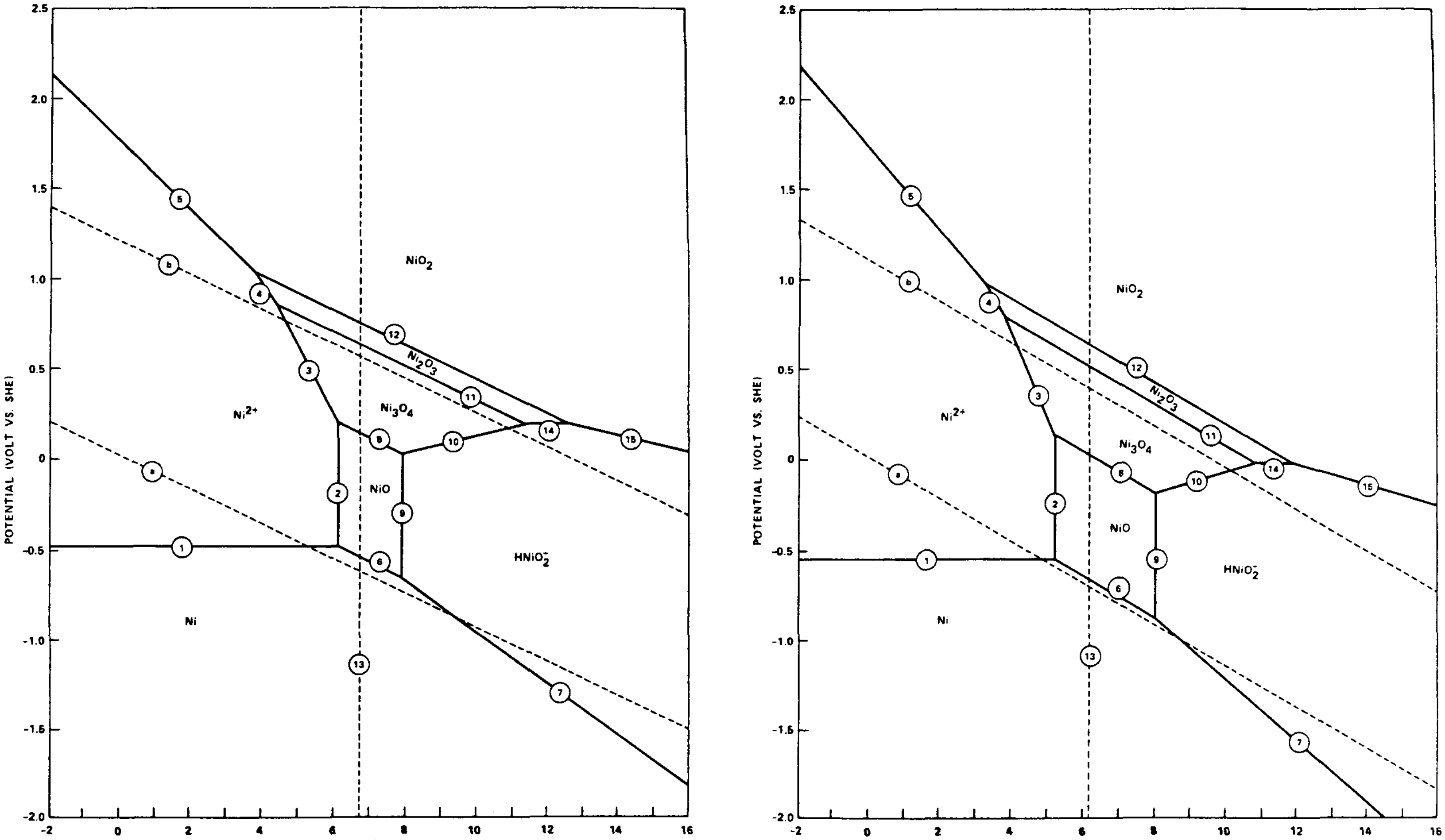

(c) @ 200°C

(d) @ 300°C

FIGURE 5 (Cont'd)

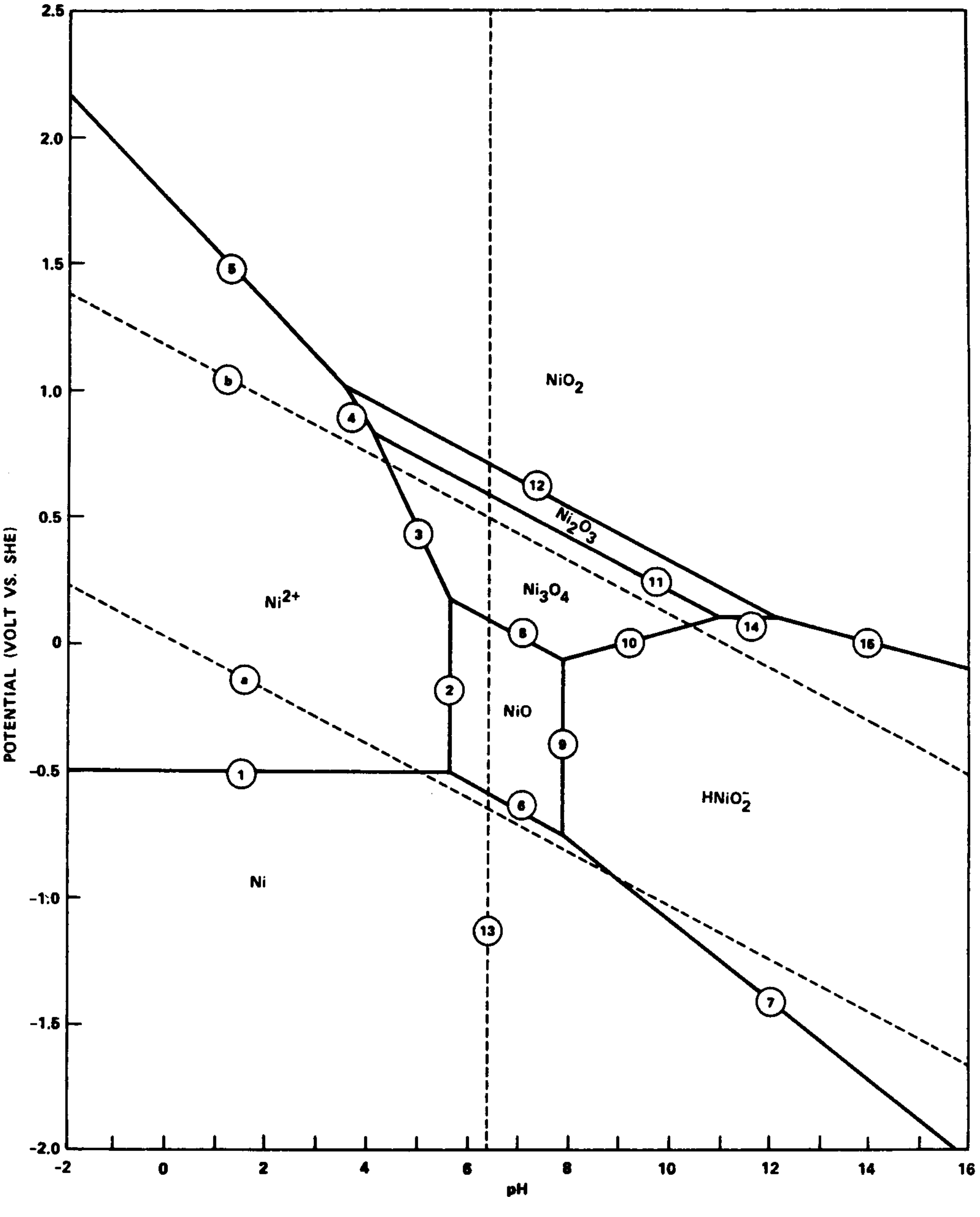

(e) @ 250°C

FIGURE 5 (Cont'd)

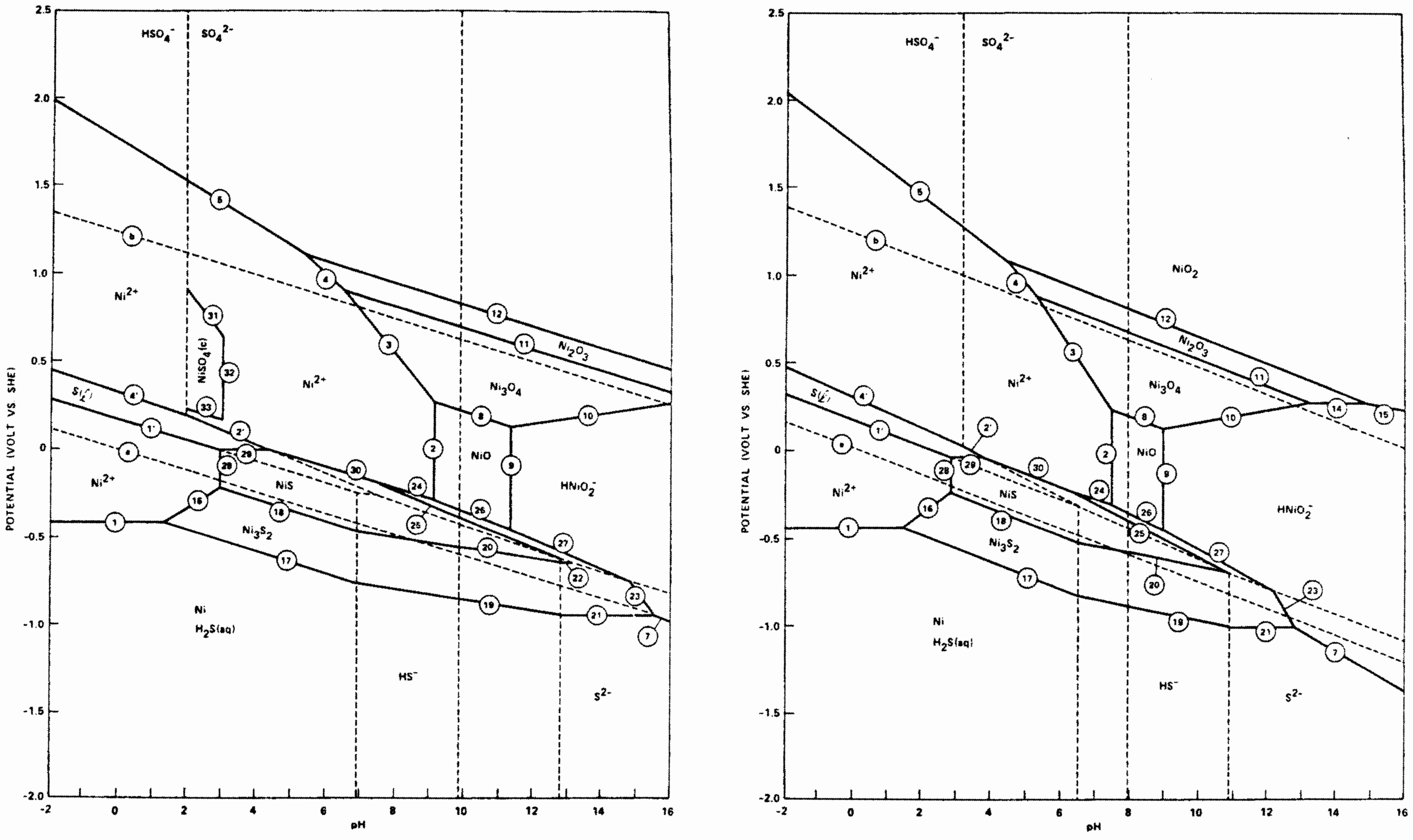

(a) @ 25°C

(b) @ 100°C

FIGURE 6 POTENTIAL-pH DIAGRAM FOR Ni-S-H_2O SYSTEM
$A_{ion} = 10^{-6}$, $A_{dissolved\ sulfide} = 10^{-1}$, $A_{gas} = 1$, $A_{solid} = 1$

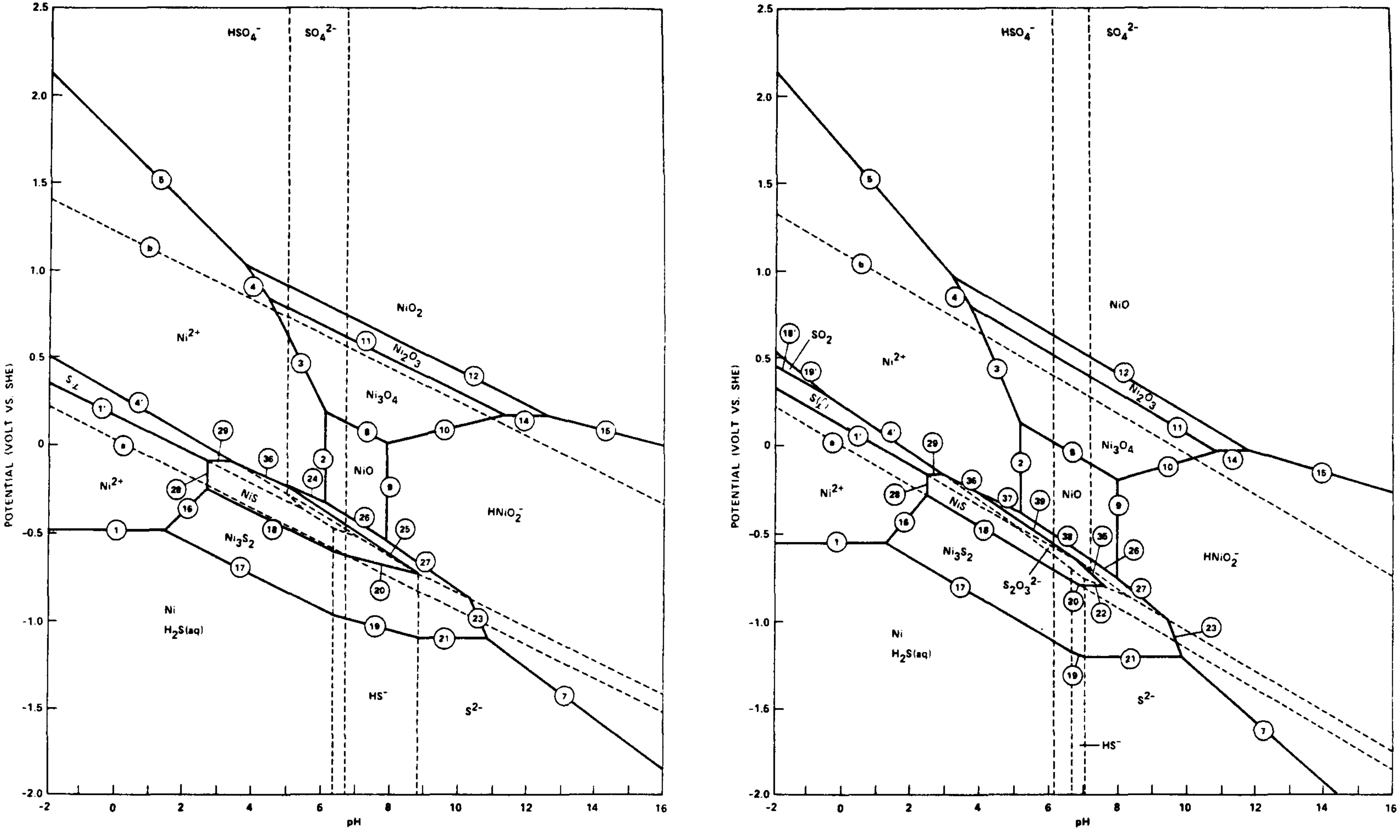

(c) @ 200°C

(d) @ 300°C

FIGURE 6 (Cont'd)

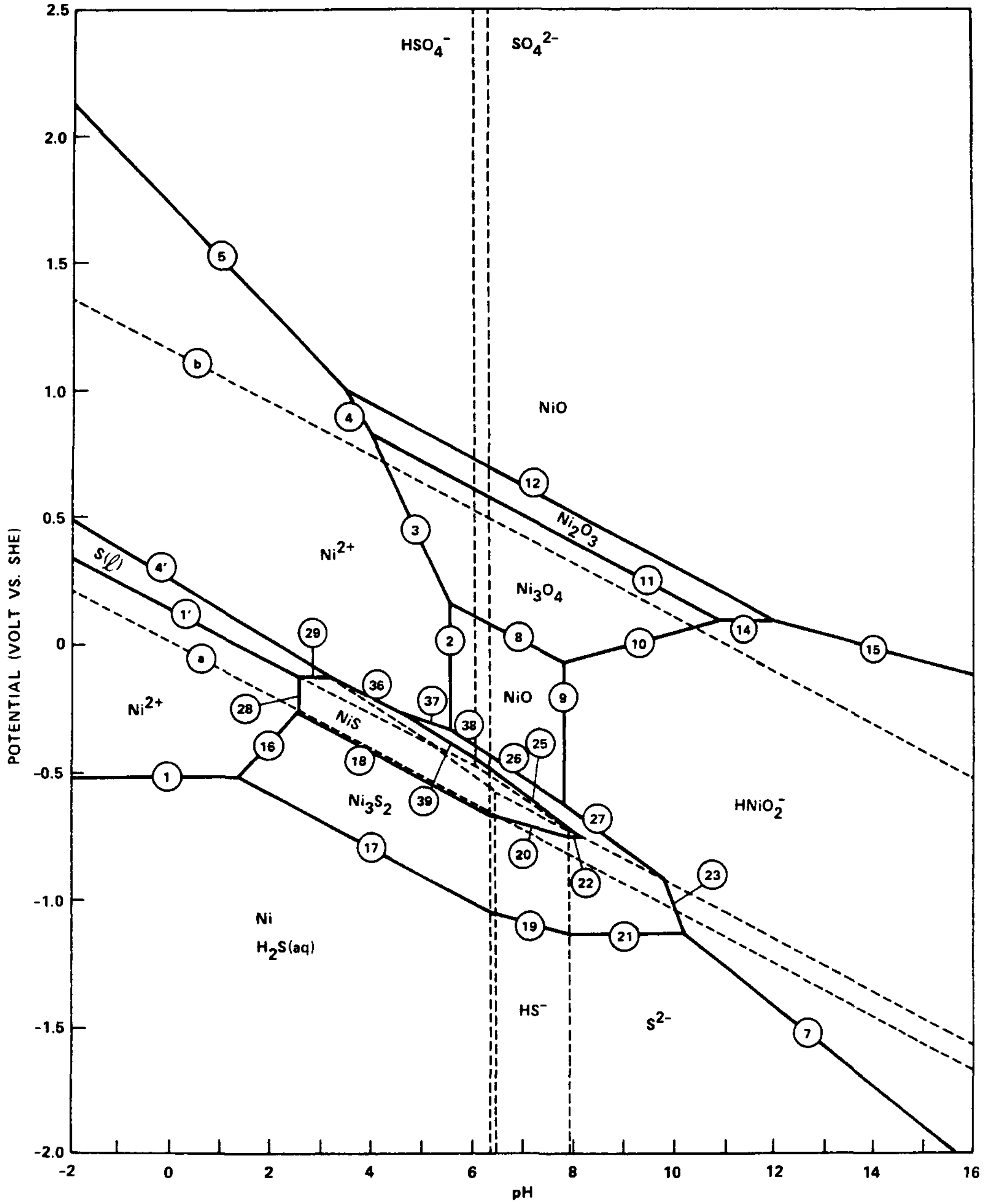

(e) @ 250°C

FIGURE 6 (Cont'd)

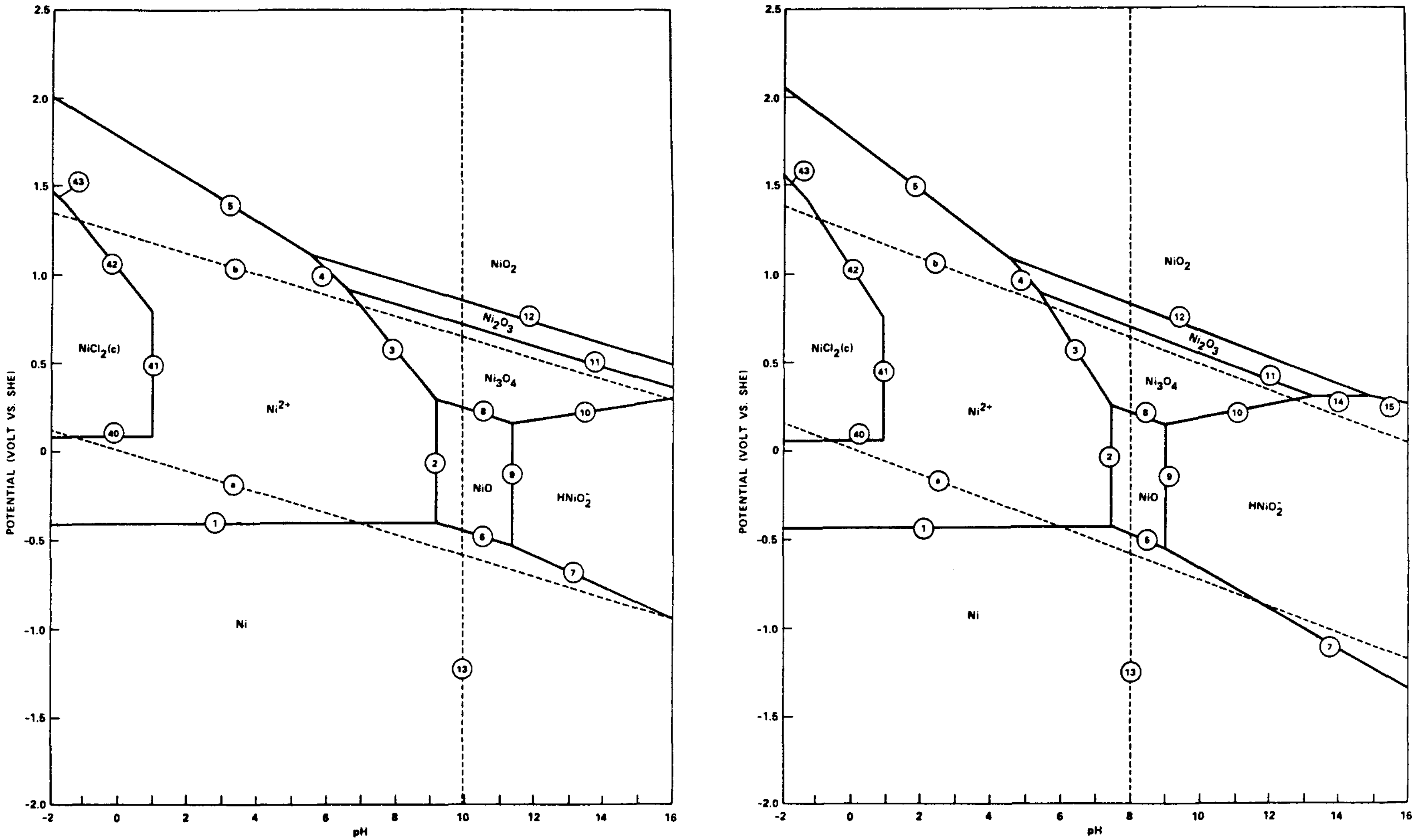

(a) @ 25°C

(b) @ 100°C

FIGURE 7 POTENTIAL-pH DIAGRAM FOR Ni-Cl$^-$-H$_2$O SYSTEM
$A_{ion} = 10^{-6}$, $A_{Cl^-} = 10^{-1}$, $A_{gas} = 1$, $A_{solid} = 1$

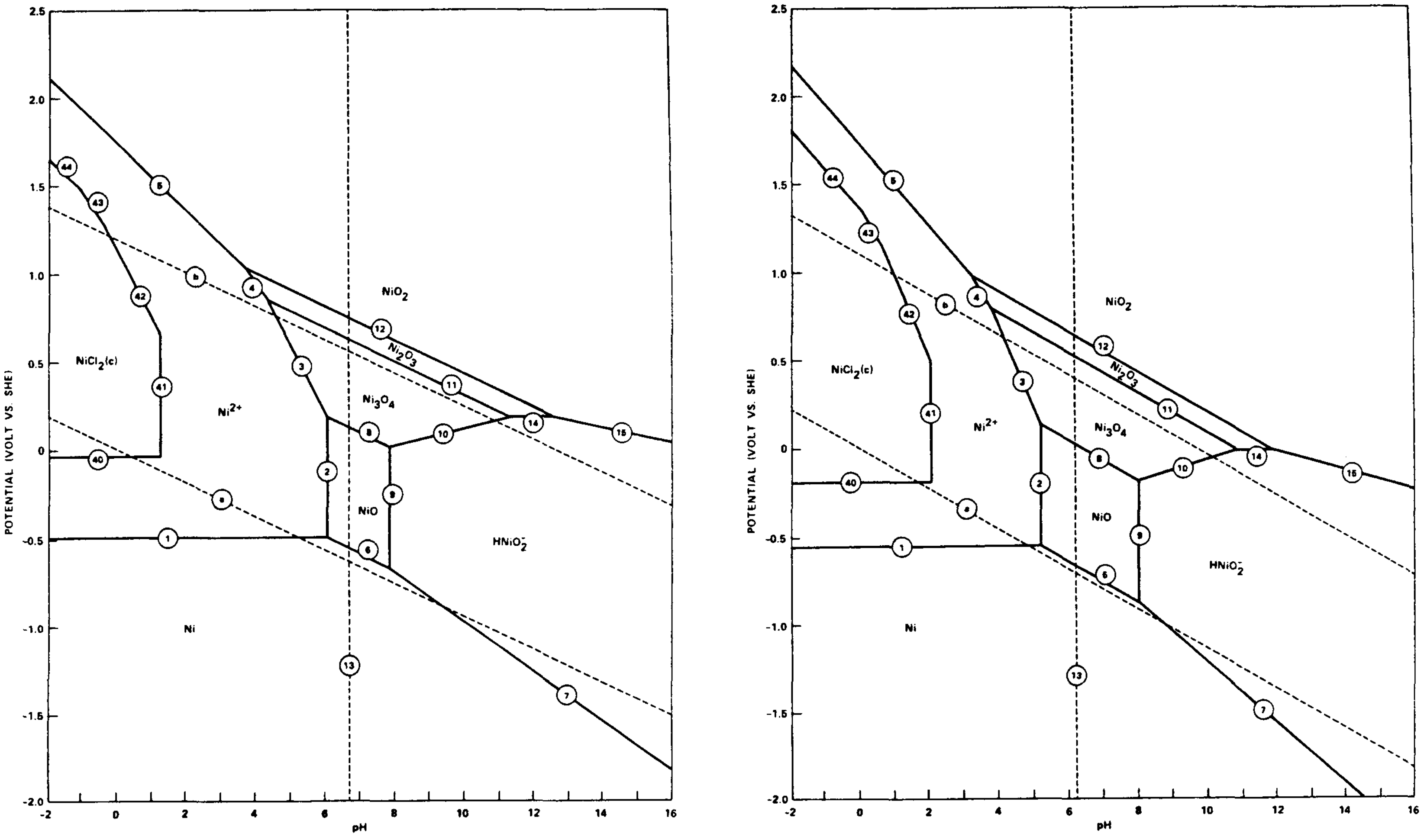

(c) @ 200°C

(d) @ 300°C

FIGURE 7 (Cont'd)

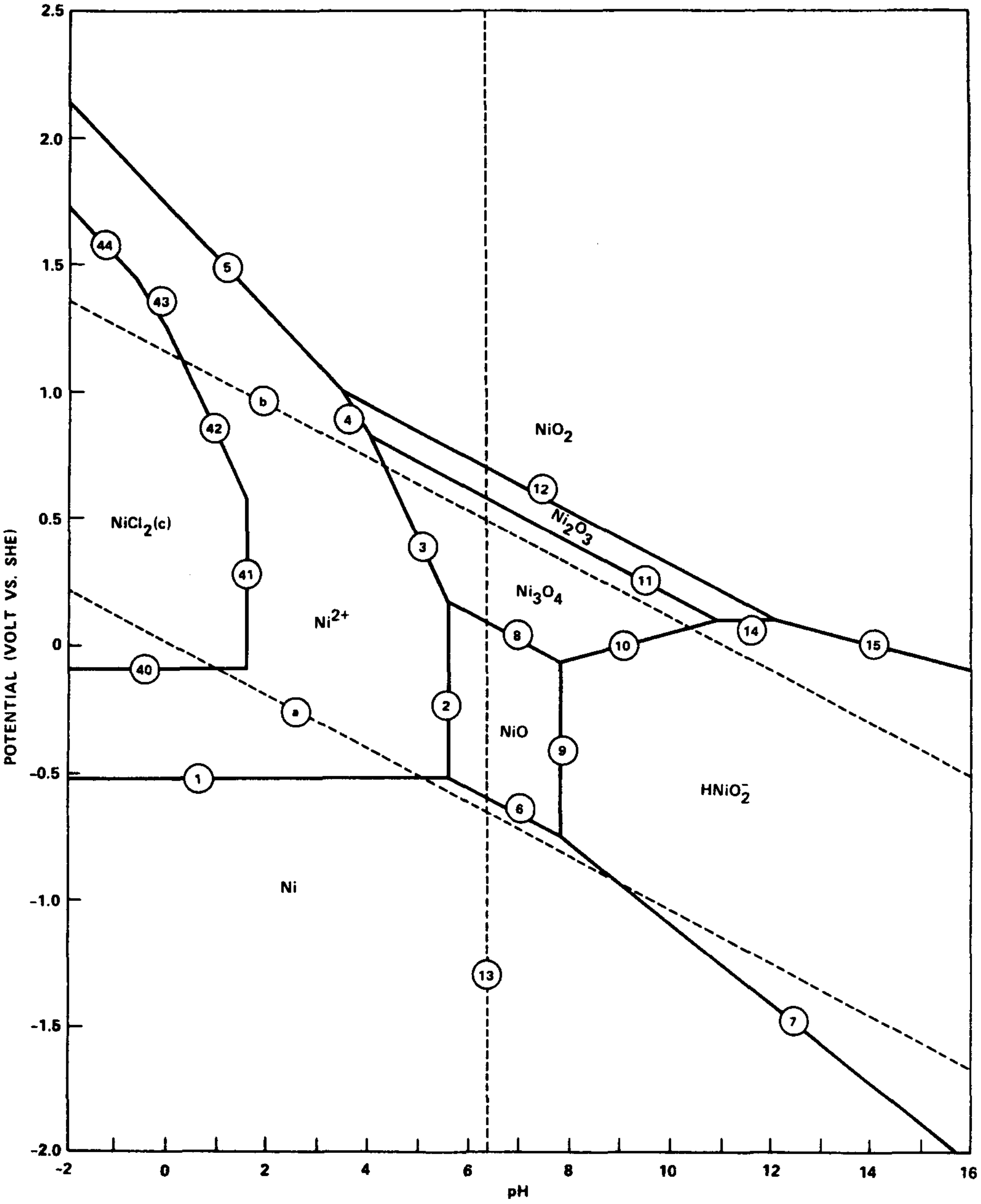

(e) @ 250°C

FIGURE 7 (Cont'd)

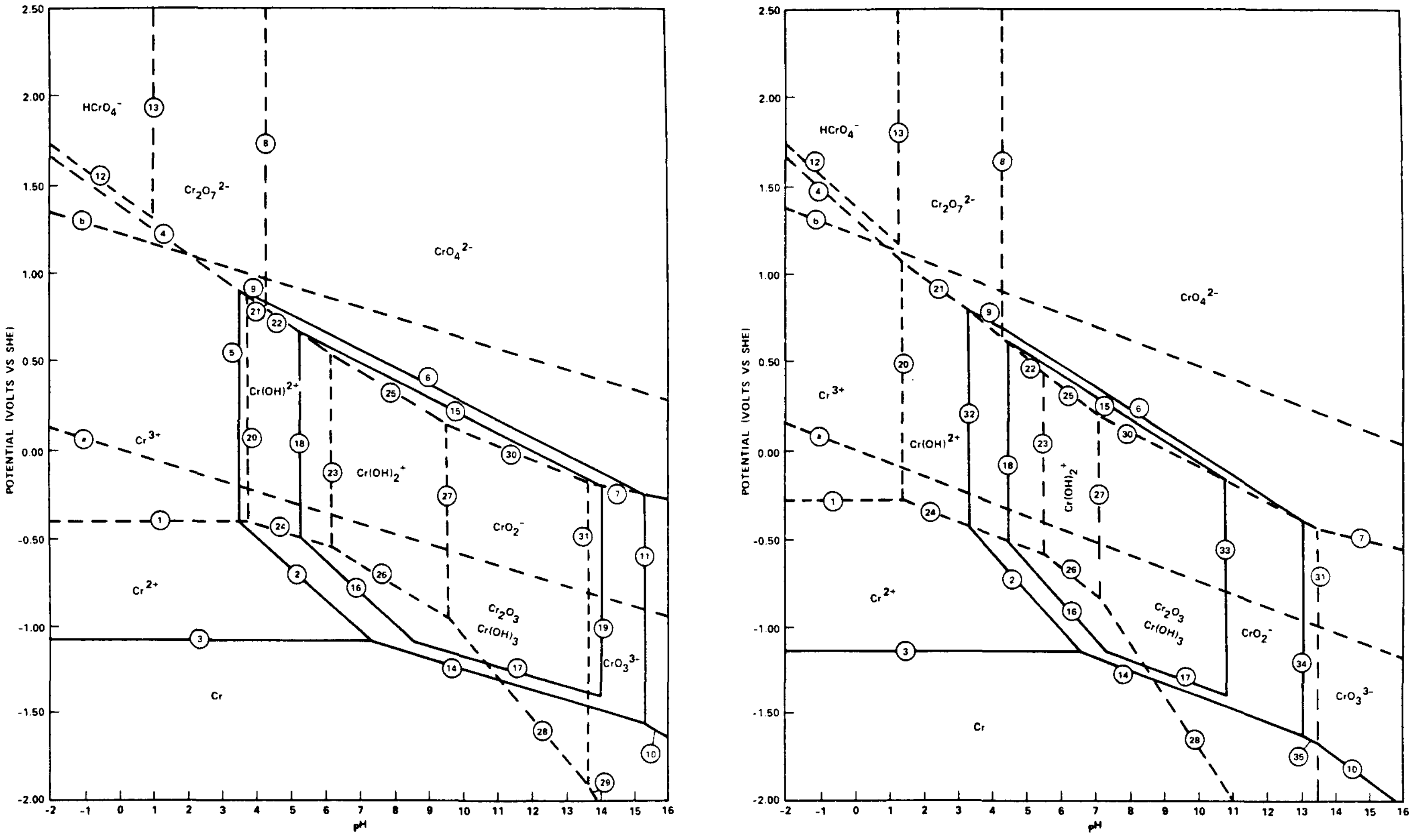

(a) @ 25°C

(b) @ 100°C

FIGURE 8 POTENTIAL-pH DIAGRAM FOR Cr-H_2O SYSTEM

$A_{ion} = 10^{-6}$, $A_{solid} = 1$, $A_{gas} = 1$

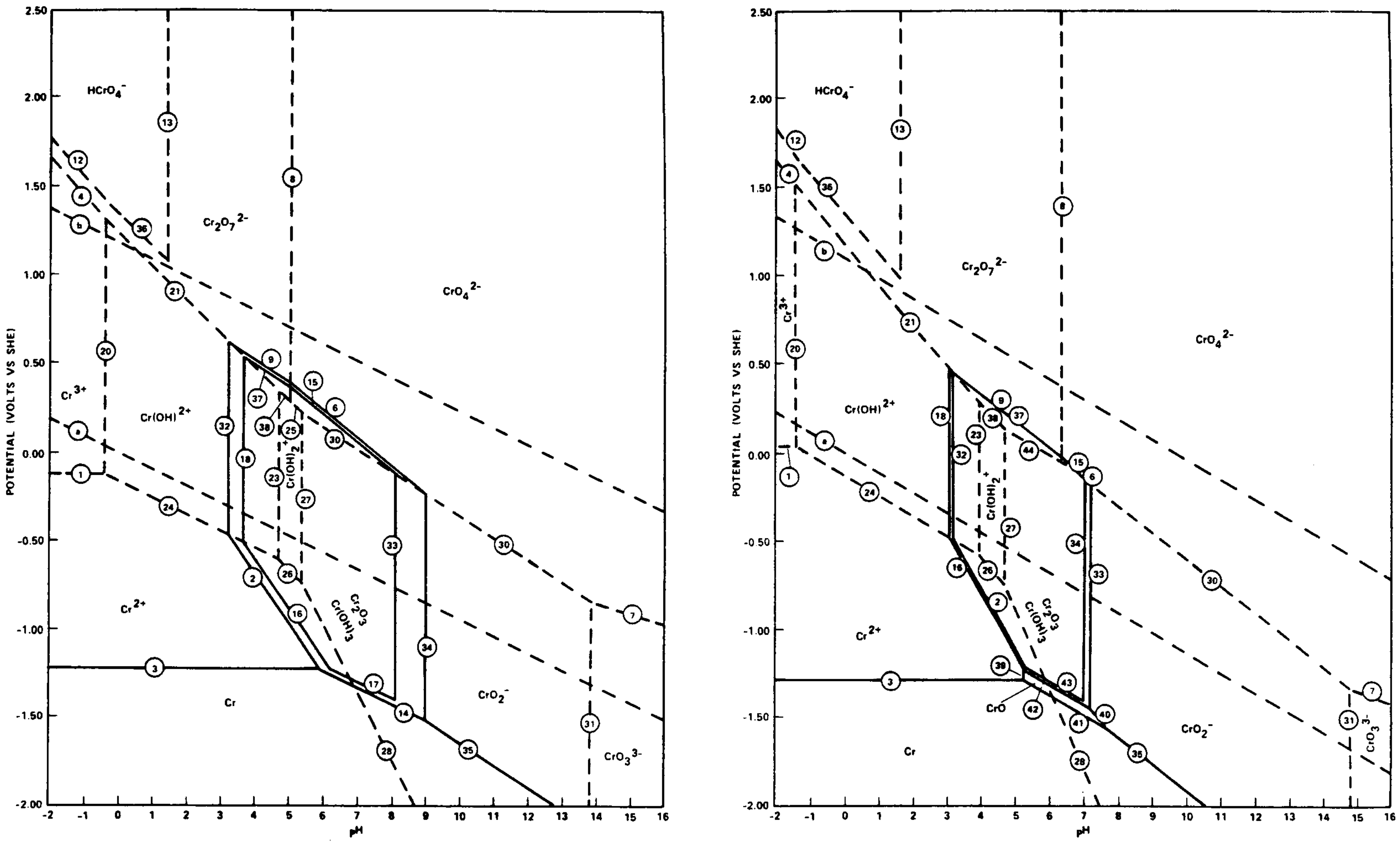

(c) @ 200°C

(d) @ 300°C

FIGURE 8 (Cont'd)

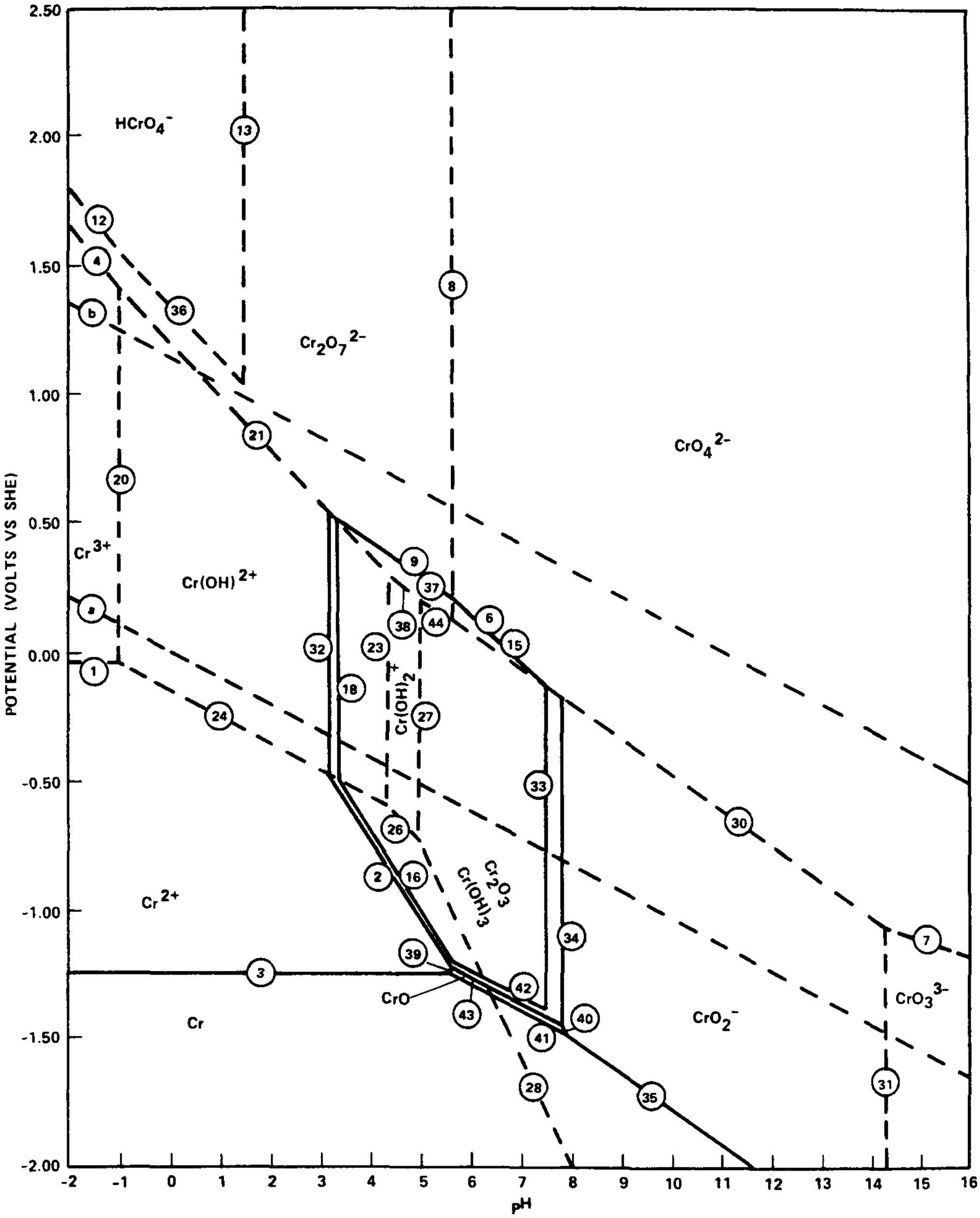

(e) @ 250°C

FIGURE 8 (Cont'd)

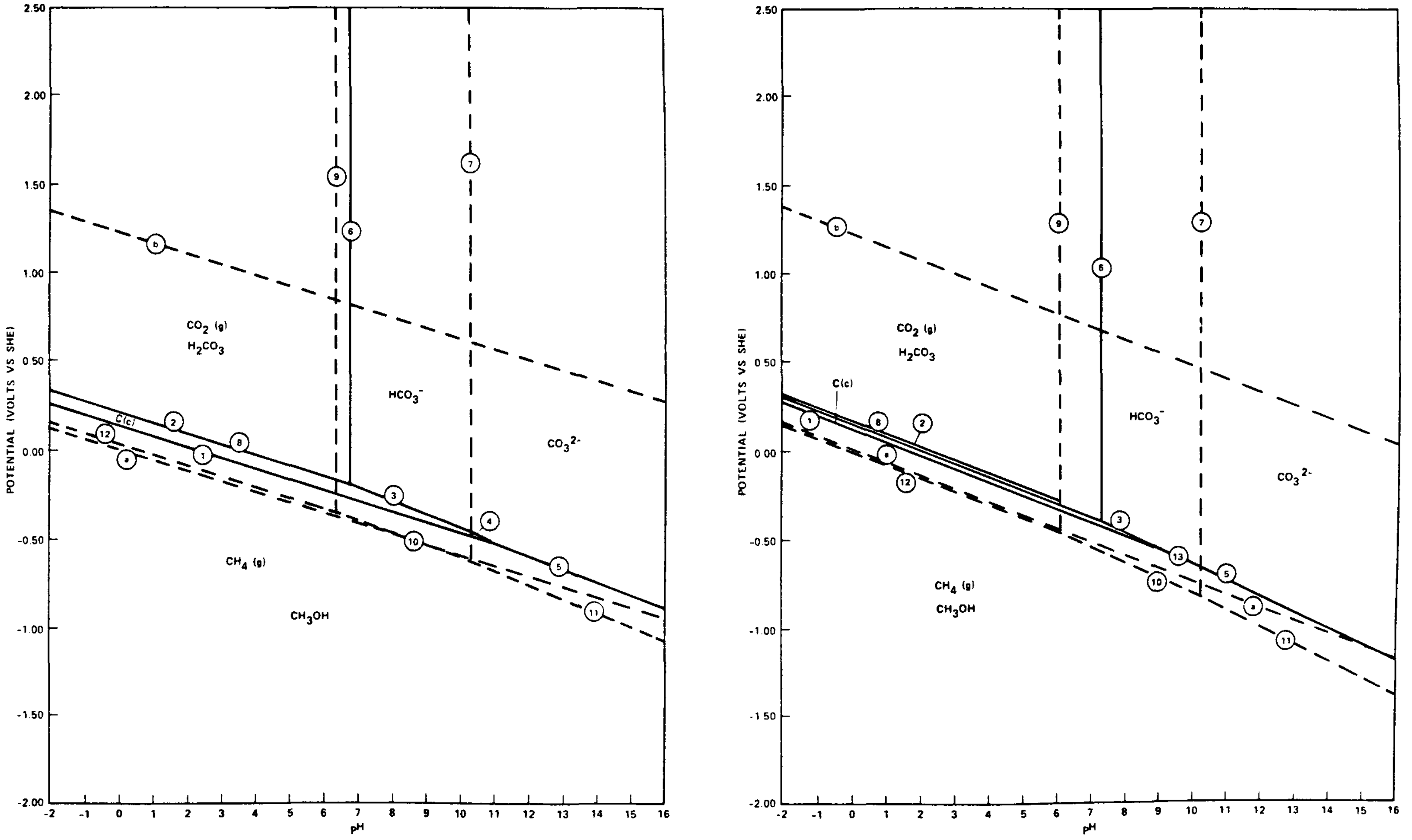

(a) @ 25°C

(b) @ 100°C

FIGURE 9 POTENTIAL-pH DIAGRAM FOR C-H_2O SYSTEM
$A_{\text{dissolved species}} = 10^{-1}$, $A_{\text{gas}} = 1$, $A_{\text{solid}} = 1$

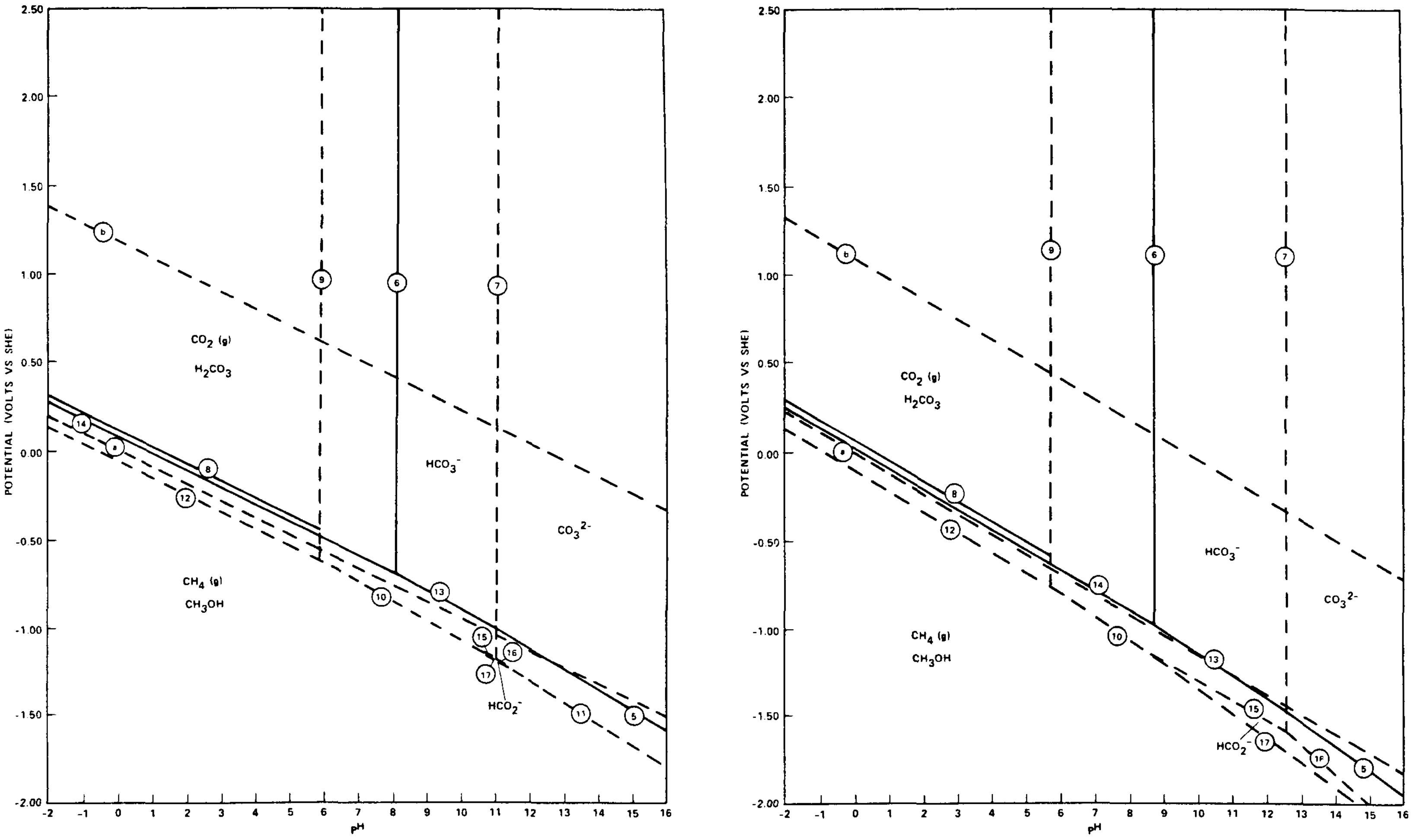

(c) @ 200°C

(d) @ 300°C

FIGURE 9 (Cont'd)

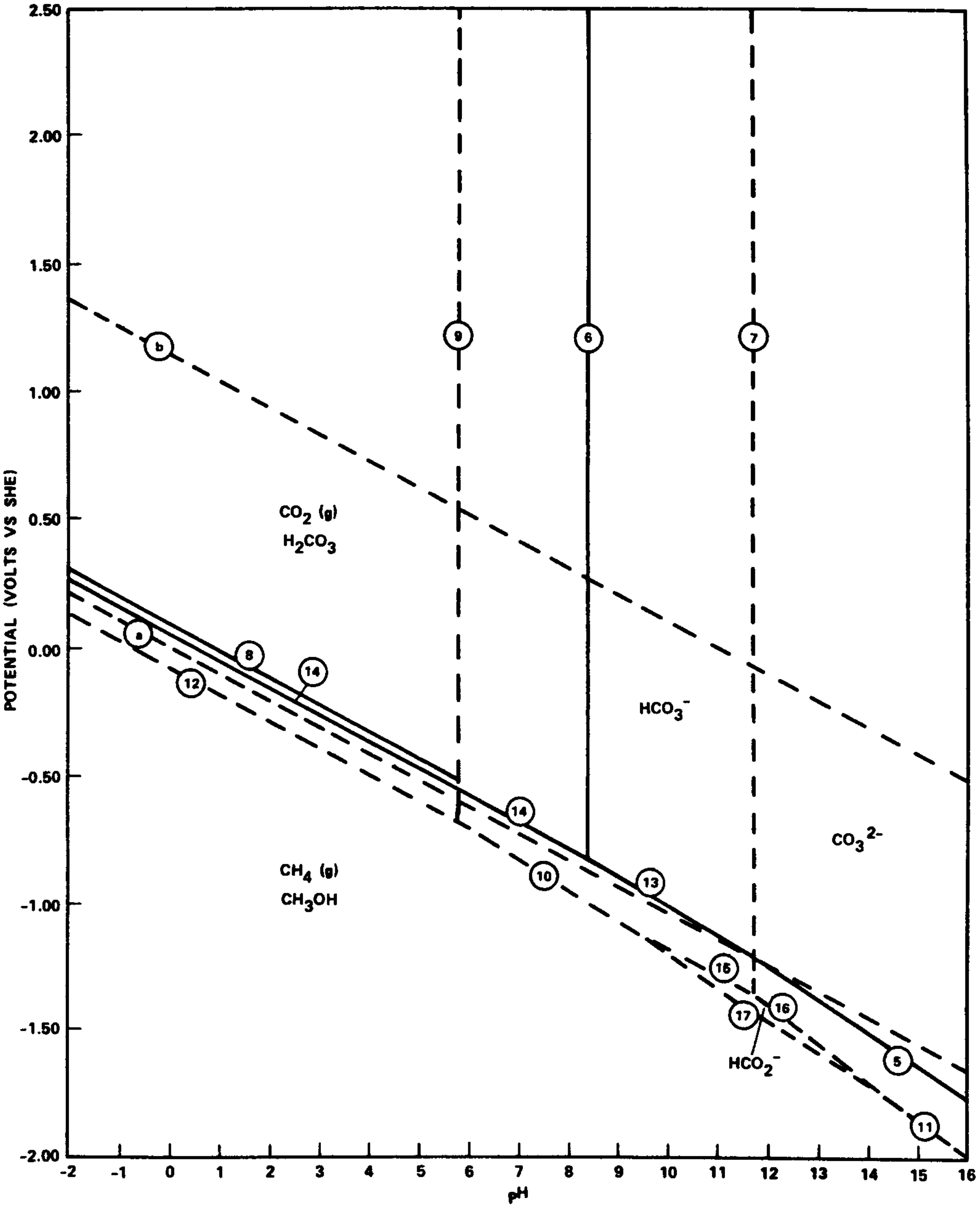

(e) @ 250°C

FIGURE 9 (Cont'd)

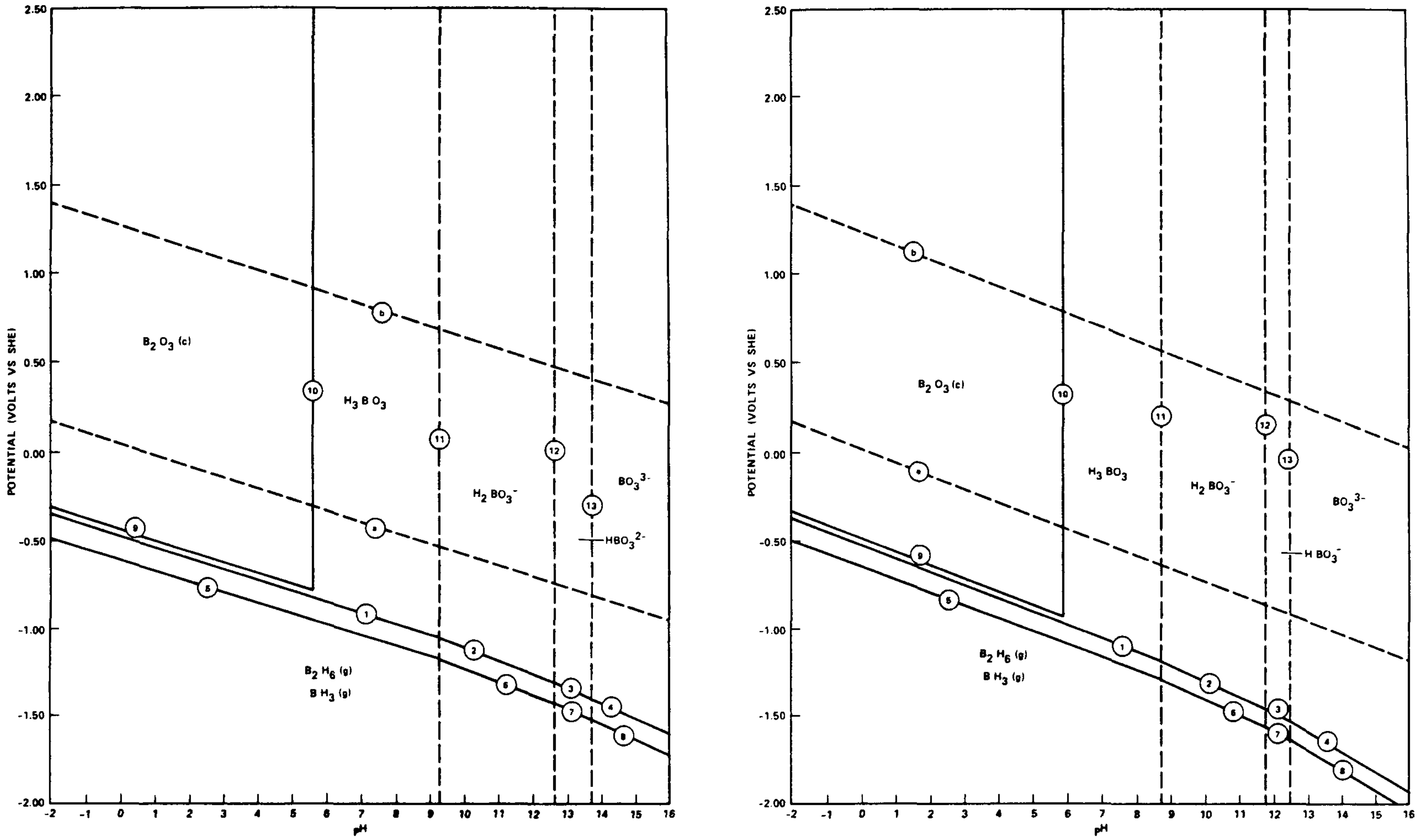

(a) @ 25°C

(b) @ 100°C

FIGURE 10 POTENTIAL-pH DIAGRAM FOR B-H_2O SYSTEM
$A_{\text{dissolved species}} = 10^{-1}$, $A_{\text{gas}} = 1$, $A_{\text{solid}} = 1$

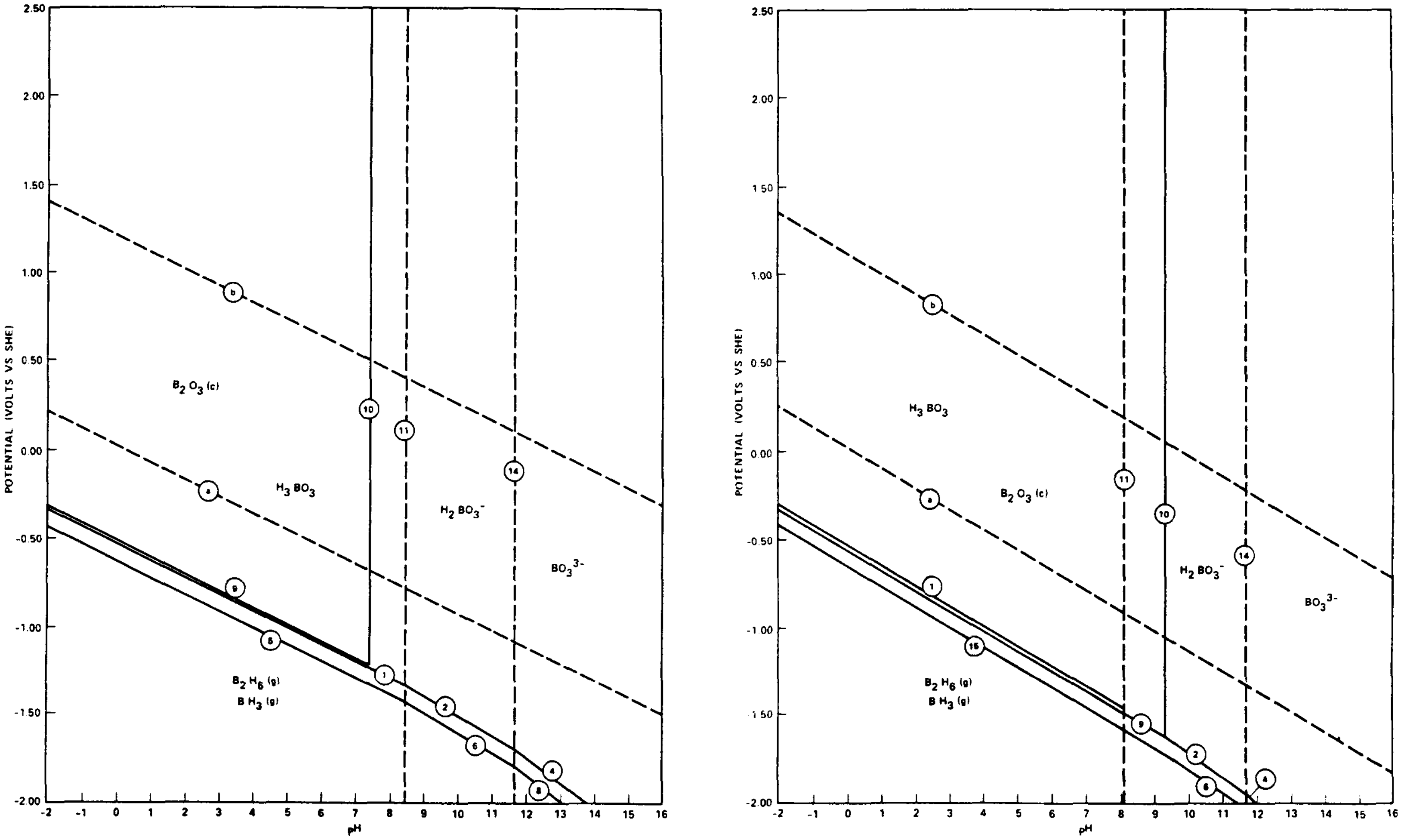

(c) @ 200°C

(d) @ 300°C

FIGURE 10 (Cont'd)

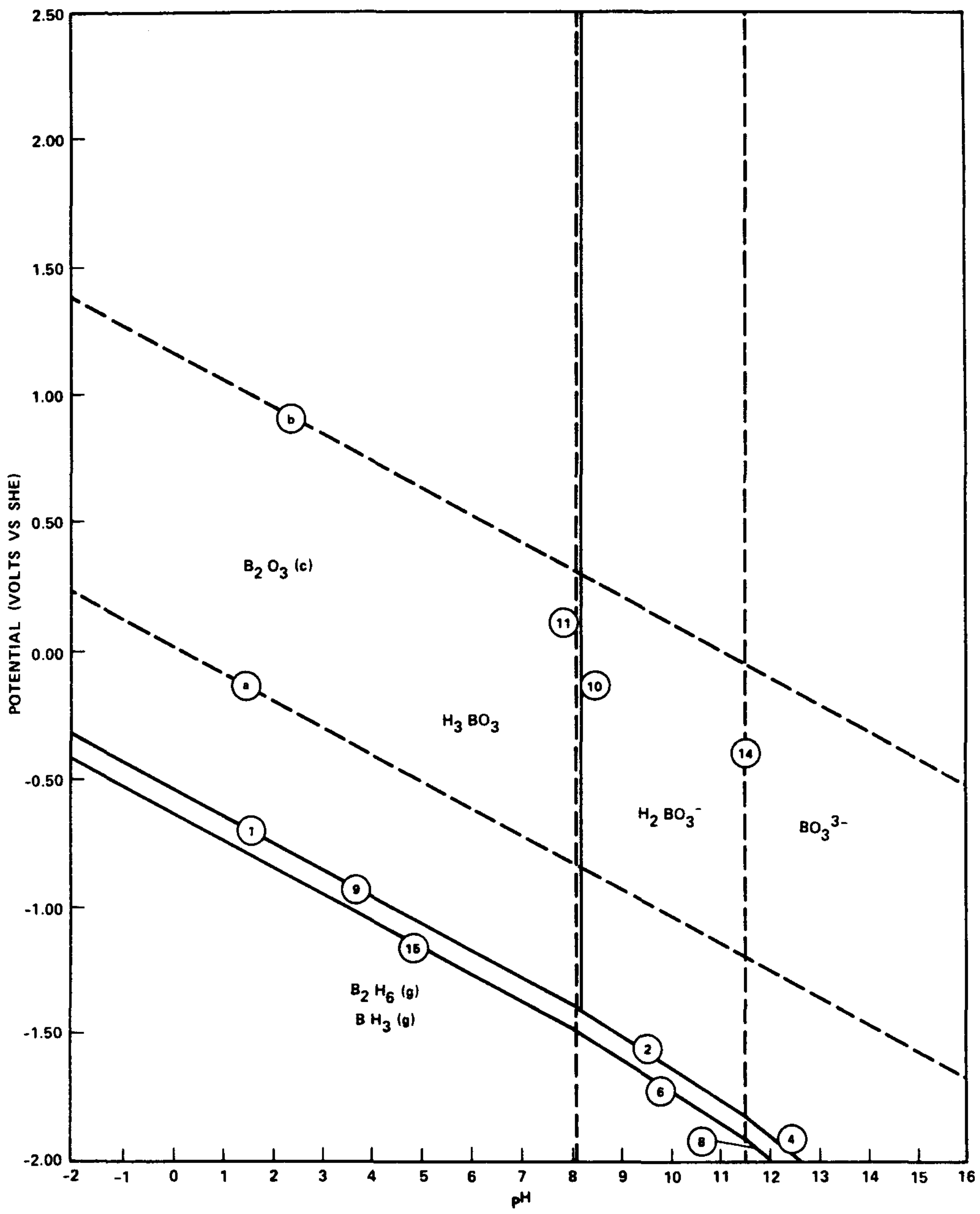

(e) @ 250°C

FIGURE 10 (Cont'd)

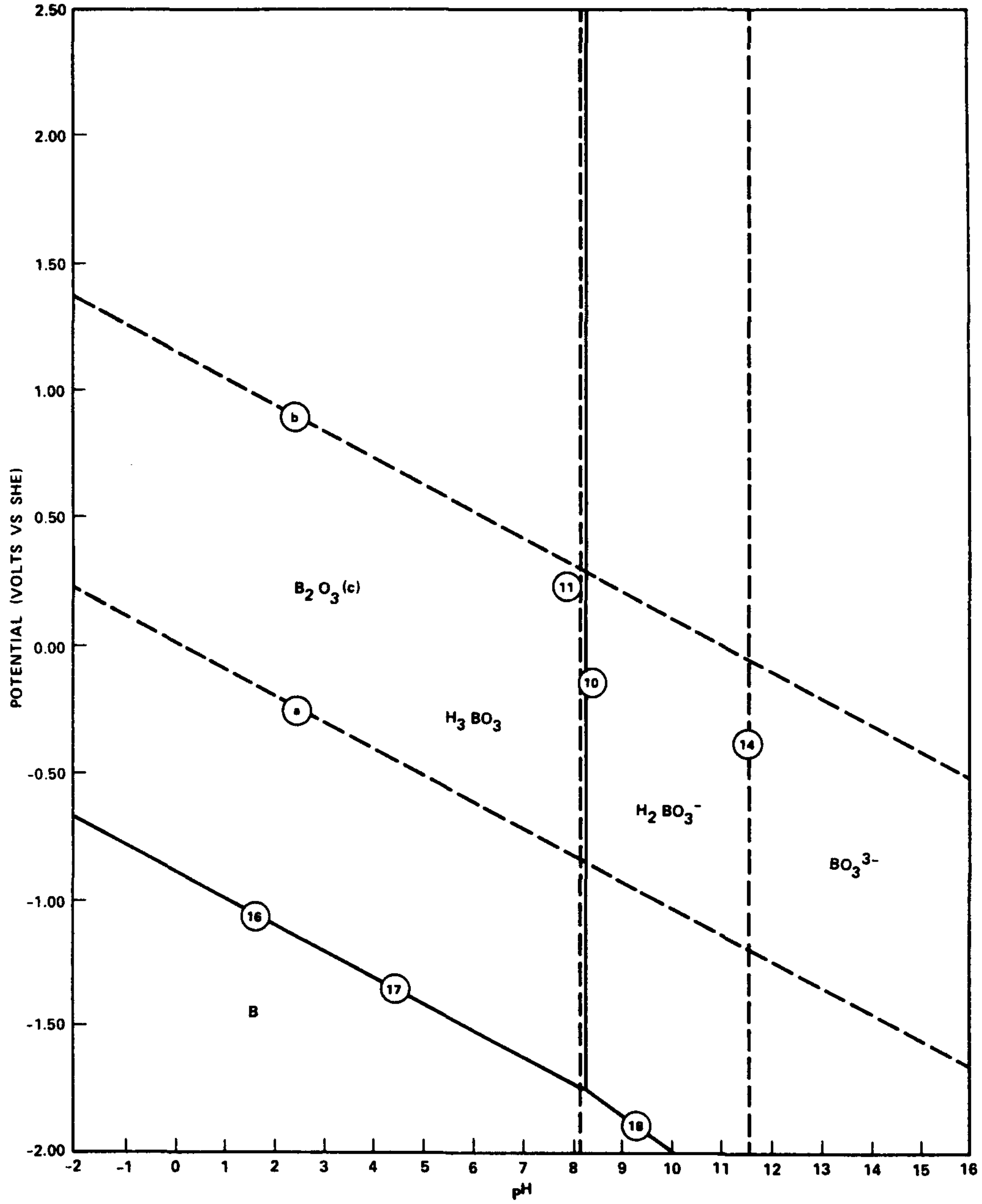

(f) WITHOUT CONSIDERATION OF BORON HYDRIDES AT 250°C

FIGURE 10 (Cont'd)

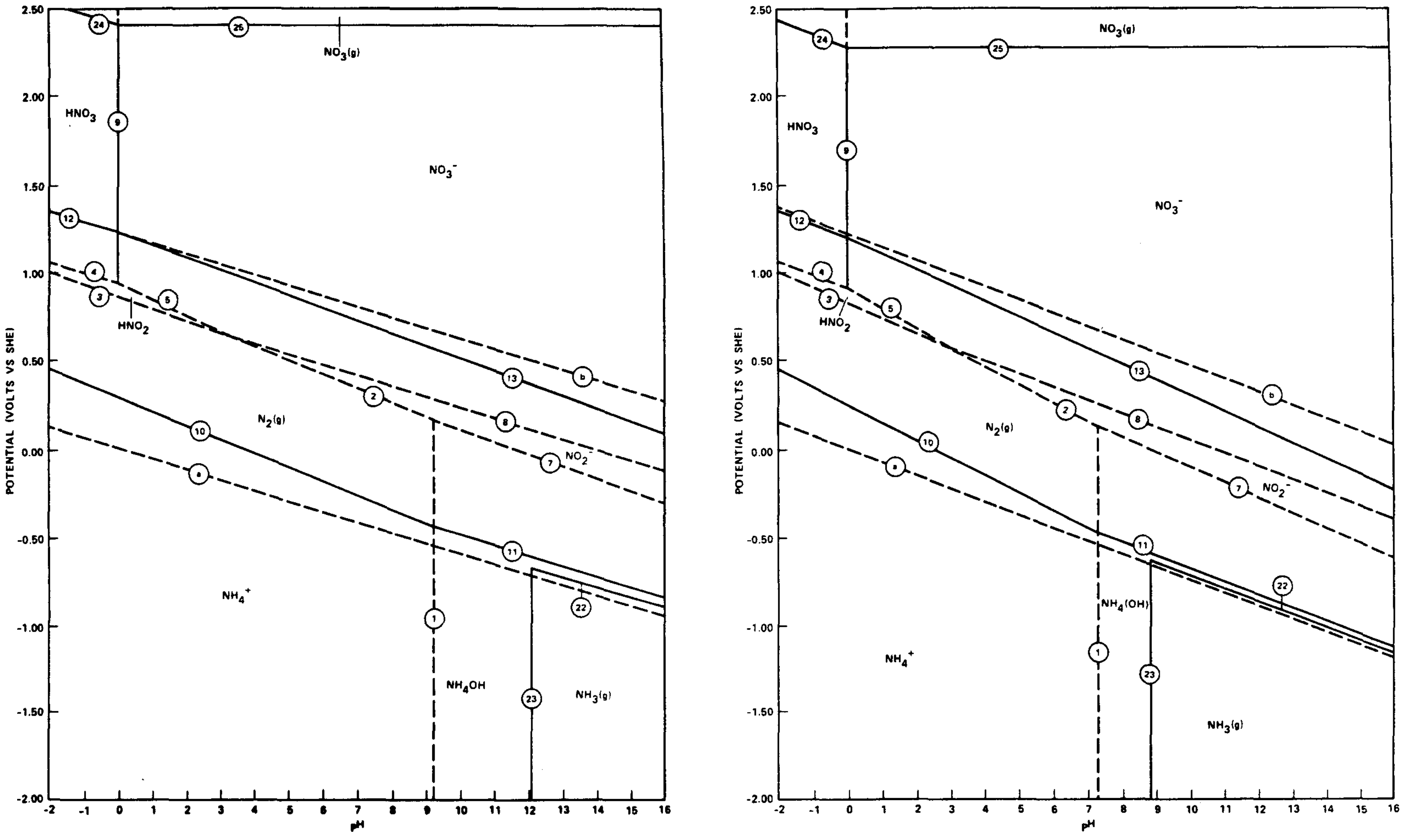

(a) @ 25°C

(b) @ 100°C

FIGURE 11 POTENTIAL-pH DIAGRAM FOR N-H_2O SYSTEMS
$A_{\text{dissolved species}} = 10^{-1}$, $A_{\text{gas}} = 1$

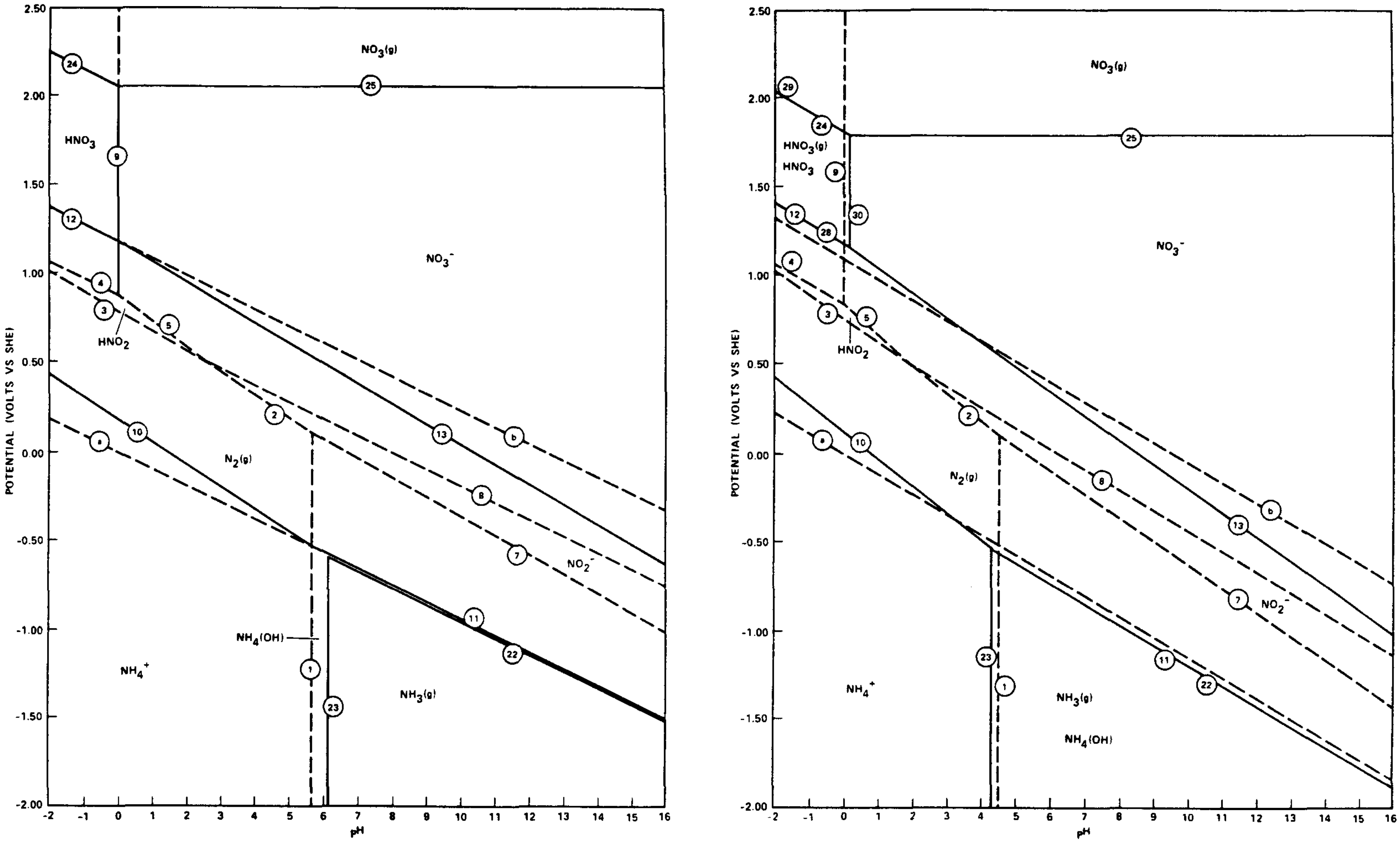

(c) @ 200°C

(d) @ 300°C

FIGURE 11 (Cont'd)

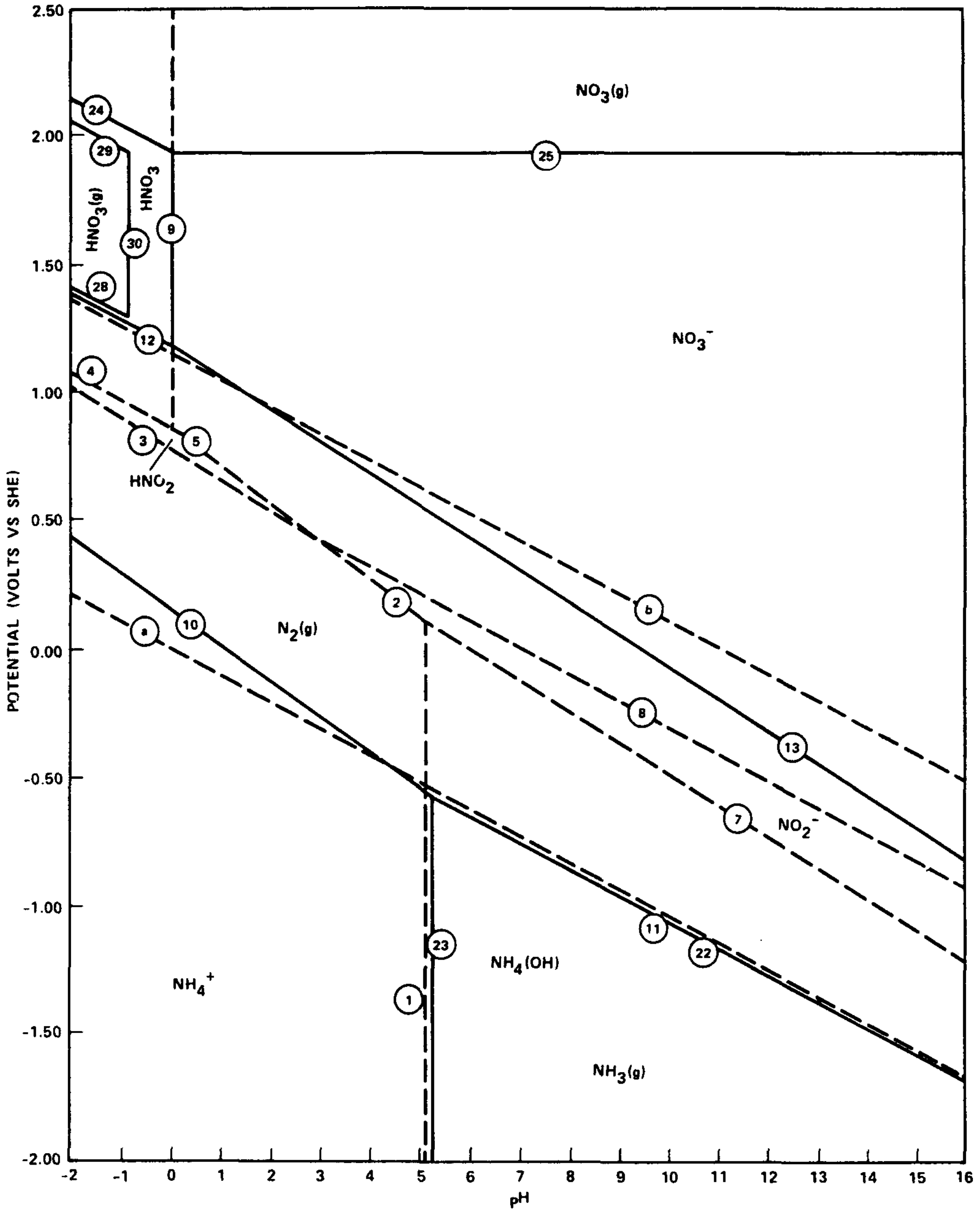

(e) @ 250°C

FIGURE 11 (Cont'd)

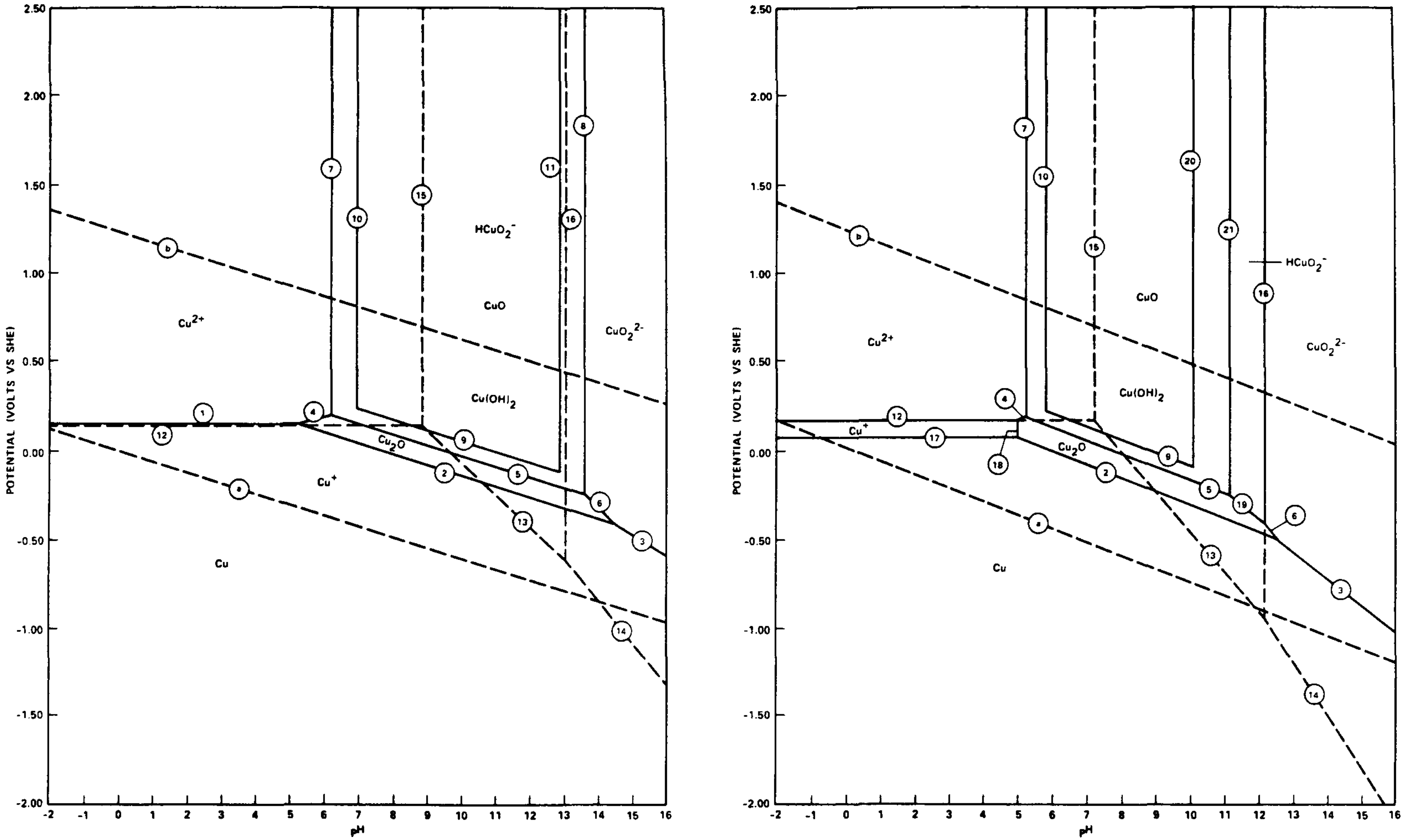

(a) @ 25°C

(b) @ 100°C

FIGURE 12 POTENTIAL-pH DIAGRAM FOR $Cu\text{-}H_2O$ SYSTEM
$A_{ion} = 10^{-6}$, $A_{solid} = 1$, $A_{gas} = 1$

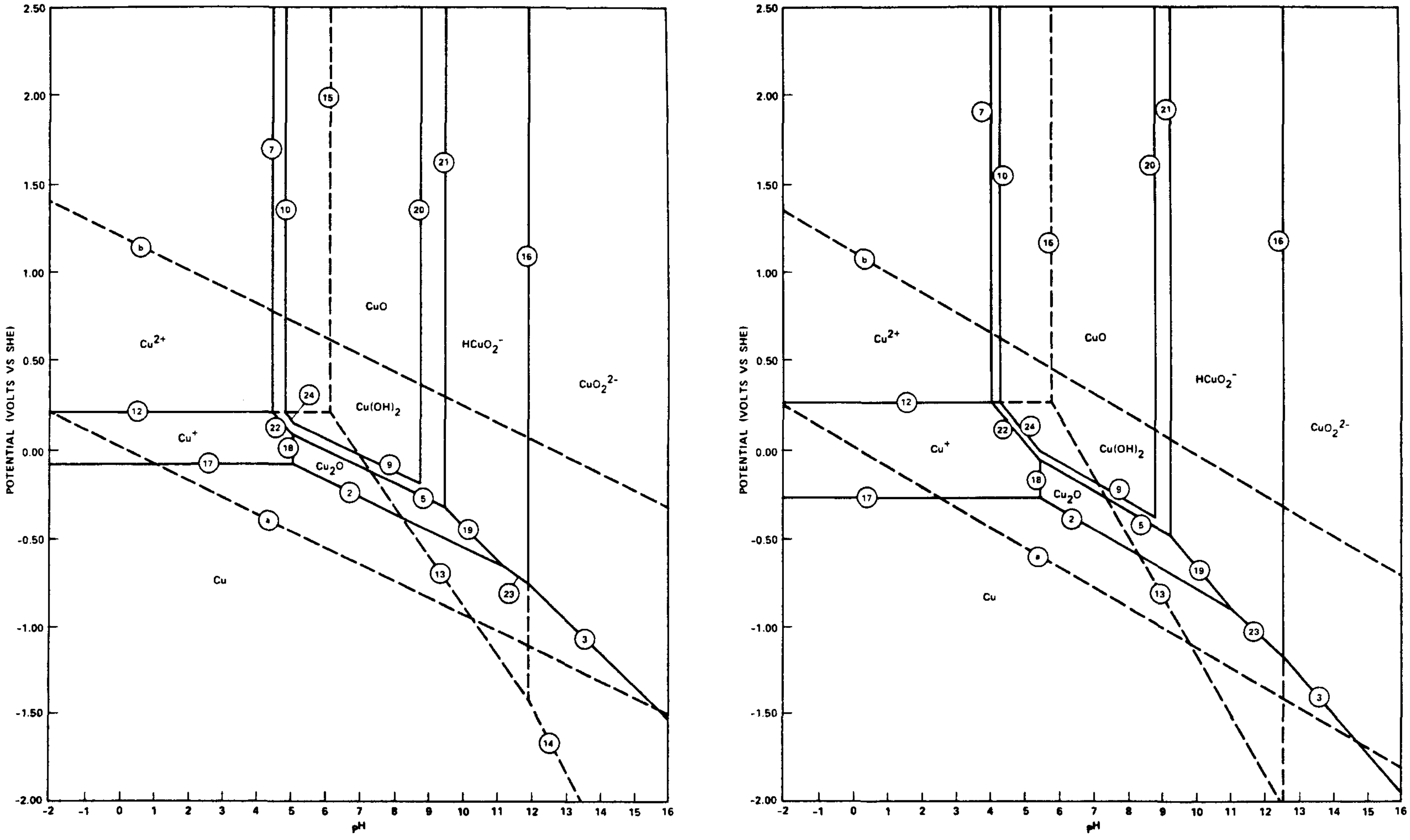

(c) @ 200°C

(d) @ 300°C

FIGURE 12 (Cont'd)

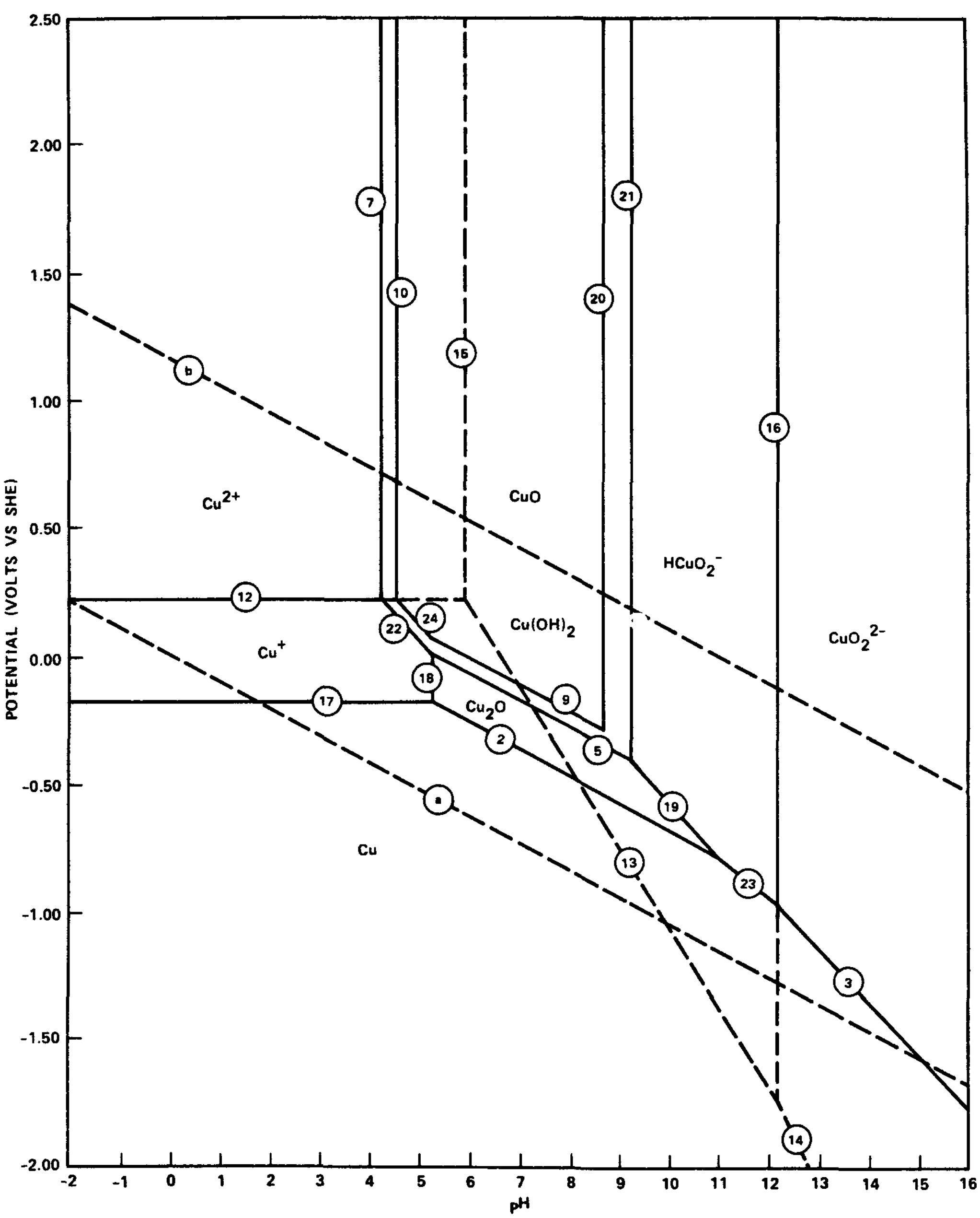

(e) @ 250°C

FIGURE 12 (Cont'd)

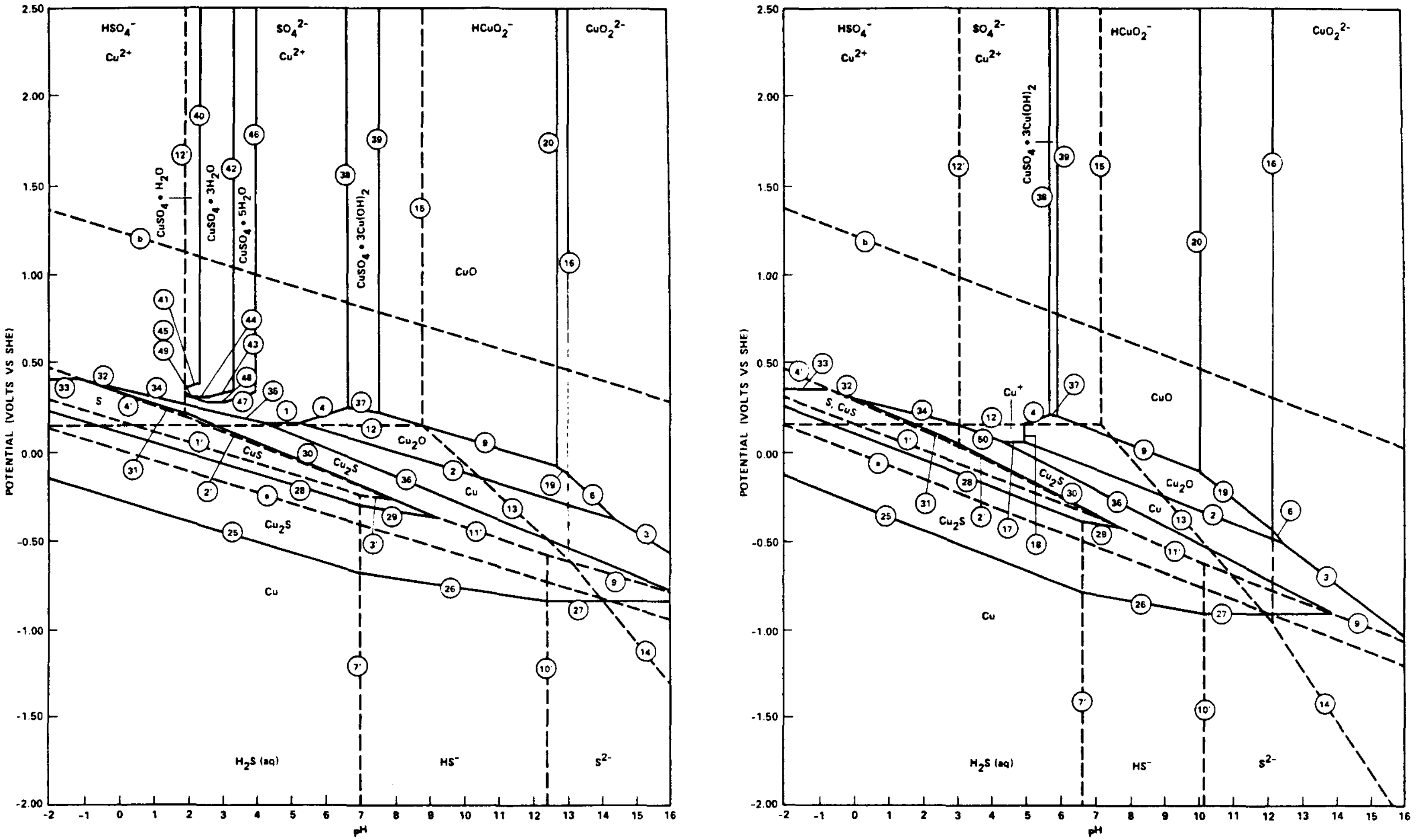

(a) @ 25°C

(b) @ 100°C

FIGURE 13 POTENTIAL-pH DIAGRAM FOR Cu-S-H_2O SYSTEM AT $A_{ion} = 10^{-6}$, $A_{dissolved\ sulfide} = 10^{-1}$, $A_{solid} = 1$, $A_{gas} = 1$

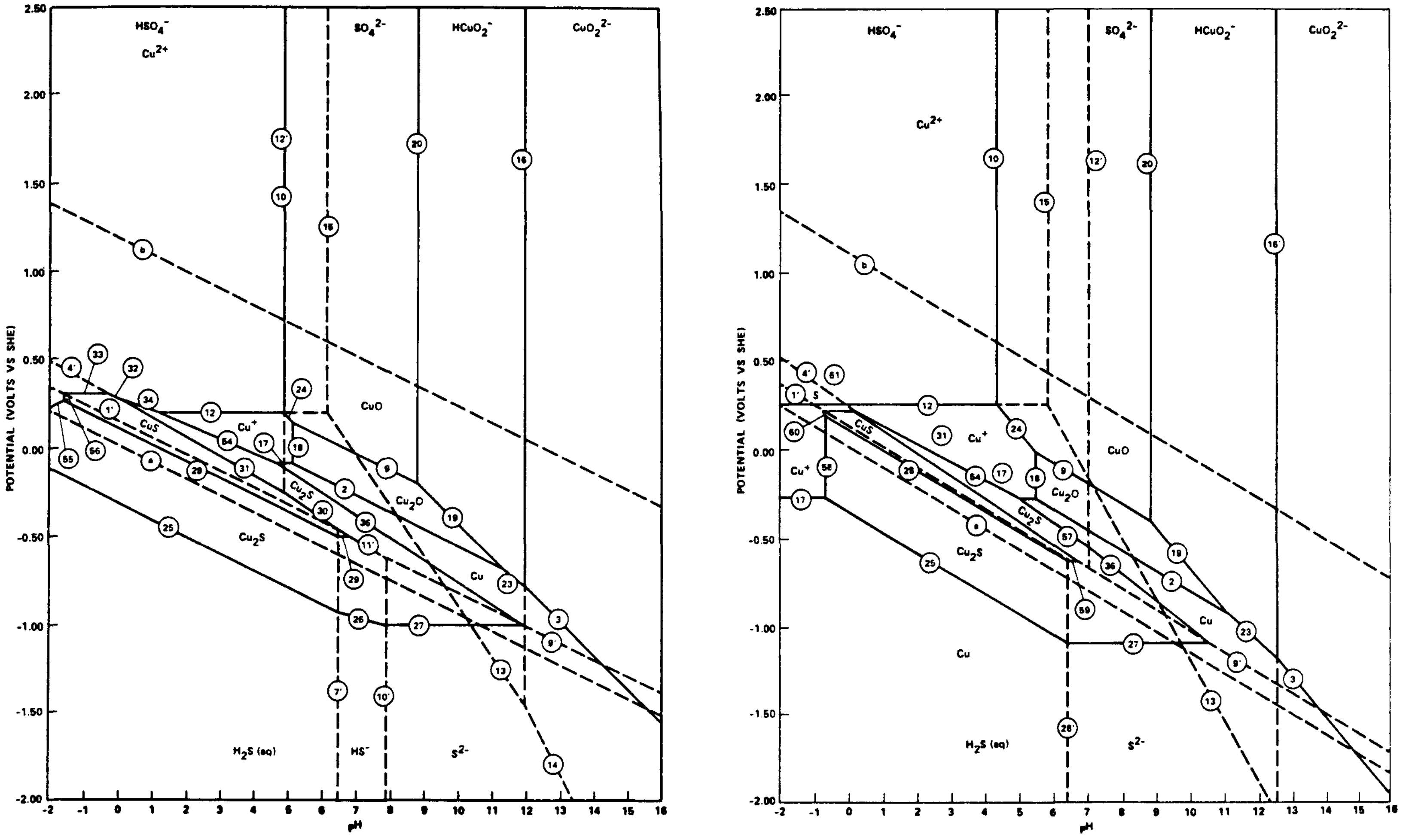

(c) @ 200°C

(d) @ 300°C

FIGURE 13 (Cont'd)

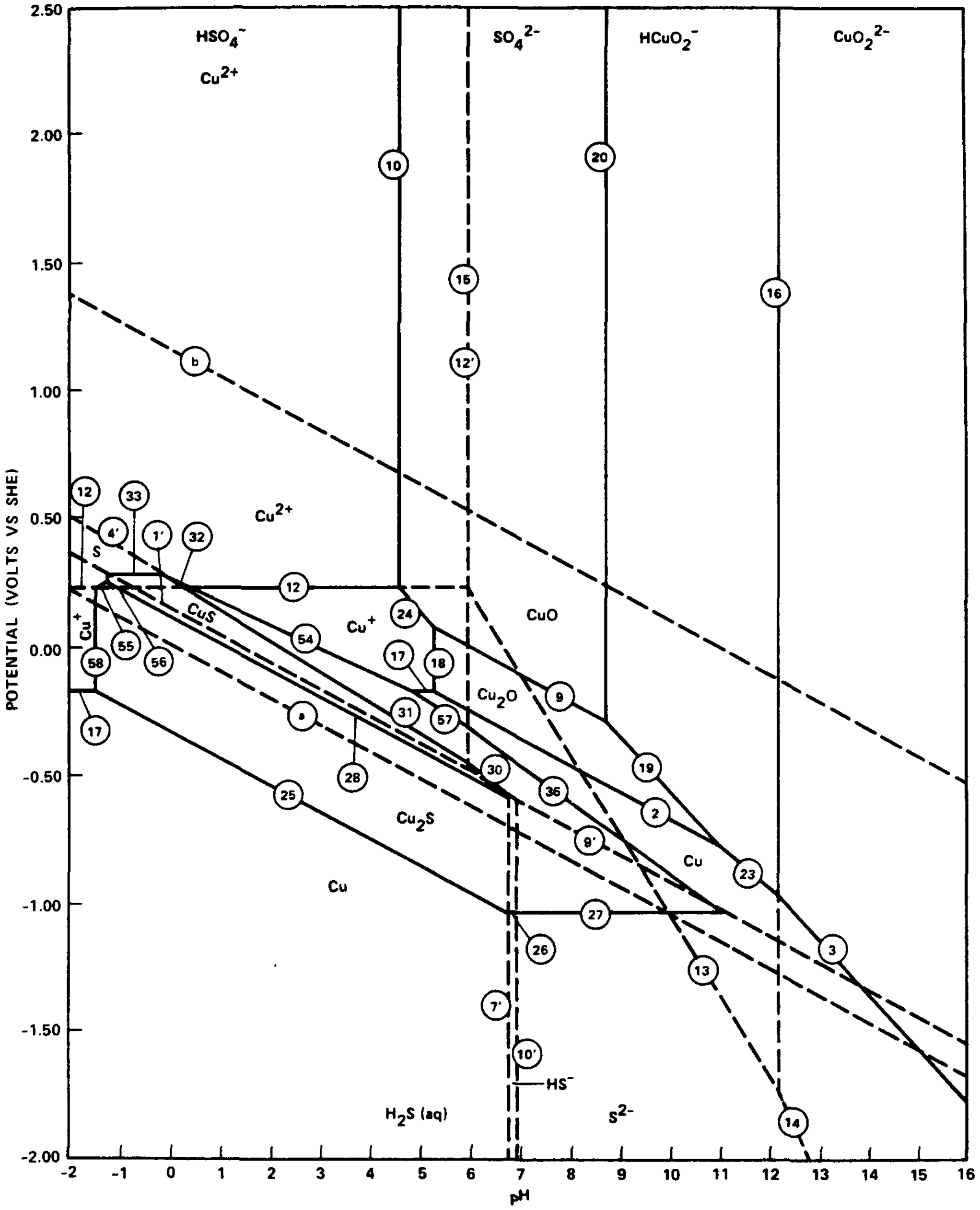

(e) @ 250°C

FIGURE 13 (Cont'd)

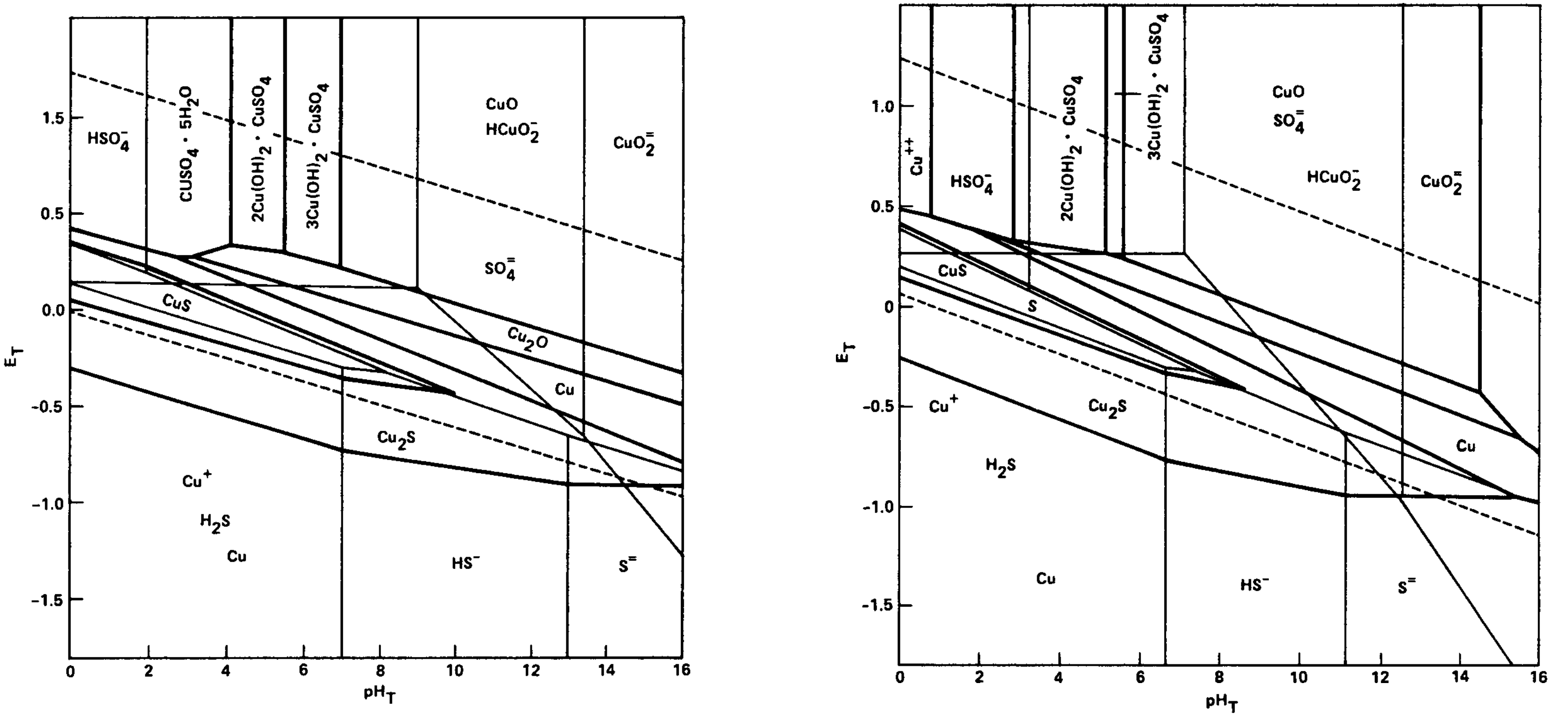

(f) E-pH DIAGRAM AT 25°C FOR THE $CuSO_4$-H_2SO_4-H_2O SYSTEM [FROM REF. 8]

(g) E-pH DIAGRAM AT 100°C FOR THE $CuSO_4$-H_2SO_4-H_2SO_4-H_2O SYSTEM [FROM REF. 8]

FIGURE 13 (Cont'd)

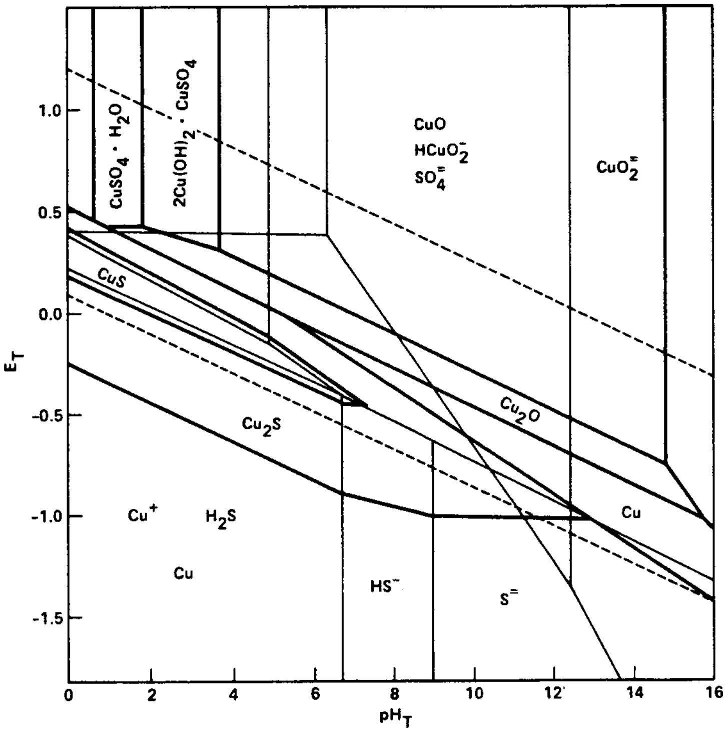

(h) E-pH DIAGRAM AT 200°C FOR THE $CuSO_4$-H_2SO_4-H_2O SYSTEM [FROM REF. 8]

FIGURE 13 (Cont'd)

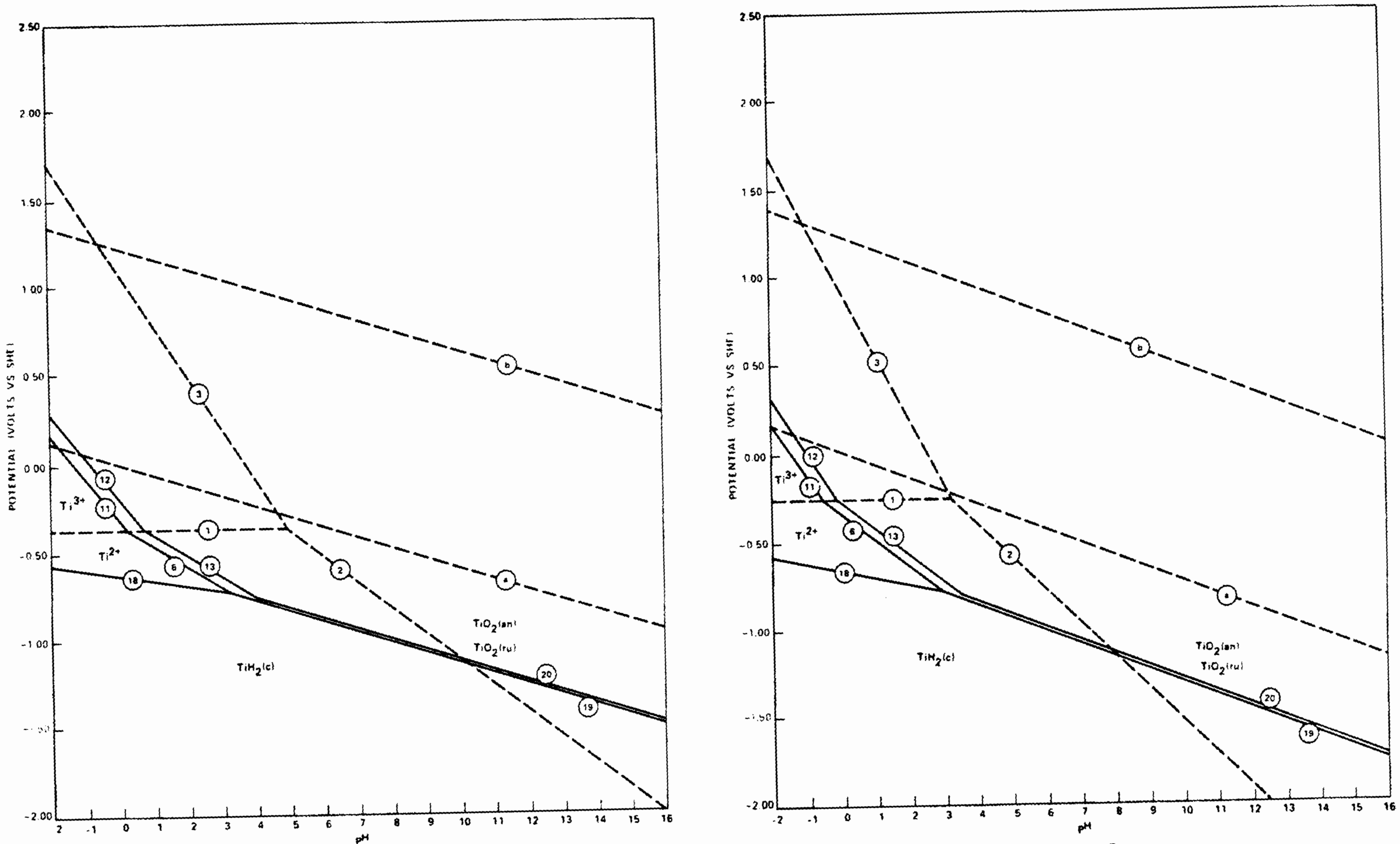

(a) @ 25°C

(b) @ 100°C

FIGURE 14 POTENTIAL-pH DIAGRAM FOR Ti-H_2O SYSTEM
$A_{ion} = 10^{-6}$, $A_{solid} = 1$, $A_{gas} = 1$

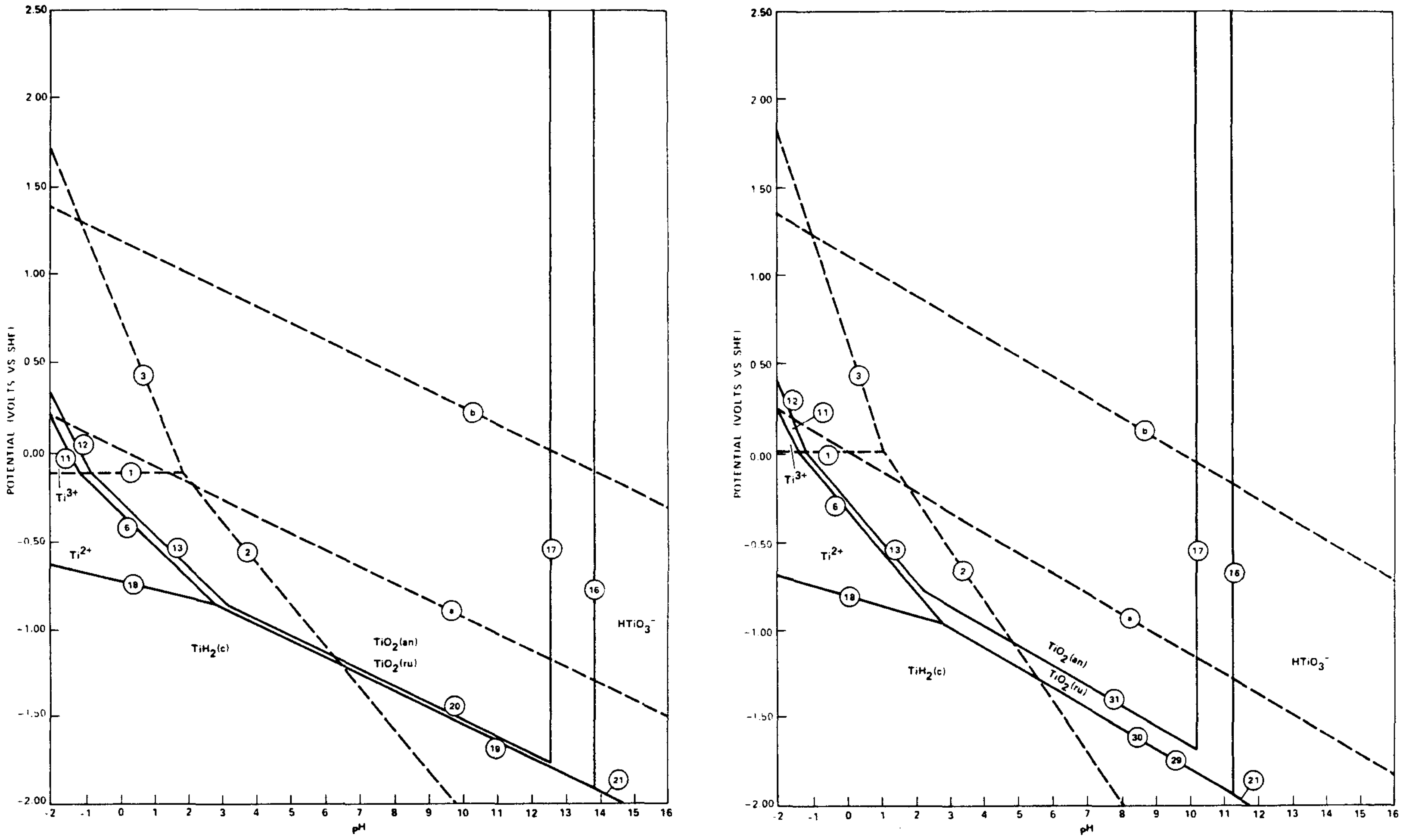

(c) @ 200°C

(d) @ 300°C

FIGURE 14 (Cont'd)

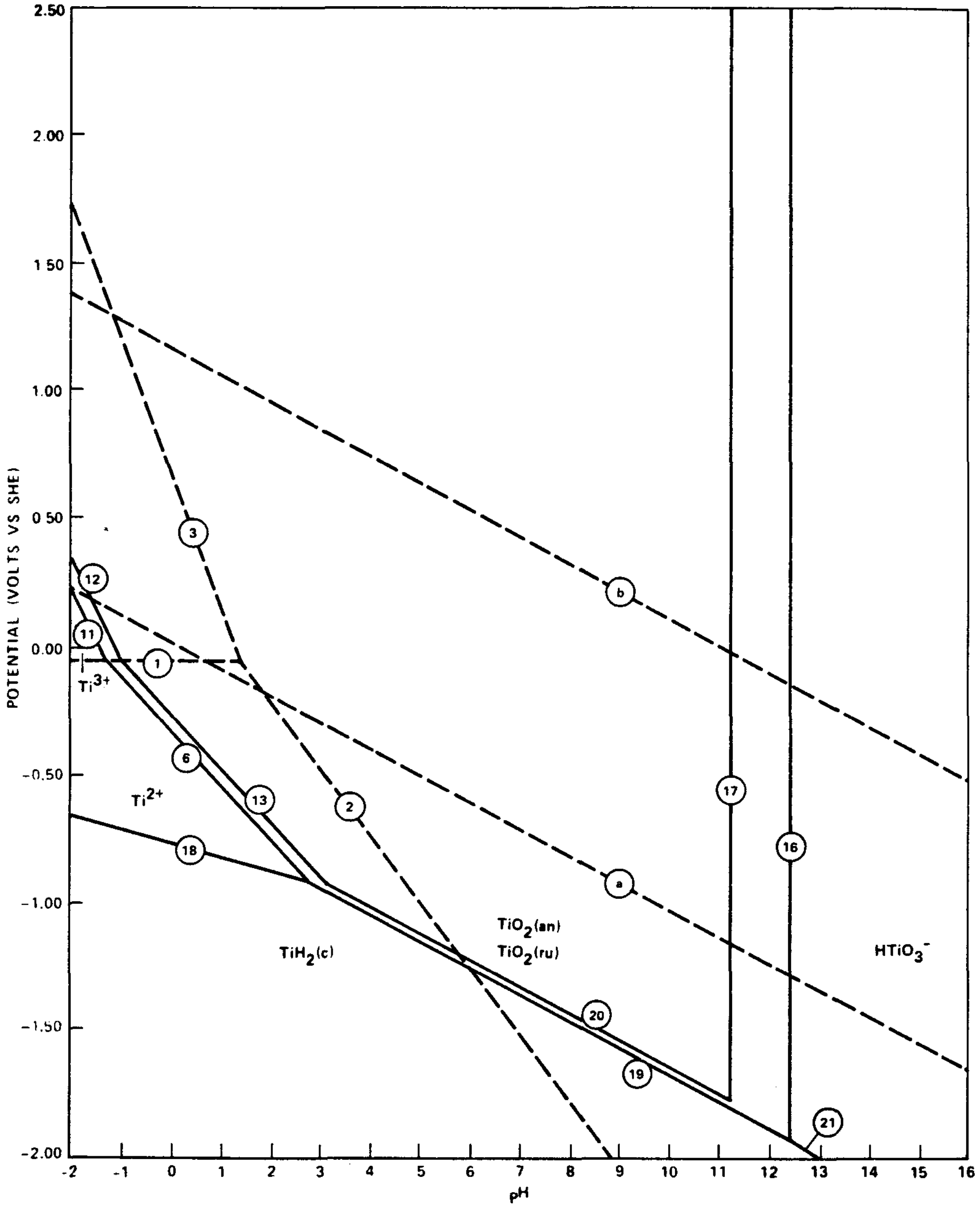

(e) @ 250°C

FIGURE 14 (Cont'd)

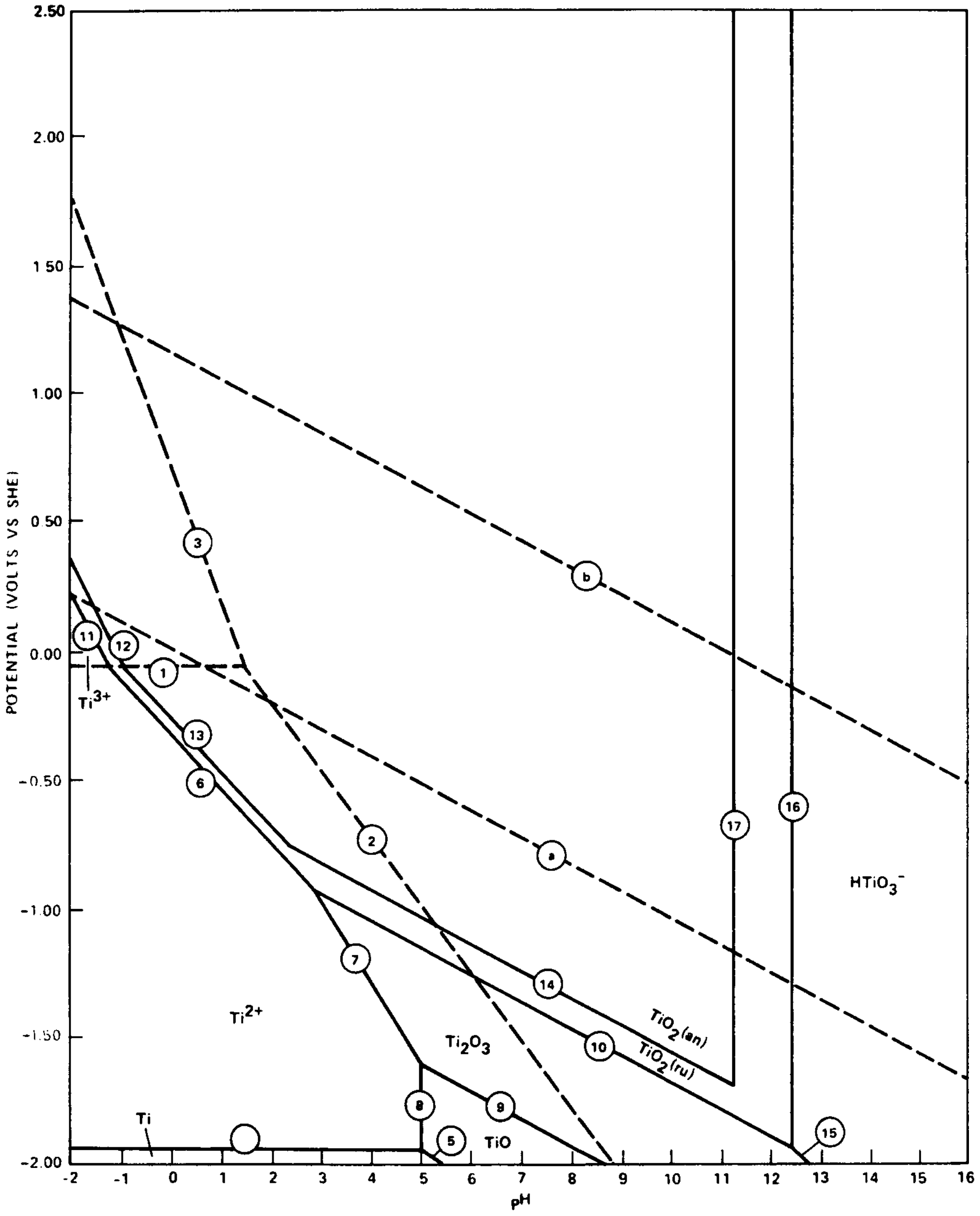

(f) WITHOUT CONSIDERATION OF TiH_2 AT 250°C

FIGURE 14 (Cont'd)

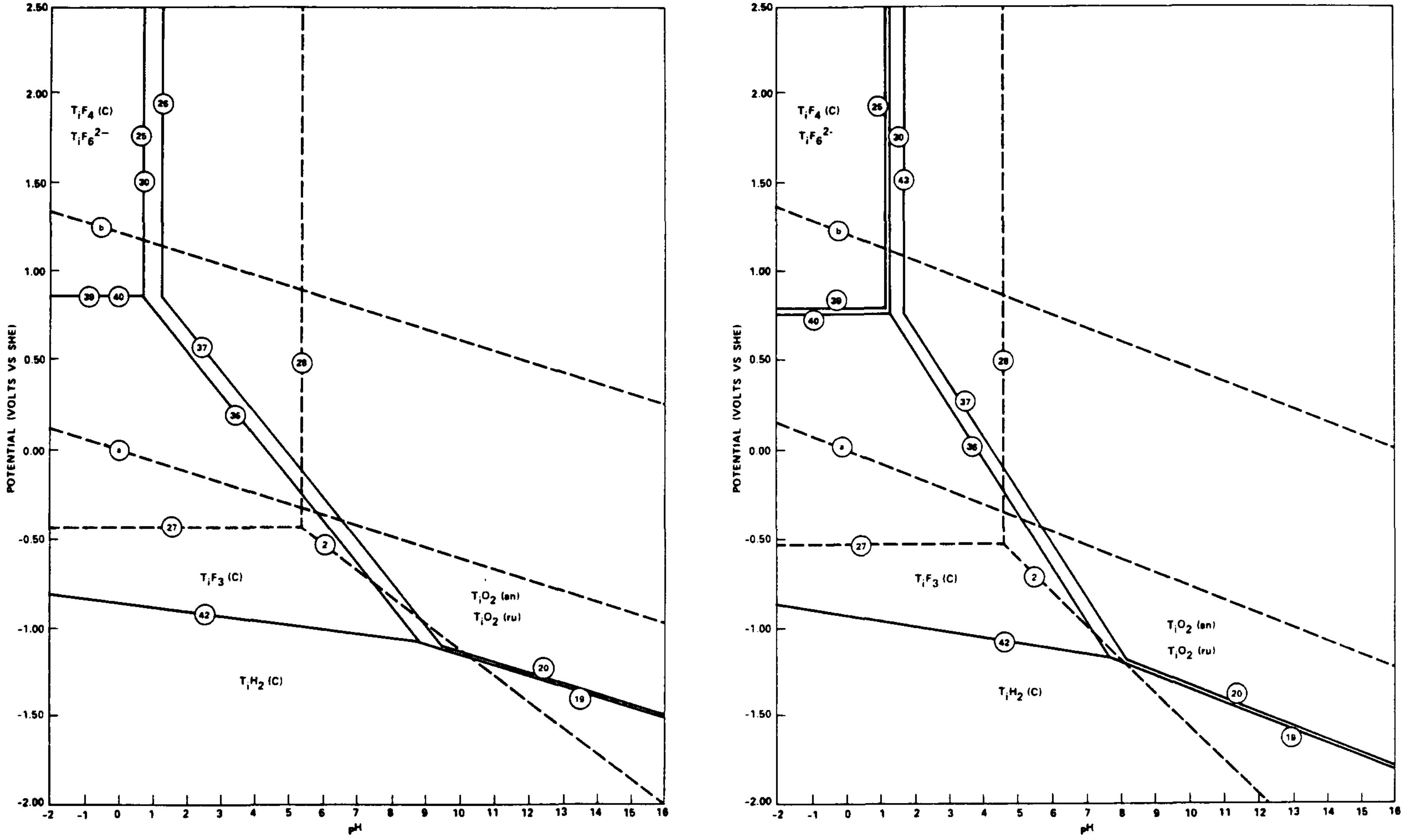

(a) @ 25°C

(b) @ 100°C

FIGURE 15 POTENTIAL-pH DIAGRAM FOR T_i-F^--H_2O SYSTEM
$A_{ion} = 10^{-6}$, $A_{dissolved\ fluoride} = 10^{-1}$, $A_{solid} = 1$, $A_{gas} = 1$

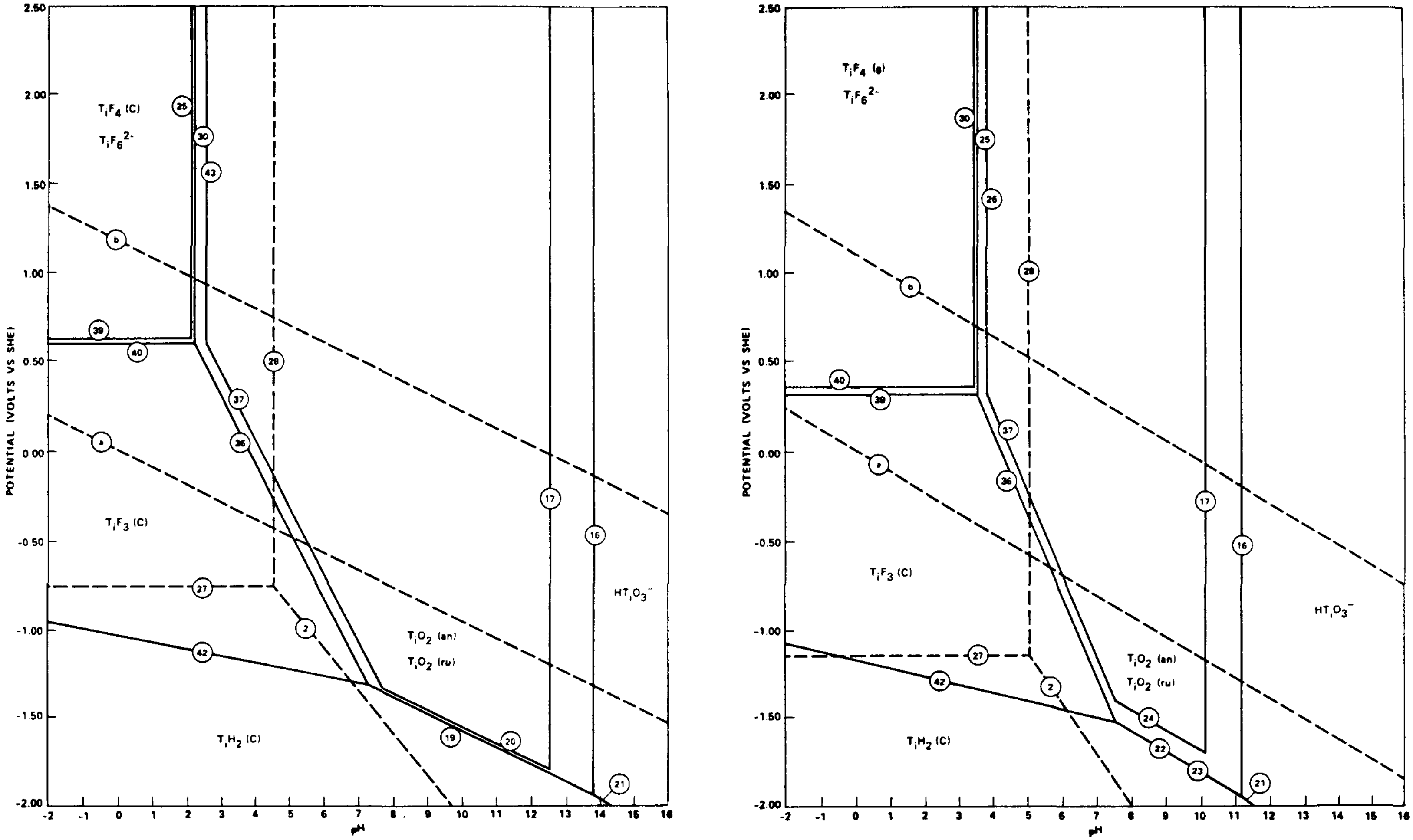

(c) @ 200°C

(d) @ 300°C

FIGURE 15 (Cont'd)

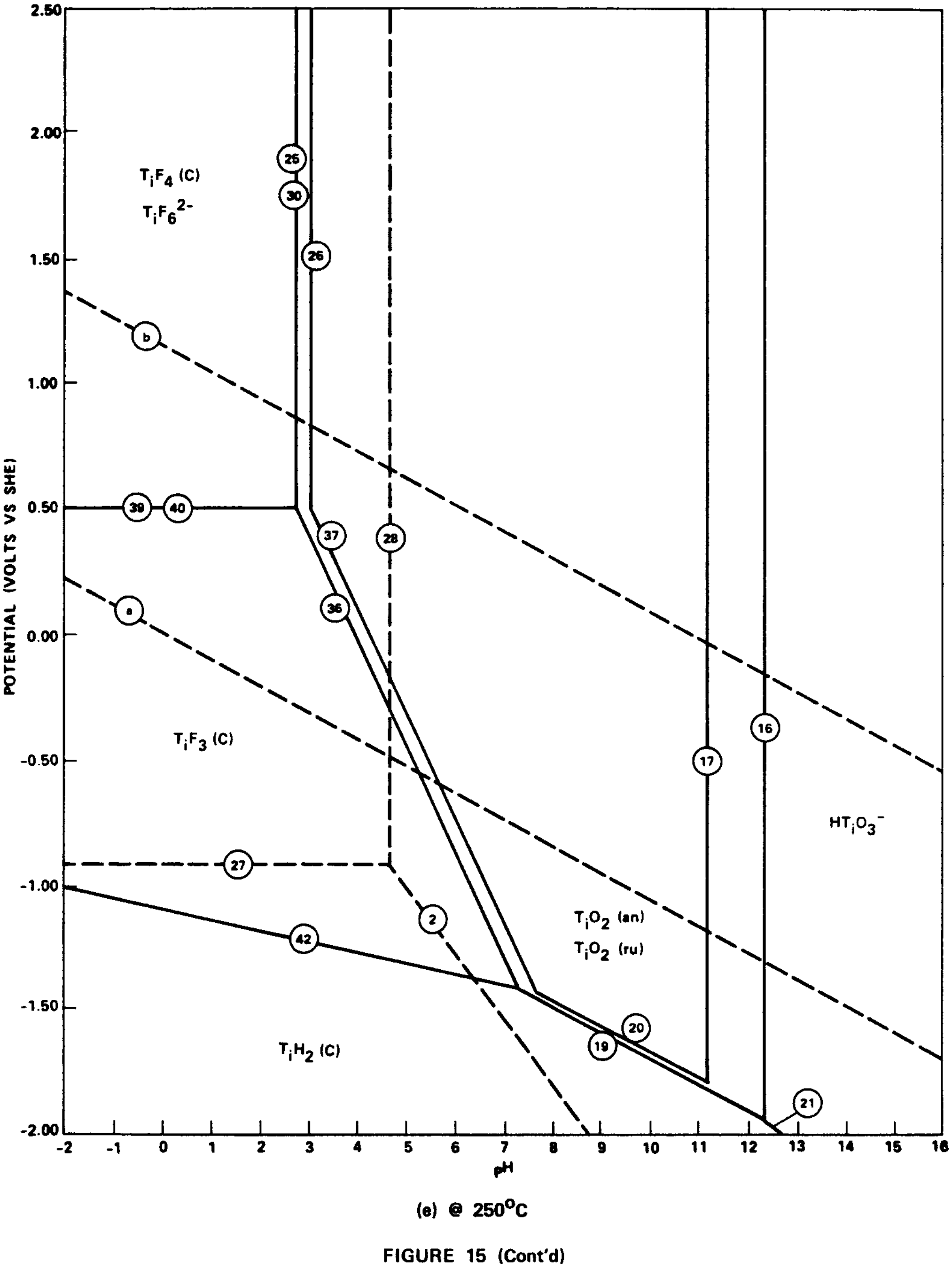

(e) @ 250°C

FIGURE 15 (Cont'd)

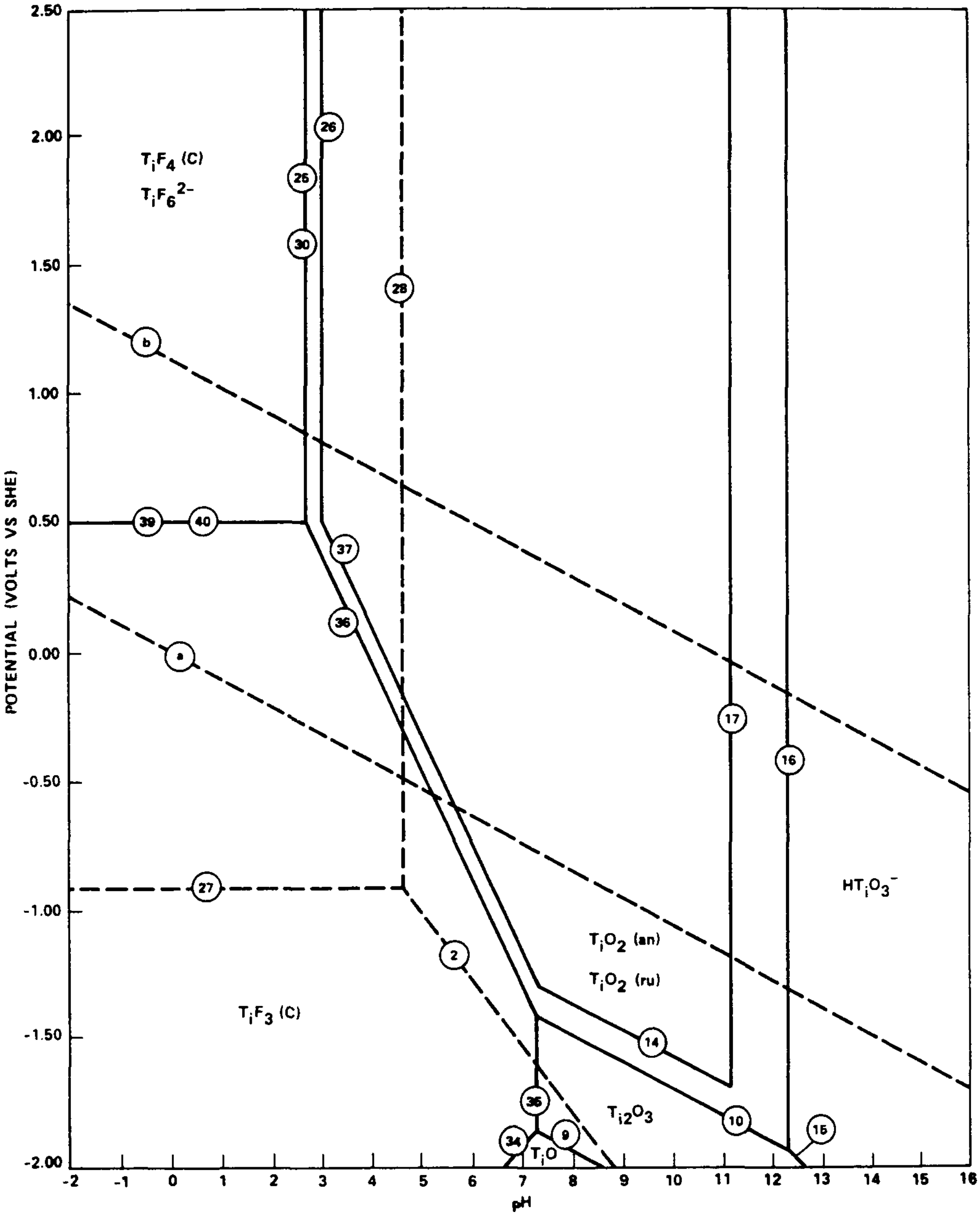

(f) WITHOUT CONSIDERATION OF T_iH_2(C) AT 250°C

FIGURE 15 (Cont'd)

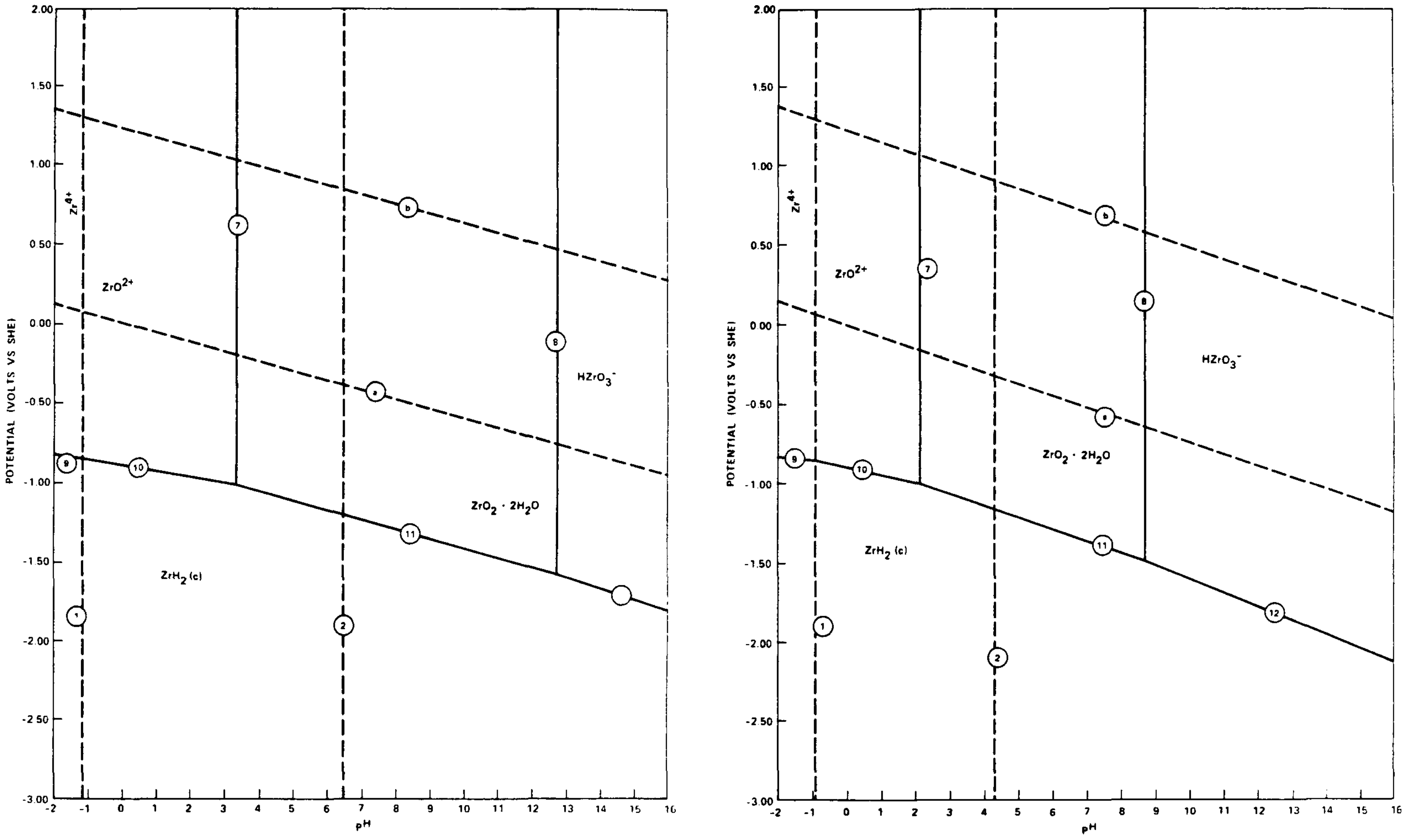

(a) @ 25°C

(b) @ 100°C

FIGURE 16 POTENTIAL-pH DIAGRAM FOR $Zr-H_2O$ SYSTEM
$A_{ion} = 10^{-6}$, $A_{solid} = 1$, $A_{gas} = 1$

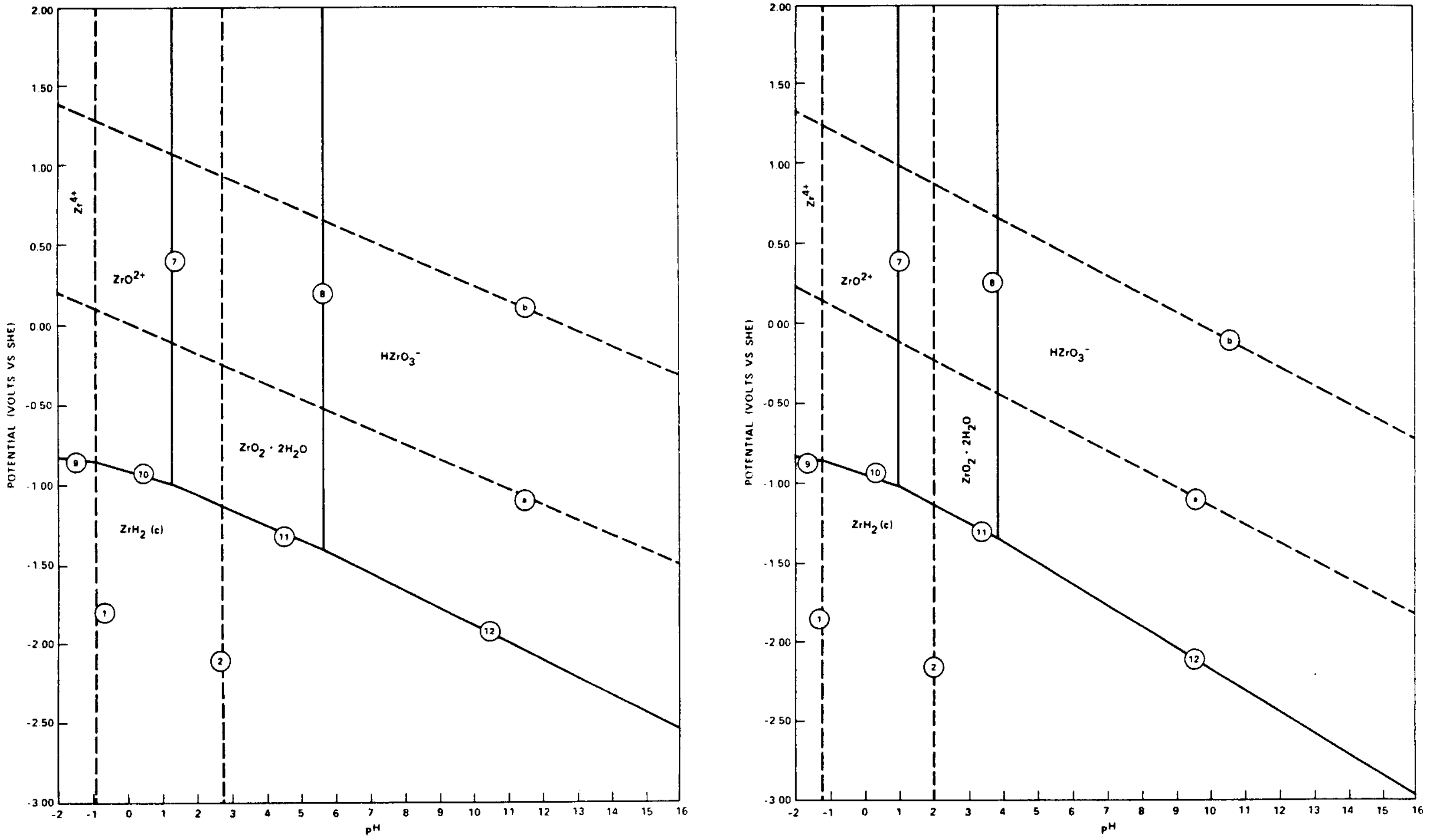

(c) @ 200°C

(d) @ 300°C

FIGURE 16 (Cont'd)

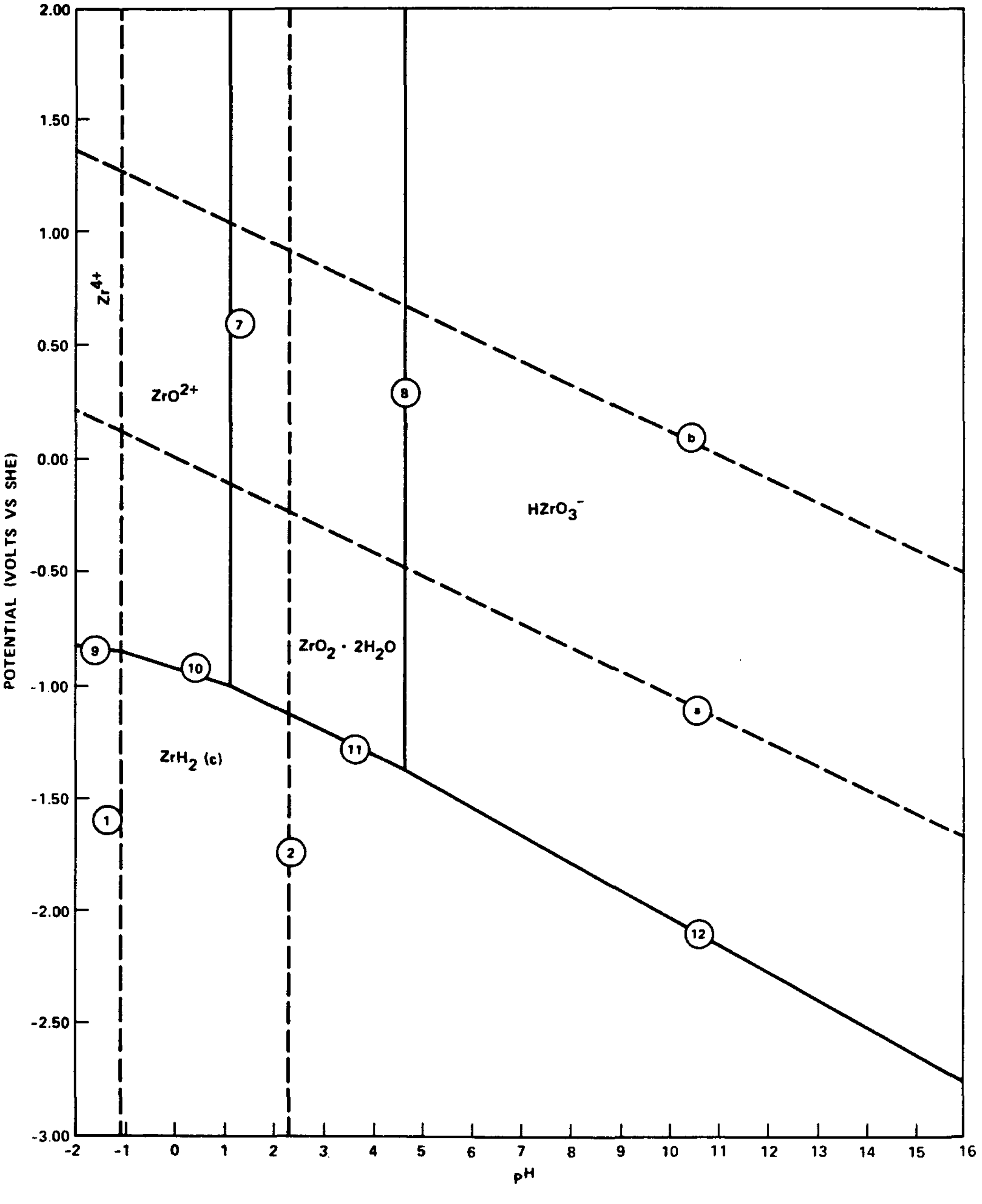

(e) @ 250°C

FIGURE 16 (Cont'd)

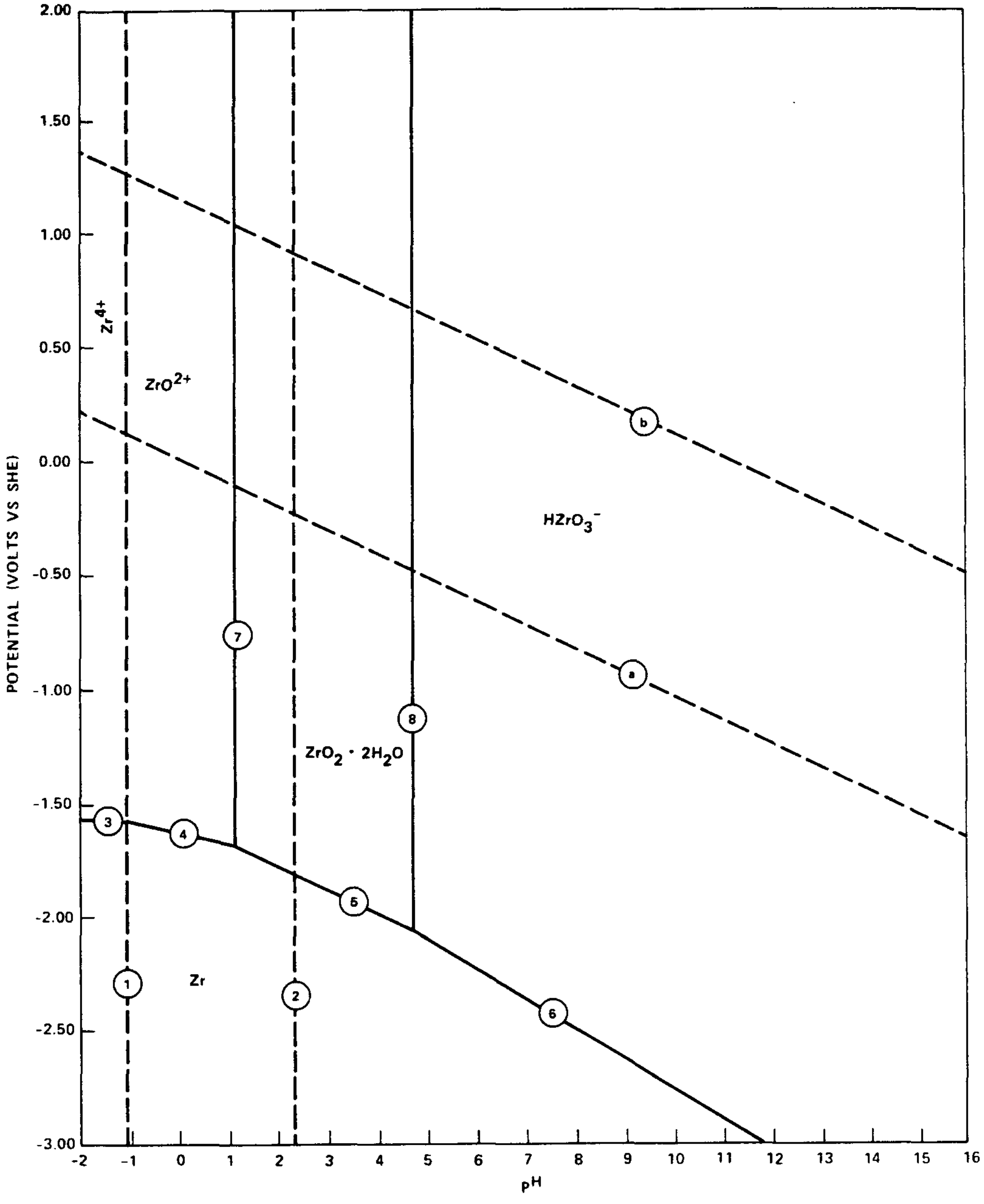

(f) WITHOUT CONSIDERATION OF ZrH_2 AT 250°C

FIGURE 16 (Cont'd)

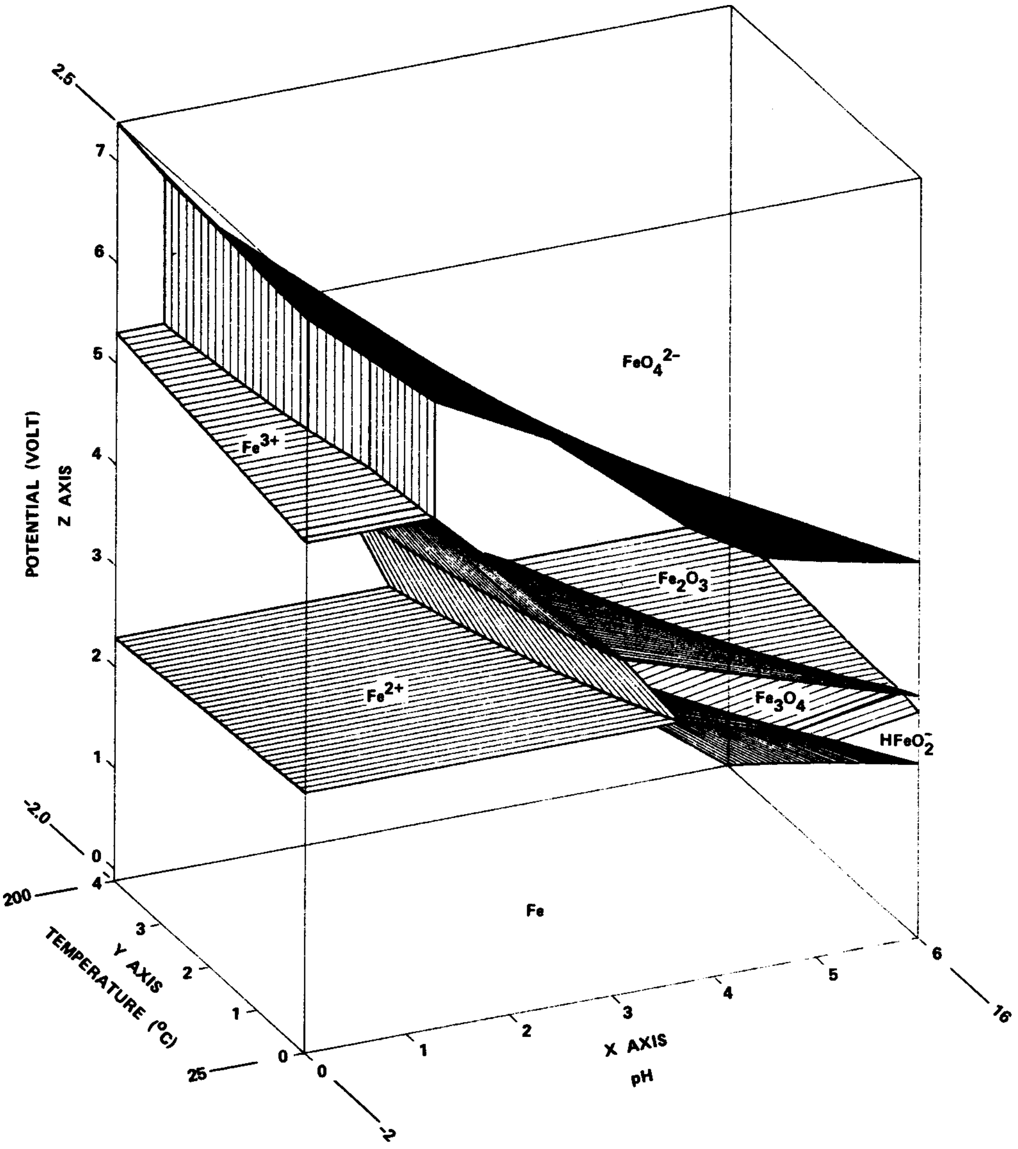

FIGURE 17 TERNARY DIAGRAM OF Fe AS FUNCTION OF POTENTIAL, TEMPERATURE AND pH

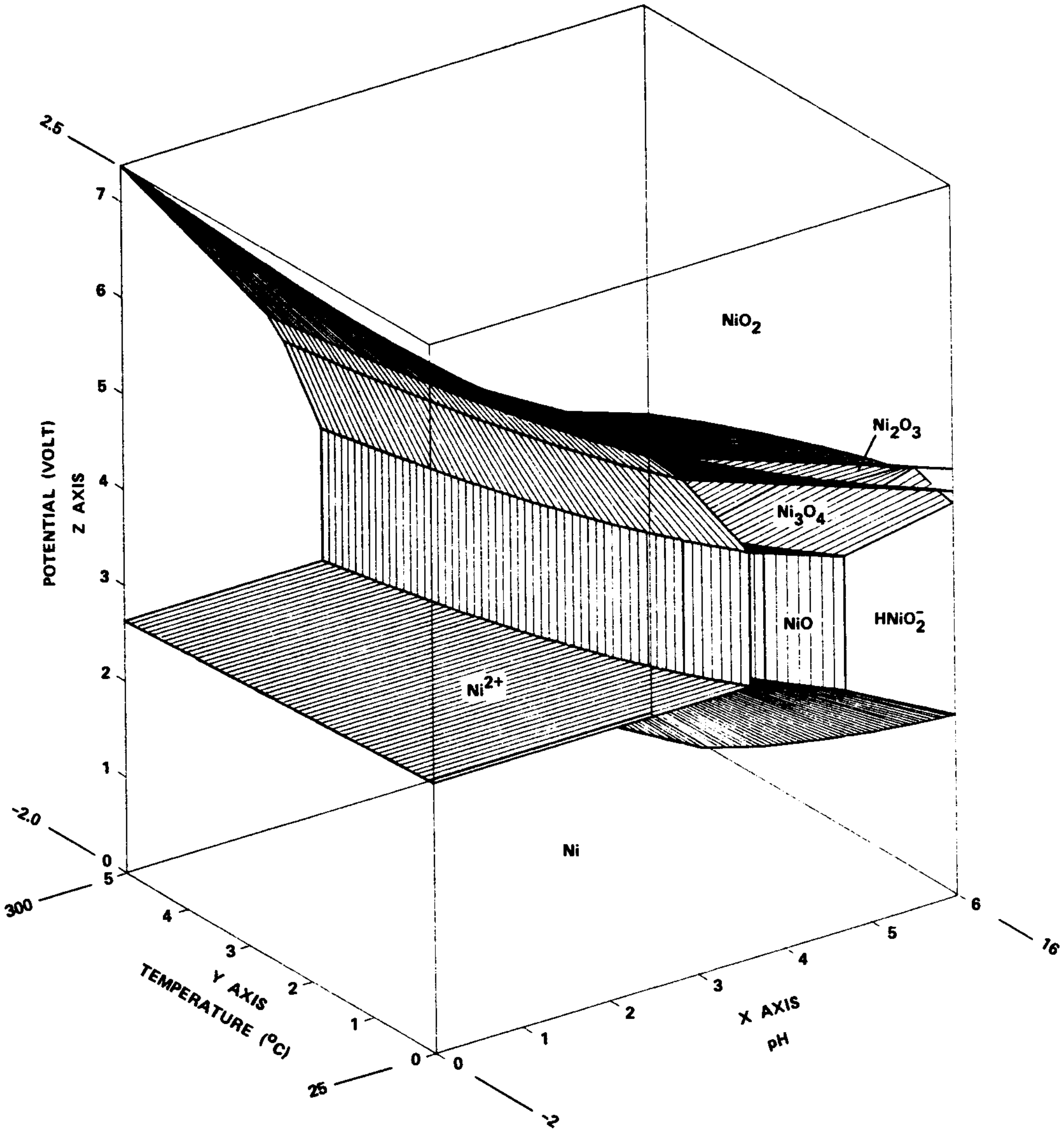

FIGURE 18 TERNARY DIAGRAM OF Ni AS FUNCTION OF POTENTIAL, TEMPERATURE AND pH

Section 6

REFERENCES

1. M. Pourbaix, Atlas of Electrochemical Equilibria in Aqueous Solutions, Pergamon Press, New York, 1966.

2. H. E. Townsend Jr., Corrosion Science, 10, 343, 1970.

3. H. E. Townsend, Proc. 4th Intern. Congress Metallic Corr., Amsterdam 1969, 477, Ed. NACE, 1972.

4. V. Asworth and P. J. Boden, Corr. Sci, 10, 709, 1970.

5. D. Lewis, J. Inorg. Nucl. Chem., 33, 2121, 1971.

6. D. Lewis; Pure and Appl. Chem., 34, 59, 1972.

7. R. J. Biernat and R. G. Robin, Electrochimica Acta, 17, 1261, 1972.

8. O. J. Kwok and R. G. Robins, International Symposium on Hydrometallurgy, Chap. 39, p. 1033, Chicago 1973, AIMMPE, New York, Ed. Evans and Shoemaker, 1973.

9. S. I. Berezima, L'electrode Ni-H, Doklad. Akad. Naouk. U.S.S.R. 77, 53, 1951.

10. F. D. Rossini, D. D. Wagman, W. H. Evans, S. Levin and I. Jaffe, "Selected Values of Chemical Thermodynamic Properties," National Bureau of Standards Circulary 500, Part 1, July 20, 1961.

11. K. K. Kelley, "Contributions to the Data on Theoretical Metallurgy XIII. High-Temperature Heat-Content, Heat-Capacity, and Entropy Data for the Elements and Inorganic Compounds," Bulletin 584, Bureau of Mines, 1960.

12. D. R. Stull and H. Prophet; JANAF Thermodynamical Tables, 2nd Edition, U. S. Department of Commerce, June 1971.

13. O. Kubaschewski and C. B. Alcock, Metallurgical Thermochemistry, 5th Edition, Pergamon Press, New York, 1979.

14. D. D. Wagman, W. H. Evans, V. B. Parker, I. Halow, S. M. Bailey, and R. H. Schumm, "Selected Values of Chemical Thermodynamic Properties," Technical Note 270-3, NBS, Jan. 1968.

15. Calculated from Criss-Cobble Correspondence Principle, C. M. Criss and J. W. Cobble, J. Am. Chem. Soc., 5385 and 5390, 1964.

16. O. Kubaschewski, E. LL. Evans and C. B. Alcock, Metallurgical Thermochemistry, 4th Edition, Pergamon Press Oxford, 1967.

17. J. M. Cobble, "Chemical Equilibria in Aqueous Systems at High Temperatures," EPRI Contract No. RP 1167-1, August 1, 1980.

18. Tentative Approximation from the Assumption of Cp = 0 Independent of Temperatures.

19. H. A. Pohl, *J. Chemical and Inorganic Data*, 6, 515, 1961.

20. D. D. Wagman, W. H. Evans, V. B. Parker, I. Halow, S. M. Bailey and R. H. Schumm, "Selected Values of Chemical Thermodynamic Properties," Technical Note 270-4, NBS, May 1969.

21. H. E. Barner, R. V. Scheuerman, *Handbook of Thermochemical Data for Compounds and Aqueous Species*, John Wiley & Sons, New York, 1978.

22. V. S. Belyanin, *Thermal Engineering*, 26 (ID), 622, 1979.

23. R. E. Connick and R. E. Powell, *J. Chemical Physics*, 21, 2206, 1953.

24. W. M. Latimer, *Oxidation Potentials*, 2nd Edition. Prentice-Hall, New Jersey, 1952.

25. R. L. Cowan and R. W. Stashle, *J. Electrochem. Soc.*, 118, 557, 1971.

26. P. A. Brook, *Corrosion Science*, 12, 197, 1972.

27. A. M. Couture and K. J. Laidler, *Can. J. Chem.*, 35, 202, 1957.

28. K. I. Laidler, *Can. J. Chemistry*, 34, 1107, 1956.

29. J. M. Cobble, "Chemical Thermodynamic Studies of Aqueous Trace Components in Light Water Reactors at High Temperature and High Pressure," EPRI Contract No. RP 311-2, Annual Report, April 1, 1976.

30. D. R. Fredrickson, R. L. Nuttall, H. E. Flotow and W. N. Hubbard, *J. Phys. Chem.* 67, 1506, 1963.

31. D. D. Wagman, W. E. Evans, V. B. Parker, I. Halow, S. M. Bailey and R. H. Schumm, "Selected Values of Chemical Thermodynamic Properties," Technical Note 270-5, NBS, 1971.

32. R. E. Powell and W. M. Latimer, *J. Chem. Phys.*, 19, 1139, 1951.